8-2011

Functional analysis of N-acetyltransferase (NAT1*14B and NAT1*10) in complete NATb and NATa mRNA.

Lori Michele Millner
University of Louisville

FUNCTIONAL ANALYSIS OF *N*-ACETYLTRANSFERASE (*NAT1*14B* AND *NAT1*10*) IN COMPLETE NATb AND NATa mRNA

By

Lori Michele Millner
B.A. University of Kentucky, 2004
M.S. University of Louisville, 2008

A Dissertation
Submitted to the Graduate Faculty of the
University of Louisville School of Medicine
in Partial Fulfillment of the Requirements
for the Degree of

Doctor of Philosophy

Department of Pharmacology and Toxicology
University of Louisville
Louisville, Kentucky

August 2011

FUNCTIONAL ANALYSIS OF *N*-ACETYLTRANSFERASE (*NAT1*14B* AND *NAT1*10*) IN COMPLETE NATb AND NATa mRNA

By

Lori Michele Millner
B.A. University of Kentucky, 2004
M.S., University of Louisville, 2008

A Dissertation Approved on

June 24, 2011

By the following Dissertation Committee:

David W. Hein, Ph.D.

J. Christopher States, Ph.D.

Kenneth a. Palmer, Ph.D.

Frederick W. Benz, Ph.D.

Russell A. Prough, Ph.D.

DEDICATION

This dissertation is dedicated to my parents

Mrs. Margaret J. Millner

and

Dr. Ozra Elmo Millner, Jr.

And to my husband,

Mr. John Michael Tandy, MBA

ACKNOWLEDGMENTS

I would like to thank my mentor, Dr. David W. Hein, for his guidance and patience during my Ph.D. training. I would also like to thank the other committee members, Drs. States, Prough, Palmer and Benz for their guidance.

I would also like to thank my husband, J. Michael Tandy, for his unending kindness and encouragement.

I would also like to thank my mom, Margaret Millner, for always believing in me and for living a life filled with faith, hope and love.

Also, I would like to thank my mother and father in-law, Jennifer and Milton Tandy, for their positive role in my life.

ABSTRACT

FUNCTIONAL ANALYSIS OF *N*-ACETYLTRANSFERASE (*NAT1*14B* AND *NAT1*10*) IN COMPLETE NATb AND NATa mRNA

Lori Millner
August 8, 2011

N-acetyltransferase 1 (NAT1) is a phase II metabolic enzyme responsible for the biotransformation of aromatic and heterocyclic amine carcinogens such as 4-aminobiphenyl (ABP). NAT1 catalyzes *N*-acetylation of arylamines as well as the *O*-acetylation of *N*-hydroxylated arylamines. *O*-acetylation leads to the formation of electrophilic intermediates that result in DNA adducts and mutations. NAT1 is transcribed from a major promoter, NATb, and an alternative promoter, NATa, resulting in mRNAs with distinct 5'-untranslated regions (UTR). NATa mRNA is expressed primarily in the kidney, liver, trachea and lung while NATb mRNA has been detected in all tissues studied. To determine if differences in 5'-UTR have functional effect upon NAT1 activity and DNA adducts or mutations following exposure to ABP, pcDNA5/FRT plasmid constructs were prepared for transfection of full length human mRNAs including the 5'-UTR derived from NATa or NATb, the open reading frame, and 888 nucleotides of the 3'-UTR. Following stable transfection of NATb/*NAT1*4* or NATa/*NAT1*4* into nucleotide excision repair (NER) deficient Chinese hamster ovary cells, *N*- and *O*-acetyltransferase activity (*in vitro* and *in situ*), mRNA, and protein expression were higher in NATb/*NAT1*4* than NATa/*NAT1*4* transfected cells ($p<0.05$). Consistent with NAT1 expression and activity, ABP-induced DNA adducts and *hypoxanthine phosphoribosyl transferase* mutants were higher ($p<0.05$) in NATb/*NAT1*4* than in

NATa/*NAT1*4* transfected cells following exposure to ABP. These NATa and NATb mRNA constructs have also been used to study variant NAT1 alleles, including *NAT1*14B* and *NAT1*10*. *NAT1*14B* is the most common allele associated with reduced *N*-acetylation activity and has been associated with increased risk for smoking induced lung cancer. NATb/*NAT1*14B* transfected cells resulted in lower V_{max} for PABA, ABP, and *N*-OH-ABP compared to cells transfected with NATb/NAT1*4. However, cells transfected with NATb/*NAT1*14B* resulted in increased V_{max}/K_m for ABP and N-OH-ABP. Cells transfected with NATb/*NAT1*14B* also resulted in increased ABP-induced DNA-adducts compared to cells transfected with NATb/*NAT1*4* transfected cell. This indicates that NAT1 14B has lowered capacity for *N*- and *O*- ABP acetylation at high substrate concentrations but higher capacity at low substrate concentration when compared to NAT1 4. NAT1 14B V_{max}/K_m compared to NAT1 4 was lower for PABA but higher for ABP and *N*-OH-ABP. This indicates that NAT1 14B is not simply associated with lowered acetylation, but is substrate dependent. Another variant allele, *NAT1*10* is the most common variant allele in many populations and has been characterized by increased acetylation activity in colon and bladder. *NAT1*10* has been associated with increased cancer risk for prostate, breast, urinary bladder cancer, gastric adenocarcinoma, colon cancers and non-Hodgkin's lymphoma. Following sequencing of *NAT1*10* genomic sources, additional polymorphisms (A1642C, ΔCT1647, C1716T, and A1735T) were observed in one source. This allele is referred to as *NAT1*10B* in this dissertation. Cells transfected with NATb/*NAT1*10* and NATb/*NAT1*10B* resulted in higher NAT1 activity, protein, mRNA, ABP-induced mutants and DNA adducts than cells transfected with NATb/*NAT1*4*. Differences between NAT1 4, NAT1 10, and NAT1 10B were also observed in NATa constructs. These studies illustrate the importance of determining NAT1 phenotypes and cancer risk based on mRNA type, substrate type and concentration.

TABLE OF CONTENTS

LIST OF TABLES

PAGE

LIST OF FIGURES

CHAPTER 1

ARYLAMINE *N*-ACETYLTRANSFERASE: AN INTRODUCTION

Arylamine *N*-acetyltransferases (NAT1 and NAT2) are an important family of cytosolic, phase II xenobiotic metabolizing enzymes. They are found in most species from prokaryotes to eukaryotes (Boukouvala and Fakis, 2005). The *N*-acetyltransferase (NAT) genes were among the first polymorphic genes to be identified, over 40 years ago. The discovery occurred in the 1950s when a new drug, isoniazid, was introduced to treat tuberculosis. Isoniazid was largely successful in treating tuberculosis, however a small percentage of patients experienced severe side effects including peripheral neuropathy and liver toxicity during treatment (Biehl and Sklavem, 1953). Following publication of biomodal distribution histograms measuring the amount of unchanged isoniazid in urine, it was determined that two groups of acetylators (rapid and slow) existed (Evans et al., 1960). It was also determined that the patients with the highest plasma isoniazid levels were generally slow acetylators (Evans et al., 1960) and that slow acetylators were most likely to develop side effects (Clark, 1985). It was later discovered that NAT2 was responsible for the metabolism of not only isoniazid, but also other hydrazine drugs including the monoamine oxidase inhibitor, phenelzine, and the anti-hypertensive drug, hydralazine (Weber and Hein, 1985). NAT is also responsible for the detoxification of many arylamine drugs such as antibacterial sulfonamides the antiarrhythmic drug procainamide, the antibiotic dapsone, and the aromatase inhibitor aminoglutethimide (Weber and Hein, 1985) (Figure 1-1).

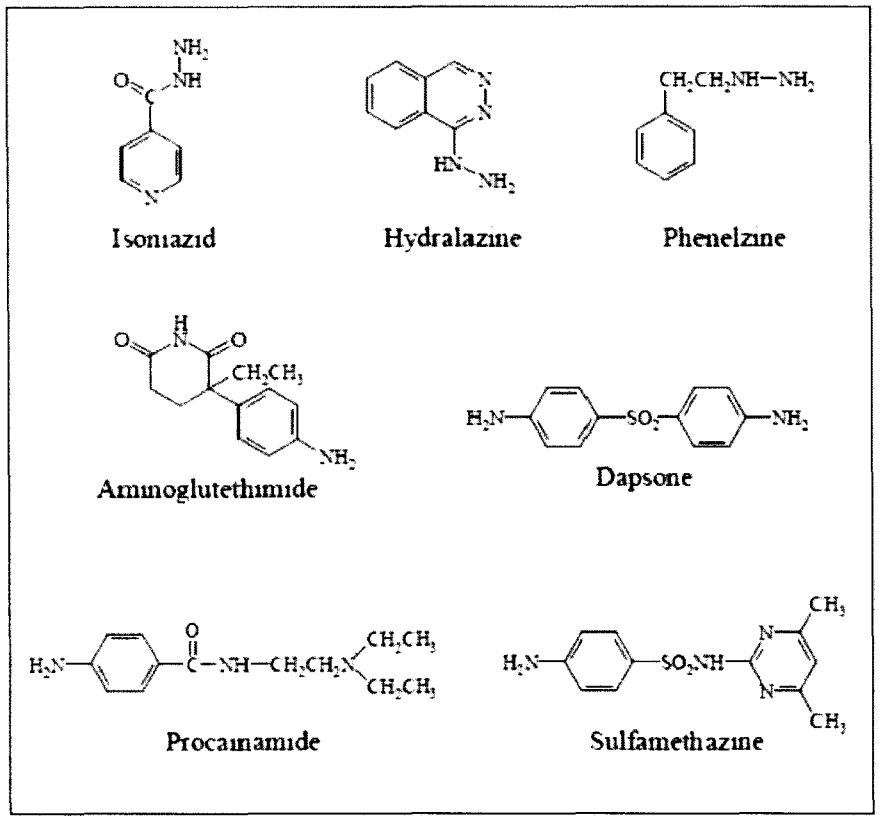

Figure 1-1: Drugs metabolized by NAT2

Drugs metabolized by NAT2 include the antitubercular drug isoniazid, the anti-hypertensive drug hydralazine, the monoamine oxidase inhibitor phenelzine, the aromatase inhibitor aminoglutethimide, the antibiotic dapsone, the antiarrhythmic drug procainamide, and the antibacterial drug sulfamethazine.

In addition to drug metabolism, NAT1 and NAT2 are responsible for the metabolism of many arylamine carcinogens. Common environmental arylamine carcinogens metabolized by NAT include aromatic amines such as 4-aminobiphenyl (ABP) and 2-aminofluorene (AF) that are components of cigarette smoke and contaminants in many products including hair and textile dyes . Heterocyclic amines include 2-amino-1-methyl-6-phenylimidazo[4,5-b]pyridine (PhIP), 2-amino-3-methylimidazo[4,5-f]quinoline (IQ), and 2-amino-3,8-dimethylimidazo[4,5-f]quinoxaline (MeIQx) which are found in meats cooked at high temperatures (Refer to Figure1-2). Heterocyclic amines form when amino acids come into contact with creatine at high temperatures (Keating and Bogen, 2004; Schut and Snyderwine, 1999).

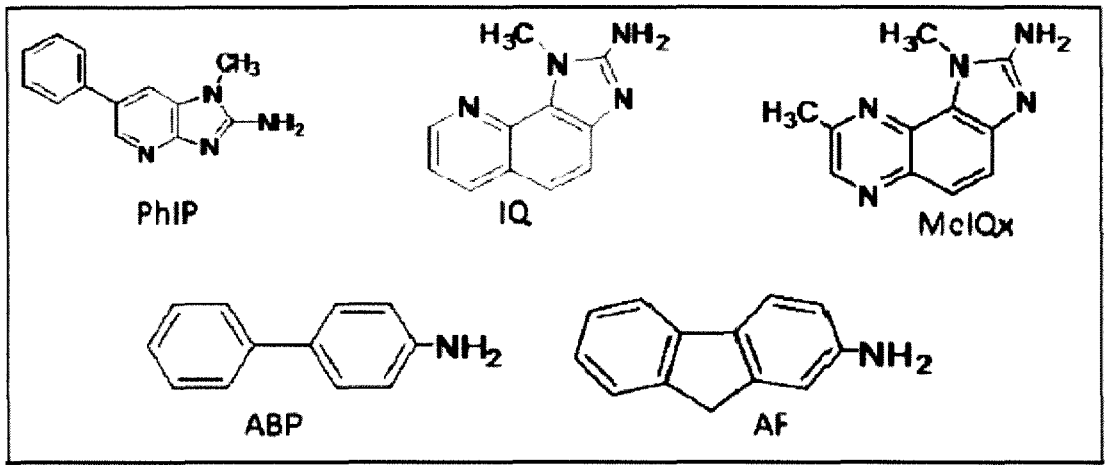

Figure 1-2: Common environmental arylamine carcinogens metabolized by NAT.

These include 4-aminobiphenyl (ABP), 2-aminofluorene (AF), 2-amino-1-methyl-6-phenylimidazo[4,5-b]pyridine (PhIP), 2-amino-3-methylimidazo[4,5-f]quinoline (IQ), 2-amino-3,8-dimethylimidazo[4,5-f]quinoxaline (MeIQx).

Role of human *N*-acetyltransferases in Carcinogen Metabolism

Carcinogens may react directly with important biological components such as DNA, protein, or lipids, but many carcinogens only exert an effect when metabolically activated by phase I or phase II enzymes. Aromatic amines such as ABP contain exocyclic amines and may be directly *N*-acetylated by NAT. NATs catalyze *N*-acetylation (Figure 1-3) by transferring an acetyl group from acetyl-CoA to the exocyclic nitrogen of an aromatic or heterocyclic amine. These compounds can then be excreted from the body. Arylamine carcinogens are primarily activated in the body by a two step process. The first step is *N*-hydroxylation carried out by the phase I metabolic enzymes, cytochrome p450s (Schut and Snyderwine, 1999). These *N*-hydroxy metabolites can be activated further by phase II enzymes such as NAT, sulfotransferases, or tRNA synthetases. NAT is an extremely important phase II enzyme. It was found to have the highest activity in mammary tissue when compared to the other most common phase II enzymes (Ghoshal et al., 1995). NAT1 and NAT2 further activate *N*-hydroxy metabolites via *O*-acetylation to form nitreum ions. These acetoxy metabolites quickly form highly electrophilic intermediates that react with DNA to form bulky adducts. If these lesions are not repaired, mutagenesis and carcinogenesis may result (Schut and Snyderwine, 1999). The interaction between environmental carcinogen exposure and genes coding for these metabolic enzymes may further modulate cancer risk.

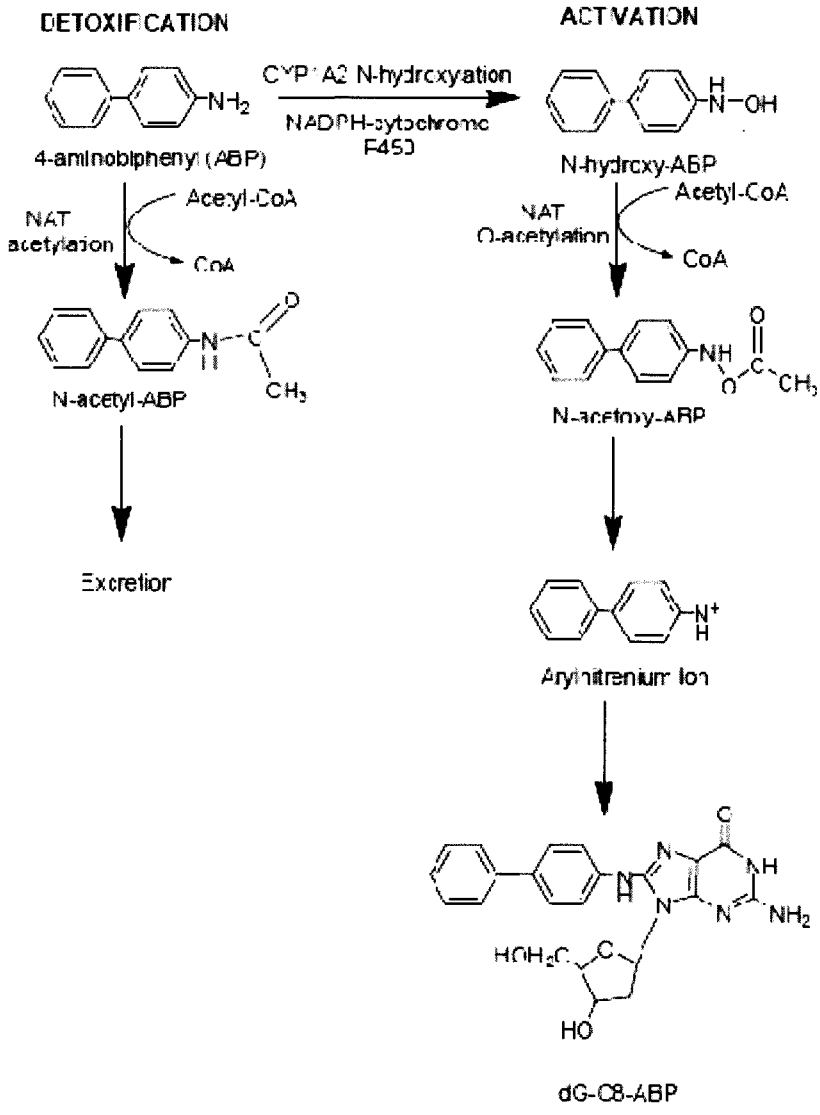

Figure 1-3: Possible Metabolic Pathways for 4-aminobiphenyl (ABP)

If the amine group is first *N*-acetylated creating *N*-acetyl-ABP, the compound can then be excreted. However, If ABP is first hydroxylated by cytochrome p450, creating *N*-hydroxy-ABP, NAT can further activate the compound by O-acetylation creating *N*-acetoxy-ABP. *N*-acetoxy-ABP is an extremely unstable compound which spontaneously breaks down to form acetic acid and a highly electrophilic arylnitrenium ion that binds covalently with nucleophilic moieties such as protein or DNA to form adducts.

In addition to activation of environmental carcinogens, NAT1 may serve in a more profound role affecting tumor development and progression. NAT1 overexpression has been implicated in enhanced density dependent cell growth and resistance to chemotherapy. In a recent study conducted in the colon adenocarcinoma cell line HT-29, a marked change in cell morphology, an increase in cell-cell contact growth inhibition and a loss of cell viability at confluence was observed when NAT1 was knocked down (Tiang et al., 2011). Additionally, knock-down of NAT1 resulted in up-regulation of E-cadherin in both HT-29 cells and in the prostate cancer cell line 22Rv1 (Tiang et al., 2011). The overexpression of NAT1 in a normal human mammary luminal epithelial cell line (HB4a) allowed those cells to continue proliferation far beyond the density of normal HB4a cells (Adam et al., 2003). The overexpressing HB4a cells also showed resistance to etoposide compared to normal HB4a cells, but it is unknown how NAT1 affects etoposide resistance (Adam et al., 2003). It has recently been demonstrated that cisplatin interacts with and inhibits NAT1 with the highest second-order rate constant among cisplatin targets (Ragunathan et al., 2008). Therefore, *NAT1* up-regulation may affect chemotherapeutic tumor sensitivity. Additionally, *NAT1* has been identified as one of the top three most overexpressed genes in estrogen receptor positive breast tumor tissues (Wakefield et al., 2008). Because NAT1 expression may have far reaching effects on tumor growth, progression and chemotherapeutic sensitivity, it is important to understand regulation of *NAT1* expression.

NAT1 Gene and Regulation

The human genome encodes two isoforms of N-acetyltransferase, NAT1 and NAT2 located on the short arm of chromosome 8 (Matas et al. 1997). Both are encoded by a single intronless coding exon containing an open reading frame (ORF) of 870 base pairs. The NAT1 and NAT2 ORFs have 87% nucleotide sequence identity (Sim et al.,

2000). Although NAT1 and NAT2 enzymes are similar in sequence, they possess different substrate selectivities and structural stabilities (Blum et al., 1990; Grant et al., 1989).

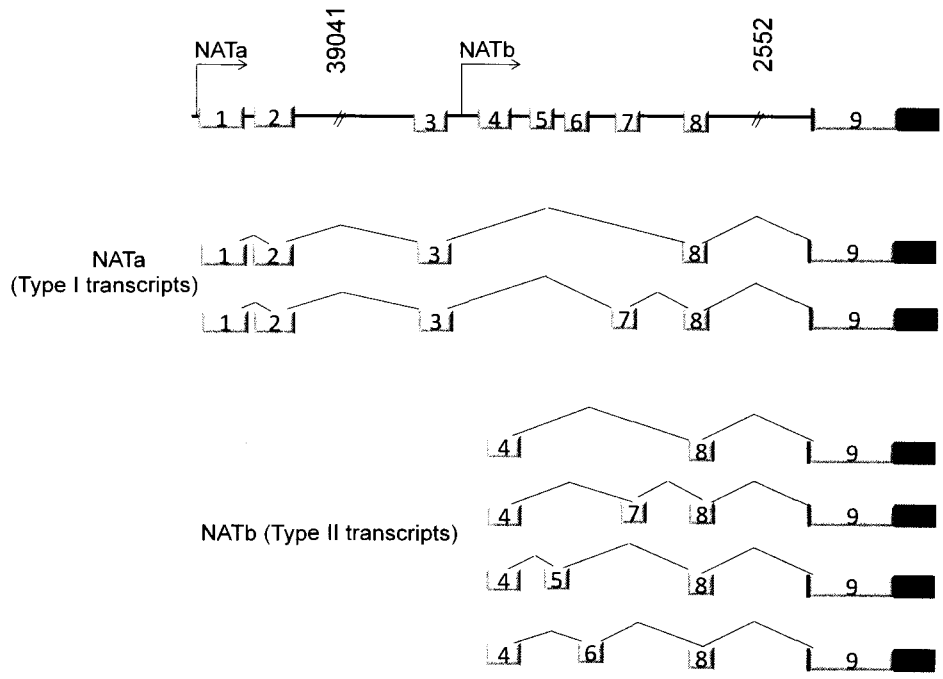

Figure 1-4: NAT1 gene structure and common transcripts

The NAT1 promoters (NATa and NATb) produce several mRNA variants with different combinations of 5'-UTR exons. All splice variants identified to date contain both exons 8 and 9. The NATa promoter drives transcription of Type 1 transcripts , whereas NATb drives transcription of Type II transcripts. Modified from Butcher et al., 2005.

The *NAT1* gene is approximately 53 kb in length and contains at least nine exons (Husain et al., 2004). Many *NAT1* transcripts have been identified containing different combinations of the 5' UTR exons originating from two separate promoters (Husain et al., 2004; Butcher et al., 2005). Differences in translational efficiencies exist between transcripts originating at each promoter, but the biological importance of this remains

unclear (Butcher et al., 2005). Six different mRNAs have been identified to begin at the first promoter, NATa (also known as P3), which is located 50.1 kb upstream of the *NAT1* ORF (Barker et al., 2006). Five different mRNAs have been identified which begin at the second promoter, NATb (also known at P1), located just upstream of exon 4 (11.8 kb of the *NAT1* ORF) (Butcher et al., 2005; Husain et al., 2004) (Figure 1-4).

The NATb promoter has been mapped to a 213 bp region upstream of exon 4 in MCF-7 cells or a 257 bp region in HT-29 cells (Butcher et al., 2005; Husain et al., 2007). Alignment with promoter sequences of NATs derived from other species revealed a conserved 16 bp palindrome and a functional Sp1 element (Husain et al., 2007). The NATb promoter lacks a TATA-box and is therefore likely a TATA-less Inr type promoter (Smale, 1997). Less is known about the alternative, NATa promoter. The NATa promoter region has been mapped to a 435 bp region upstream of exon 1 (Barker et al., 2006). The relative strength of the NATa promoter was low compared to the NATb promoter and pGL3-control (containing the strong SV40 promoter) in HepG2 cells (Barker et al., 2006; Husain et al., 2004). However, the relative contribution of transcripts derived from the NATa promoter is not known. Transcripts derived from the NATb promoter have been found in all tissues studied but transcripts derived from the NATa promoter have been found in liver, kidney, lung, and trachea (Barker et al., 2006; Husain et al., 2004). It is possible that NATa transcripts are expressed in a wider range of tissues, but only when the cell is under specific environmental stress or in a disease state. For example, expression of NATa transcripts has recently been reported in several ER-positive breast cancer cell lines where NAT1 overexpression is observed (Wakefield et al., 2008).

NAT1 Population Frequencies

*NAT1*4* is present at high frequencies in most populations. The highest *NAT1*4* allelic frequencies have been reported in the American, French, Canadian, Lebanese, Chinese and German populations (Table 1-1). *NAT1*4* is not the most frequent allele in the South African population, where *NAT1*10* has the highest allelic frequency. In the Lebanese population, allelic frequency for *NAT1*14B* is 23.8%, while in most other populations the allelic frequency is less than 5% (Table 1). Although the NAT1 allele population frequencies included here are not exhaustive, they represent populations found on four different continents.

Table 1-1: NAT1 allelic frequencies in selected populations

Allele	USA (Iowa)	France	Canada	Germany	Lebanon	China	South Africa (Blacks)
*NAT1*4*	74.2	74.7	70.3	72.4	56	49.6	48.5
*NAT1*10*	17.4	17.8	25	20.4	10.7	40	50.5
*NAT1*14B*	2	3.7	2.6	0.6	23.8	ND	ND

(NAT1 allele frequencies from Cascorbi et al., 2001; Dhaini and Levy et al., 2001; Lo-Guidice et al., 2000; Loktionov et al., 2002; Vaziri et al., 2001; Zhangwei et al., 2006; Zheng et al., 1999).

*NAT1*14B*

*NAT1*14B* is the most common NAT1 allele associated with reduced acetylation activity. *NAT1*14B* is characterized by a SNP found in the ORF (560G>A) which causes an amino acid substitution (R187Q). Evidence suggests that NAT1 14B is a slow acetylator due to the R187Q substitution which causes decreased or no acetylation activity in NAT1 14B (Grant et al., 1997; Hughes et al., 1998). In addition to a decrease

in *N*- and *O*-acetyltransferase activity, there is also decreased protein level (Zhu and Hein, 2007). The R187Q substitution is believed to interfere with the ability of the NAT1 protein to be acetylated, therefore NAT1 14B is unstable, ubiquitinated, and then degraded by the 26 S proteasome (Butcher et al., 2004).

*NAT1*14B* is associated with an increased risk of smoking-induced lung cancer. The OR for smoking induced lung cancer was 4.0 (95% confidence interval 0.8-19.6) for homozygous rapid (*NAT1*4* or *NAT1*3*) acetylators, whereas the risk was found to be 11.0 (95% confidence interval 1.3-106.5) for heterozygous slow (*NAT1*14B* or *NAT1*15*) acetylators (Bouchardy et al., 1998) compared to non-smokers. *NAT1*14B* is present at low frequencies in many populations with the exception of the Lebanese population where the *NAT1*14B* allelic frequency was reported to be 23.8% (Dhaini and Levy, 2000).

*NAT1*10*

*NAT1*10* is characterized by two SNPs located in the region 3' to the open reading frame including T1088A and C1095A. There are no amino acid changes due to the polymorphisms, but the T1088A causes a change in the second potential polyadenylation signal (ATTAAA). The signal is not destroyed, but it is shifted 3' three nucleotides. It has been speculated that this change in polyadenylation signal may give rise to a difference in mRNA stability and modulated acetylation activity of NAT1 10 (Bell et al., 1995a).

*NAT1*10* is putatively considered to be a rapid acetylator, however there are many conflicting results about the acetylator phenotype of *NAT1*10*. Bell et al. reported significantly higher enzyme activity in urinary bladder and colon tissue for individuals heterozygous for *NAT1*10/1*4* compared to those individuals homozygous for *NAT1*4*. Similar findings were reported in colorectal tissue. In contrast, another study employing

recombinantly expressed alleles reported no difference between NAT1 10 and NAT1 4 activities (de Leon et al., 2000).

*NAT1*10* is of great interest because it has been associated with increased risk of so many different forms of cancer, however the molecular contribution remains unclear. Specifically, *NAT1*10* heterozygous genotype is associated with an odds ratio (OR) of 1.60 for non-Hodgkin lymphoma (Morton et al., 2006), an OR of 2.2 for gastric adenocarcinoma (Boissy et al., 2000), and an OR of 2.17 for prostate cancer (Hein et al., 2002) when compared to the homozygous *NAT1*4* genotype. It is clear that cancer risk associated with *NAT1*10* is further modulated by exposure to environmental carcinogens found in cigarette smoke, meats cooked at high temperatures, and hair dye. Frequent consumption of red meat in combination with the *NAT1*10* allele is associated with increased risk for colorectal cancer (Lilla et al., 2006). The use of dark, permanent hair dye in combination with *NAT1*10* increases the risk for non-Hodgkin lymphoma (Morton et al., 2007). Heavy smokers possessing the *NAT1*10* allele have increased risk for pancreatic cancer compared to non-smokers (Li et al., 2006) and an as well as increased risk for breast cancer (Zheng et al., 1999).

Although the contribution of *NAT1*10* to increased cancer risk is not well understood, molecular epidemiological studies have given us some clues. This study focuses on the association between cancer risk and the combination of *NAT1*10* and exposure to amine carcinogens. It is imperative that the phenotype of *NAT1*10* be clearly defined in order to understand the association of *NAT1*10* genotype with increased cancer risk.

DNA Repair Deficient Chinese Hamster Ovary Cells

The experiments described in this dissertation employ a strain of Chinese hamster ovary (CHO) cells referred to as UV5 cells that are deficient in the DNA nucleotide excision repair (NER) pathway. UV5 cells are deficient in transcription factor IIH (TFIIH), a multisubunit protein complex required for both transcription catalyzed by RNA polymerase II and NER (Drapkin et al., 1994). Specifically, UV5 cells have a mutation in ERCC2 which is linked to excision repair deficiency and results in the genetic disease xeroderma pigmentosum group D (XPD) (Schaeffer et al., 1994). This cell line is used to detect endpoints caused by mutagenesis and adduct formation because bulky adduct removal is compromised. This cell line was chosen to facilitate studying the genotoxic effects of aromatic amines due to metabolism by cytochrome p450 and NAT1 alleles. In addition to NER deficiency, the UV5 cell line is commonly used because of its robust growth, ease in mutagenesis studies, and its ability to be transfected without affecting plating efficiencies (Li et al., 1987).

The UV5 cells that are employed in this study have been stably transfected with human cytochrome p450 (*CYP1A1)*. This cell line allows genotoxic effects to be studied that require metabolic activation by CYP1A1 and NAT1. UV5 cells expressing *CYP1A2* and various *NAT2* alleles have been used to compare the genotoxic effects of PhIP and MeIQx (Bendaly et al., 2007; Metry et al., 2007;). The experiments described in this dissertation express human CYP1A1 because, like human NAT1, it is expressed extrahepatically. These experiments employed NER-deficient CHO cells expressing human *CYP1A1* and various *NAT1* alleles to compare *NAT1* polymorphism effects on aromatic amine metabolism, DNA adduct formation and mutation frequency.

4-aminobiphenyl

This study uses the aromatic amine 4-amiobiphenyl (ABP). ABP is a common environmental carcinogen and a potent bladder carcinogen (IARC, 1987). NAT1 is expressed extrahepatically, including bladder tissue (Badawi et al., 1995), therefore, NAT1 metabolism is likely important for ABP-induced bladder cancer.

ABP was widely used as an antioxidant in the rubber industry (IARC, 1987). Once its carcinogenic properties were discovered, it was strictly prohibited by federal regulation. However, ABP can still be found as a contaminant in color additives, paints, food colors, leather, textile dyes, diesel-exhaust particles, cooking oil fumes and commercial hair dyes (Nauwelaers et al., 2011). ABP is also still found in the aluminum industry (Guzzo et al., 2008). Cigarette smoke is a major source of ABP exposure. Mainstream smoke has been reported to contain up to 23 ng per cigarette and sidestream smoke has been reported to contain up to 140 ng per cigarette (Hoffmann et al., 1997). Following exposure, ABP is metabolized in the liver by *N*-acetylation, *N*-glucuronidation, or hydroxylation (Seyler et al., 2010). Hemoglobin (Hb) adducts have been reported to be 75.8 pg/g Hb (66.5-86.5) in smokers and 29.9 pg/g Hb (24.7-36.2) in nonsmokers (Seyler et al., 2010).

Flp-In System™

To create a model system to investigate the carcinogenic effect of ABP exposure with different NAT1 alleles, Invitrogen's Flp-In™ System was used to create a CHO cell line stably expressing a single copy of NAT1. The Flp-In™ system utilizes a Saccharomyces cerevisiae-derived DNA recombination system. NAT1 was integrated into a specific site in the CHO genome by a recombinase (Flp) and site-specific

recombination (Craig, 1988; Sauer, 1994). The *NAT1* alleles were cloned into an expression vector, the pcDNA5/FRT (Figure 1-5) which utilizes the CMV promoter to drive constitutive expression of *NAT1*. The pcDNA5/FRT expression vector was co-transfected with the pOG44 vector, which constitutively expresses the Flp recombinase.

Figure 1-5: pcDNA5/FRT Expression Vector

The pcDNA5/FRT is the chosen expression vector into which the *NAT1* DNA was ligated. The polyadenylation signal was removed prior to ligation of *NAT1* DNA. The vector contains one FRT site which allows it to be stably integrated into the CHO cell genome. (Modified from invitrogen.com)

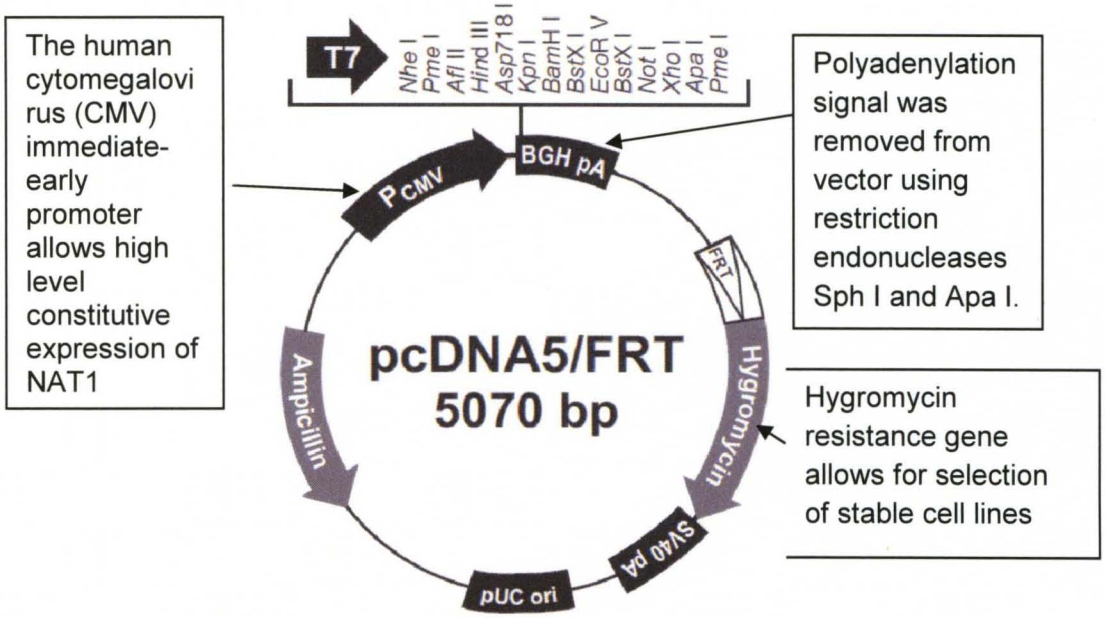

SPECIFIC AIMS

Specific Aim I

Create pcDNA5/FRT vector constructs which contain the human *NAT1* alleles including NATa and NATb 5'-UTR exons, the open reading frame, and 885 base pairs of the region 3' to the open reading frame (with 6 potential polyadenylation signals). In addition to the reference *NAT1*4*, constructs containing individual or combinations of genetic polymorphisms present in *NAT1*10, NAT1*11*, and *NAT1*14* will be constructed.

Specific Aim II

Prepare and characterize nucleotide excision repair deficient Chinese hamster ovary cells expressing human *CYP1A1* transfected with pcDNA5/FRT vectors containing human *NAT1* constructs. The functional effects of genetic polymorphisms in *NAT1*10, NAT1*11,* and *NAT1*14* will be compared to the reference allele *NAT1*4* in transient transfection experiments. Functional assays will include determinations of *N*- and *O*-acetylation catalytic activities (HPLC assays), mRNA levels (Taqman assays) and protein levels (Western blot assays).

Specific Aim III

Test effects of *NAT1* polymorphisms in stable CHO cell transfectants after exposure to various aromatic and heterocyclic amine carcinogens on levels of covalent DNA adduct formation (liquid chromatography-mass spectrometry assays) and mutagenicity (hprt mutants).

CHAPTER 2

NATb/*NAT1*4* PROMOTES GREATER ARYLAMINE *N*-ACETYLTRANSFERASE 1 MEDIATED DNA ADDUCTS AND MUTATIONS THAN NATa/*NAT1*4* FOLLOWING EXPOSURE TO 4-AMINOBIPHENYL

INTRODUCTION

Human arylamine *N*-acetyltransferase 1 (NAT1) is a phase II cytosolic enzyme responsible for the biotransformation of many arylamine compounds including pharmaceuticals and environmental carcinogens. A common environmental carcinogen found in cigarette smoke is an aromatic amine, 4-aminobiphenyl (ABP) (Internation Agency for Research on Cancer, 1987). Arylamines such as ABP can be inactivated via *N*-acetylation (Hein et al., 1993). However, if ABP is first hydroxylated by cytochrome p4501A1 (CYP1A1), the hydroxyl-ABP then can be further activated by NAT1-catalyzed *O*-acetylation resulting in *N*-acetoxy-ABP (Hein et al., 1993). This compound is very unstable and spontaneously degrades to form a nitrenium ion that can react with DNA to produce bulky adducts. If these adducts are not repaired, mutagenesis can occur and result in cancer initiation.

The only known endogenous NAT1 substrate is p-aminobenzoylglutamate (PABG), a catabolite of folate (Wakefield et al., 2007). *NAT1* has been associated with various birth defects (Jensen et al., 2005; Lammer et al., 2004) that may be related to deficiencies in folate metabolism. *NAT1* polymorphisms and maternal smoking have been associated with increased incidence of oral clefts, spina bifidia and increased limb

deficiency defects (Carmichael et al., 2006; Jensen et al., 2006). *NAT1* polymorphisms have also been associated with increased risk for breast (Ambrosone et al., 2007; Millikan et al., 1998), pancreatic (Li et al., 2006; Suzuki et al., 2008), urinary bladder (Gago-Dominguez et al., 2003; Sanderson et al., 2007) and colorectal cancers (Bell et al., 1995a; Shin et al., 2008), non-Hodgkin lymphoma (Kilfoy et al., 2010; Morton et al., 2006), mammary cell growth (Adam et al., 2003) and breast cancer survival (Ring et al., 2006). However, other studies have concluded that NAT1 polymorphism status is not associated with increased risk to bladder, esophageal, prostate or gastric cancers (Kidd et al., 2011; McGrath et al., 2006; Wideroff et al., 2007). NAT1 has also been implicated in cell growth and survival. Studies have shown that overexpression of NAT1 increased density dependent cell proliferation, and knock-down of NAT1 resulted in marked change in cell morphology, an increase in cell-cell contact inhibition and a loss of cell viability at confluence (Adam et al., 2003; Tiang et al., 2011). *NAT1*4* is referred to as the referent allele because it was the most common allele in the population in which it was first identified (Vatsis and Weber, 1993). To date, 26 human *NAT1* alleles have been identified (http://louisville.edu/medschool/pharmacology/consensus-human-arylamine-n-acetyltransferase-gene-nomenclature/). Although the effects of *NAT1* polymorphisms on catalytic activity have been studied, the results are ambiguous. Within single NAT1 genotypes, conflicting phenotypes have been reported, and the relationship between phenotype and genotype remains poorly understood. Since factors other than genotype are likely affecting phenotype, it is important to understand transcriptional and translational control of *NAT1*.

The *NAT1* gene spans 53 kb and contains nine exons (Figure 2-1a). Several *NAT1* transcripts have been identified containing various combinations of 5'-untranslated region (UTR) exons and are known to originate from two distinct promoters, NATa and

NATb. NATb, the major promoter, is located 11.8 kb upstream of the open reading frame (ORF). NATb promotes transcription of Type II transcripts and the major transcript, Type IIA, has been detected in all tissues studied to date (Boukouvala and Sim, 2005; Husain et al., 2004). An alternative promoter, NATa, originates 51.5 kb upstream of the *NAT1* ORF and promotes transcription of Type I transcripts expressed primarily in kidney, lung, liver, and trachea (Barker et al., 2006; Boukouvala and Sim, 2005). The NAT1 gene is induced following exposure to androgens and NAT1 protein stability is affected by the presence of substrates (Minchin et al., 2007).

Recent analyses of genome-wide Pol II distribution in Drosophila and mammalian systems have reported that regulation of many genes occurs after transcription initiation (Aida et al., 2006; Nechaev et al., 2010) providing evidence for regulatory control in the 5'-UTR that is distinct from promoter regulatory control. Recent studies have shown that between 30-50% of all human genes utilize alternative promoters (Cooper et al., 2006; Takeda et al., 2007) to allow for cell, tissue and disease specific expression. To determine if differences in 5'-UTR have functional effect upon NAT1 activity, DNA adducts or mutations following exposure to ABP, pcDNA5/FRT plasmid constructs were prepared for transfection of full length human mRNAs including the 5'-UTR derived from NATa or NATb, the *NAT1*4* open reading frame, and 888 nucleotides of the 3'-UTR. The constructs were cloned into two expression vectors utilizing two different constitutive promoters, (CMV and the EF1α promoters) to examine regulatory control located in the 5'-UTR. The cells transfected with NATa/*NAT1*4* and NATb/*NAT1*4* constructs were characterized for NAT1 mRNA and protein expression, *N*- and *O*-acetyltransferase activity (*in vitro* and *in situ*), ABP-induced DNA adducts and *hypoxanthine phosphoribosyl transferase (hprt)* mutations following exposure to ABP.

METHODS

Polyadenylation Site Removal

The bovine growth hormone (BGH) polyadenylation site from the pcDNA5/FRT (Invitrogen, Carlsbad, CA) vector was removed to allow the endogenous *NAT1* polyadenylation sites to be active. This was accomplished by digestion at 37°C with restriction endonucleases, *ApaI* and *SphI* (New England Biolabs, Ipswich, MA), followed by overhang digestion with T4 DNA polymerase (Invitrogen) and ligation with T4 Ligase (Invitrogen).

NATb/*NAT1*4* and NATa/*NAT1*4* Constructs

NATb/*NAT1*4* and NATa/*NAT1*4* constructs were created utilizing gene splicing via overlap extension (Horton et al., 1989) by amplifying the 5'-UTR and the coding region/3'-UTR separately and then fusing the two regions together. Beginning with frequently used transcription start sites, the 5'-UTRs (Barker et al., 2006; Husain et al., 2004) were amplified from cDNA prepared from RNA isolated from homozygous *NAT1*4* HepG2 cells. All primer sequences used are shown in Table 1. The primers used to amplify the NATb 5'-UTR region were Lkm40P1 and NAT1 (3') ORF Rev while the primers used to amplify the NATa 5'-UTR region were Lkm41P1 and NAT1 (3') ORF Rev. The coding region and 3'-UTR were amplified as one piece from *NAT1*4* human genomic DNA with *NAT1*4/NAT1*4* genotype. The forward primer used to amplify the coding region/3'-UTR was NAT1 (3') ORF Forward while the reverse primer was pcDNA5distal Reverse. The two sections, the 5'-UTR and the coding region/3'UTR, were fused together via overlap extention and amplification of the entire product using nested primers. The forward nested primer for NATb was P1 Fwd Inr NheI while the forward nested primer for NATa was P3 Fwd Inr NheI. The reverse nested primer for both NATa

and NATb constructs was NAT1 Kpn Rev. Both forward nested primers included the *KpnI* endonuclease restriction site and both reverse nested primers contained the *NheI* endonuclease restriction site to facilitate cloning. The pcDNA5/FRT vector and NATa/*NAT1*4* and NATb/*NAT1*4* allelic segments were digested at 37^{0}C with restriction endonucleases *KpnI* and *NheI* (New England Biolabs). The *NAT1* constructs were then ligated into pcDNA5/FRT using T4 ligase (Invitrogen). These same *NAT1* constructs were also cloned into a second expression vector, pEF1/5V-His (Invitrogen). The NATb/*NAT1*4* construct was amplified using the forward primer, NATb Forward pEF1, while the NATa/*NAT1*4* construct was amplified using the forward primer NATa Forward pEF1. Both forward primers contained the *BamHI* restriction site. Both constructs were amplified using the reverse primer NATa/b Reverse pEF1 which contained the *EcoRV* restriction site. Both NATa/*NAT1*4* and *NATb/NAT1*4* and pEF1/5V-His were digested with the restriction endonucleases, *BamHI* and *EcoRV* (New England Biolabs), followed by ligation into the vector using T4 ligase (Invitrogen). All constructs were sequenced to ensure integrity of allelic segments and junction sites.

Cell Culture

UV5-CHO cells, a nuclease excision repair (NER)-deficient derivative of AA8 which are hypersensitive to bulky DNA lesions, were obtained from the ATCC (catalog number: CRL-1865). Unless otherwise noted, cells were incubated at 37□C in 5% CO_2 in complete alpha-modified minimal essential medium (α-MEM, Lonza, Walkersville, MD) without L-glutamine, ribosides, and deoxyribosides supplemented with 10% fetal bovine serum (Hyclone, Logan, UT), 100 units/mL penicillin (Lonza), 100 µg/mL streptomycin (Lonza), and 2 mM L-glutamine (Lonza). The UV5/CHO cells used in this study were previously stably transfected with a single Flp Recombination Target (FRT) integration site (Metry et al., 2007). The FRT site allowed stable transfecions to utilize the Flp-In

System (Invitrogen). When co-transfected with pOG44 (Invitrogen), a Flp recombinase expression plasmid, a site-specific, conserved recombination event of pcDNA5/FRT (containing either NATa/*NAT1*4* or NATb/*NAT1*4)* occurs at the FRT site. The FRT site allows recombination to occur immediately downstream of the hygromycin resistance gene, allowing for hygromycin selectivity only after Flp-recombinase mediated integration. The UV5/FRT cells were further modified by stable integration of human *CYP1A1* and NADPH-cytochrome P450 reductase gene (*POR*) (Metry et al., 2007). They are referred to in this manuscript as UV5/*1A1* cells.

Transient Transfection

UV5/*1A1* cells were transiently transfected with pcDNA5/FRT (Invitrogen) or pEF1/V5-His (Invitrogen) containing NATa/*NAT1*4* and NATb/*NAT1*4* constructs using Lipofectamine reagent (Invitrogen) following the manufacturer's recommendations. UV5/1A1 cells were co-transfected with pCMV-SPORT-βgal (β-galactosidase transfection control plasmid, Invitrogen). The cells were harvested the next day. Lysate was prepared by centrifuging the cells and resuspending pellet in homogenization buffer (20 mM $NaPO_4$ pH 7.4, 1 mM EDTA, 1 mM DTT, 0.1 mM PMSF, 2 μg/mL aprotinin and 2 mM pepstatin A). The resuspended cell pellet was subjected to 3 rounds of freezing at -80°C and thawing at 37°C and then centrifuged at 15,000xg for 10 min. The supernatant was used to measure *N*-acetyltransferase activity and β-galactosidase activity.

Stable Transfections

Stable transfections were carried out using the Flp-In System (Invitrogen) into UV5/*1A1* cells that were previously stably transfected with a FRT site (as noted above).

The pcDNA5/FRT plasmids containing human NATa/*NAT1*4* or NATb/*NAT1*4* were co-transfected with pOG44 (Invitrogen), a Flp recombinase expression plasmid. UV5/*1A1* cells were stably transfected with pcDNA5/FRT containing NATa/*NAT1*4* and NATb/*NAT1*4* constructs using Effectene transfection reagent (Qiagen, Valencia, CA) following the manufacturer's recommendations. Since the pcDNA5/FRT vector contains a hygromycin resistance cassette, cells were passaged in complete α-MEM containing 600 μg/mL hygromycin (Invitrogen) to select for cells containing the pcDNA5/FRT plasmid. Hygromycin resistant colonies were selected approximately 10 days after transfection and isolated with cloning cylinders.

Measurement of *N*-Acetyltransferase Enzymatic Activity

In vitro assays using the NAT1 specific substrate para-aminobenzoic acid (PABA) or 4-aminobiphenyl (ABP) were conducted and acetylated products were separated utilizing HPLC (Hein et al., 2006). Reactions containing 50 μL cell lysate, PABA or ABP (300 μM) and acetyl coenzyme A (1 mM) were incubated at 37˚C for 10 min. Reactions were terminated by the addition of 1/10 volume of 1M acetic acid and centrifuged at 15,000Xg for 10 min. Supernatant was injected into a (125 mm X 4 mm; 5 μM pore size) reverse phase C18 column. Reactants and products were eluted using a Beckman System Gold high performance liquid chromatograph (HPLC) system. HPLC separation of *N*-acetyl-PABA was achieved using a gradient of 96:4 sodium perchlorate pH 2.5:acetonitrile (ACN) to 88:12 sodium perchlorate pH 2.5: ACN over 3 min and was quantitated by absorbance at 280 nm. HPLC separation of *N*-acetyl-ABP was achieved using a gradient of 85:15 sodium perchlorate pH 2.5:ACN to 35:65 sodium perchlorate pH 2.5:ACN over 10 min and was quantitated by absorbance at 260 nm. Measurements were adjusted according to baseline measurements using lysates of the UV5/*CYP1A1* cell line. Both stably and transiently transfected cells were normalized by the amount of

total protein. Assays involving transiently transfected cells and PABA used β-galactosidase activity to control for transfection efficiency. To correct for transfection efficiency, β-galactosidase plasmids (pCMV-sport-βgal) were co-transfected with pcDNA5/FRT or pEF1/5V-His. β-galactosidase activity was measured in reactions containing 30 µL cell lysate, 70 µL of 4 mg/mL *ortho*-nitrophenyl-β-D-galactopyranoside (ONPG), and 200 µL of cleavage buffer (60 mM Na_2HPO_4, 40 mM NaH_2PO_4, and 1 mM $MgSO_4$, pH 7.0). The reaction was incubated for 30 min at 37°C. The reaction was terminated by the addition of 500 µL of 1 M sodium carbonate and absorbance at 420 nm was measured. Protein concentrations were measured using the method of Bradford (Bio-Rad, Hercules, CA). The β-galactosidase activities were normalized to total protein and the resulting values were used to correct for the effect of any differences in transfection efficiency. *In situ N*-acetyltransferase activity was studied in a whole cell assay using media spiked with differing concentrations of PABA (10 – 300 µM). The cells were incubated at 37°C and media was collected after 5 h, 1/10 volume of 1M acetic acid was added, and the mixture was centrifuged at 13,000xg for 10 min. The supernatant was injected into the reverse phase HPLC column and *N*-acetyl-PABA was separated and quantitated as described above.

Measurement of *O*-Acetyltransferase Enzymatic Activity

N-hydroxy-4-aminobiphenyl (*N*-OH-ABP) *O*-acetyltransferase assays were conducted as previously described (Metry et al., 2007). Assays containing 100 µg total protein, 1 mM acetyl coenzyme A, 1 mg/mL deoxyguanosine (dG), and 100 µM *N*-OH-ABP were incubated at 37°C for 10 min. Reactions were stopped with the addition of 100 µL of water saturated ethyl acetate and centrifuged at 13,000xg for 10 min. The organic phase was removed, evaporated to dryness and the residue was dissolved in 100 µL of 10% ACN. HPLC separation was achieved using a gradient of 80:20 sodium

perchlorate pH 2.5:ACN to 50:50 sodium perchlorate pH 2.5:ACN over 3 min and dG-C8-ABP adduct was detected at 300 nm.

Measurement of NAT1 Protein

The amount of NAT1 produced in UV5/*1A1* cells stably transfected with NATa/*NAT1*4* or NATb/*NAT1*4* was determined by western blot. Cell lysates were isolated as described above. Varying amounts of lysate were mixed 1:1 with 5% β-mercaptoethanol in Laemmli buffer (Bio-Rad), boiled for 5 min, and resolved by 12% SDS-PAGE. The proteins were then transferred by semi-dry electroblotting to polyvinylidene fluoride (PVDF) membranes. The membranes were probed with a polyclonal rabbit anti-hNAT1 ES195 (1:1000) kindly provided by Edith Sim (Stanley et al., 1996) and with horseradish peroxidase (HRP)-conjugated secondary goat anti-rabbit IgG antibody (1:20,000) (Pierce, Rockford, IL). Supersignal West Pico Chemiluminescent Substrate was used for detection (Pierce) and densitometric analysis was performed using Quantity One Software (Bio-Rad).

Measurement of NAT1 mRNA

Total RNA was isolated from cells using the RNeasy kit (Qiagen) followed by removal of contaminating DNA by treatment with TurboDNase Free (Ambion, Austin, TX). Synthesis of cDNA was performed using qScript cDNA Synthesis Kit (Quanta Biosciences, Gaithersburg, MD) using 1 μg of total RNA in a 20 μL reaction per the manufacturer's protocol. Quantitative RT-PCR (RT-qPCR) assays were used to assess the relative amount of *NAT1* mRNA in cells stably transfected with NATa/*NAT1*4* compared to cells stably transfected with NATb/*NAT1*4*. The Step One Plus (Applied Biosystems, Foster City, CA) was used to perform qRT-PCR in reactions containing 1x final concentration of qScript One-Step Fast mix (Quanta Biosciences), 300 nM of each

primer and 100 nM of probe in a total volume of 20 µL. For qRT-PCR of *NAT1* mRNA, a TaqMan probe was used with NAT1 Total Splice Forward and NAT1 Total Splice Reverse primers (Table 1) designed using Primer Express 1.5 software (Applied Biosystems). An initial incubation at 50°C was carried out for 2 min and at 94°C for 10 min followed by 40 cycles of 95°C for 15 seconds and 60°C for 1 minute. TaqMan® Ribosomal RNA Control Reagents for quantitation of the endogenous control, 18S rRNA, (Applied Biosystems) were used to determine ΔCt (*NAT1* Ct –18S rRNA Ct). ΔΔCt was determined by subtraction of the smallest ΔCt and relative amounts of *NAT1* mRNA were calculated using $2^{-\Delta\Delta Ct}$ as previously described (Barker et al., 2006).

Measurement of NAT1 mRNA Stability

Dishes (100 x 20 mm) containing 8 x 10^6 stably transfected NATa/*NAT1*4* and NATb/*NAT1*4* cells were treated with complete α-MEM media spiked with 10 ug/mL of the transcription inhibitor, Actinomycin D (Sigma, St. Louis, MO). Cells were collected at 0, 2, 4, 6, and 8 hour time points and total RNA was isolated as described above. Relative *NAT1* mRNA levels were determined from cells transfected with NATa/*NAT1*4* or NATb/*NAT1*4* utilizing qRT-PCR assays as described above. The first-order rate decay constant (slope) of *NAT1* mRNA was determined by linear regression.

DNA Isolation and dG-C8-ABP Quantitation

DNA was isolated and dG-C8-ABP adducts were quantitated with modifications to a previously described method (Metry et al., 2007). Cells grown to approximately 80% confluency in 15 cm dishes were incubated in complete α-MEM media containing 1.56, 3.13, 6.25, 12.5 µM ABP or vehicle alone (0.5% DMSO) at 37°C. The cells were collected following 24 h of treatment, centrifuged for 5 min at 13,000xg, and the pellet was resuspended in 2 volumes of homogenization buffer (20 mM sodium phosphate pH

7.4, 1 mM EDTA), 0.1 volumes of 10% SDS and 0.1 volume of 20 mg/mL Proteinase K and allowed to incubate overnight at 37□C. The DNA was extracted using phenol/chloroform:isoamyl alcohol and precipitated with isopropanol. The pellet was dried and resuspended in 500 µL of DNA adduct buffer (5 mM Tris pH 7.4, 1 mM $CaCl_2$, 1 mM $ZnCl_2$, and 10 mM $MgCl_2$). The DNA was quantitated by spectrophotometry at A_{260}. Five hundred pg of internal standard (dG-C8-ABP-d5, Toronto Research Chemicals, North York, Ontario, Canada) was added to 30 µg of sample DNA, treated with 10 units *DNase I* (US Biological, Swampscott, MA) for 1 h at 37°C followed by treatment with 10 units nuclease P1 (Sigma) for 6 h. The reactions were then treated with 10 units of alkaline phosphatase (Sigma) overnight at 37°C. The samples were then loaded onto PepClean C-18 Spin Columns (Thermo Fisher Scientific), washed with 10% acetonitrile (ACN), eluted with 50% ACN by centrifugation at 2000xg and dried. The samples were reconstituted with 25 µL 5% ACN in 2.5 mM NH_4HCO_3 just before analysis and 10 µL of the sample was analyzed by Accela LC System (Thermo Scientific, San Jose, CA) coupled with a LTQ-Orbitrap XL mass spectrometer (Thermo Scientific, San Jose, CA). Samples were loaded onto a 30 × 1mm × 1.9 µm Hypersil GOLD column (Thermo Scientific, San Jose, CA) and eluted with a 12.5 minute binary solvent gradient (Solvent A: 5% ACN/0.1% formic acid and Solvent B: 95% ACN/0.1% formic acid) at 50 µl/min. The gradient started from 5% Solvent B, increased linearly to 75% Solvent B in 10 min, and then remained at 75% B for 2.5 min. The eluates were ionized by electrospray isonization and dG-C8-ABP and dG-C8-ABP-d5 were detected with linear ion trap and detected by multiple reaction monitoring using the transitions of m/z 435.2 to m/z 319.2 (dG-C8-ABP) and m/z 440.2 to m/z 324.2 (dG-C8-ABP-d5). Concentrations of dG-C8-ABP were calculated from peak areas of dG-C8-ABP and dG-C8-ABP-d5 with a calibration curve from synthetic dG-C8-ABP and dG-C8-ABP-d5.

Measurement of Cytotoxicity and Mutagenesis

Assays for cell cytoxicity and mutagenesis were carried as previously described (Wu et al., 1997) with slight modifications. Cells were grown in HAT medium (30 mM hypoxanthine, 0.1 mM aminopterin, and 30 mM thymidine) for 12 doublings. Cells ($1x10^6$) were plated, allowed to grow for 24 h and were then treated with 1.56, 3.13, 6.25 or 12.5 μM ABP (Sigma) or vehicle alone (0.5% DMSO) in media. After 48 h, cells were plated to determine survival and mutagenic response to ABP. To determine cloning efficiency following each dose of ABP, 100 cells were plated in triplicate in 6 well-plates and allowed to grow for 7 days in non-selective media. Colonies were counted and expressed as percent of vehicle control. To determine mutagenic response following ABP exposure, $5x10^5$ cells were plated and sub-cultured for 7 days and then seeded with $1x10^5$ cells/100 x 20 mm dish (10 replicates) in complete αMEM containing 40 mM 6-thioguanine (Sigma). Mutant *hprt* cells were allowed to grow for 7 days and colonies were counted to determine ABP-induced mutants and corrected by cloning efficiency.

Statistical Analysis

Statistical differences were determined using either an unpaired student's t-test or one-way ANOVA using Prism Software by Graphpad (La Jolla, CA).

RESULTS

PABA *N*-Acetylation Following Transfection of NATb/*NAT1*4* or NATa/*NAT1*4*

PABA *N*-acetylation activity was 9- to 12-fold ($p<0.05$) higher in CHO cells transfected with NATb/*NAT1*4* than NATa/*NAT1*4* following both transient and stable transfections (Figure 2-2 a,b) utilizing the CMV promoter. Figure 2-2b shows average PABA *N*-acetylation for 3 stable clones of each NATb/*NAT1*4* and NATa/*NAT1*4.* One clone representative was selected from each group to conduct all further assays. To ensure that the difference was not promoter specific, *N*-acetylation activity was also measured following transfection with constructs utilizing the EF1α promoter. PABA *N*-acetylation activity was 6-fold ($p<0.0001$) higher in CHO cells transiently transfected with NATb/*NAT1*4* than NATa/*NAT1*4* (Figure 2-2c) utilizing the EF1α promoter. To more accurately model *in vivo N*-acetylation and to confirm the *in vitro* results, an *in situ* assay was performed using PABA as the substrate in a dose response experiment (Figure 2-2d). The *in situ* assay showed that significantly ($p<0.05$) more PABA *N*-acetylation activity was observed in cells stably transfected with NATb/*NAT1*4* than NATa/*NAT1*4* at all concentrations tested (Figure 2-2d) utilizing the CMV promoter. As shown in figure 2-3, PABA *N*-acetylation activity also was significantly higher in COS-1 cells transiently transfected with NATb/*NAT1*4* than with NATa/*NAT1*4* utilizing either the CMV ($p<0.005$) or EF1α ($p<0.0001$) promoters.

ABP *N*-Acetylation and *N*-hydroxy-ABP *O*-acetylation Following Transfection of NATb/*NAT1*4* or NATa/*NAT1*4*

Cells stably transfected with NATb/*NAT1*4* were found to have 7-fold ($p<0.0001$) higher ABP *N*-acetylation activity than cells stably transfected with NATa/*NAT1*4* (Figure 2-4a) utilizing the CMV promoter. *O*-acetyltransferase activity using *N*-OH-ABP as the substrate also was found to be 7-fold ($p<0.05$) higher in cells stably transfected with NATb/*NAT1*4* than NATa/*NAT1*4* (Figure 2-4b) utilizing CMV promoter.

Expression of NAT1 Protein Following Transfection of NATb/*NAT1*4* or NATa/*NAT1*4*

NAT1 expression was determined by western blot in cells stably transfected with NATb/*NAT1*4* and NATa/*NAT1*4* utilizing the CMV promoter. Four-fold ($p<0.05$) more NAT1 was found in cells stably transfected with NATb/*NAT1*4* than cells transfected with NATa/*NAT1*4* following densitometric analysis (Figure 2-5).

Expression of NAT1 mRNA Following Transfection of NATb/*NAT1*4* or NATa/*NAT1*4*

As shown in Figure 2-6a, 4-fold more NAT1 mRNA was detected in cells stably transfected with NATb/*NAT1*4* than in cells transfected with NATa/*NAT1*4* ($p<0.05$) utilizing the CMV promoter. To determine the cause of the difference in NAT1 steady-state mRNA between cells stably transfected with NATb/*NAT1*4* and in cells transfected with NATa/*NAT1*4*, an mRNA stability assay was performed in the presence of actinomycin-D. No significant ($p>0.05$) difference in the NAT1 mRNA first-order decay constant was observed between NAT1 mRNA derived from cells stably transfected with NATb/*NAT1*4* versus NATa/*NAT1*4* (Figure 2-6b).

Cytoxicity, dG-C8-ABP Adduct and *hprt* Mutations from ABP in UV5/*1A1* Cells Stably Transfected With NATb/*NAT1*4* or NATa/*NAT1*4*

CYP1A1 mediated hydroxylation and NAT1 *O*-acetylation result in DNA adducts and mutations, if not repaired. Significantly ($p<0.05$) greater cytoxicity (Figure 2-7a), dG-C8-ABP adducts (Figure 2-7b) and *hprt* mutants (Figure 2-7c) were detected in cells stably transfected with NATb/*NAT1*4* than NATa/*NAT1*4* utilizing the CMV promoter at each ABP concentration tested up to 12.5 μM.

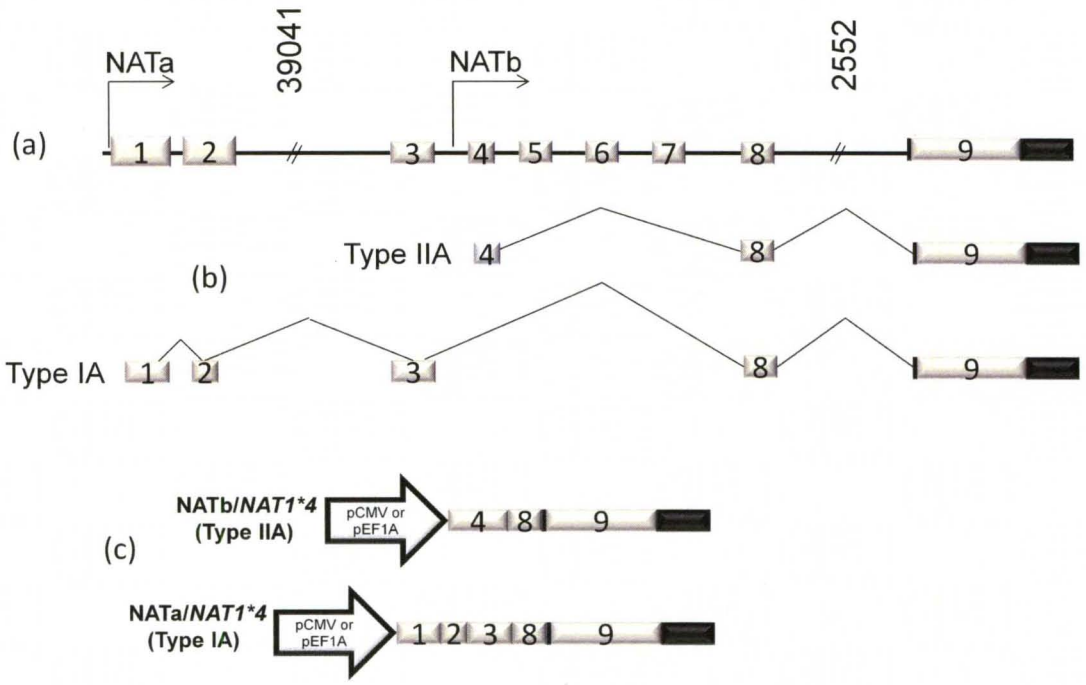

Figure 2-1: Genomic Organization of NAT1 gene

(a) Genomic organization of NAT1 gene; (b) Type IIA and Type IA NAT1 RNA (c) and representative NATb/*NAT1*4* and NATa/*NAT1*4* constructs. (modified from 41).

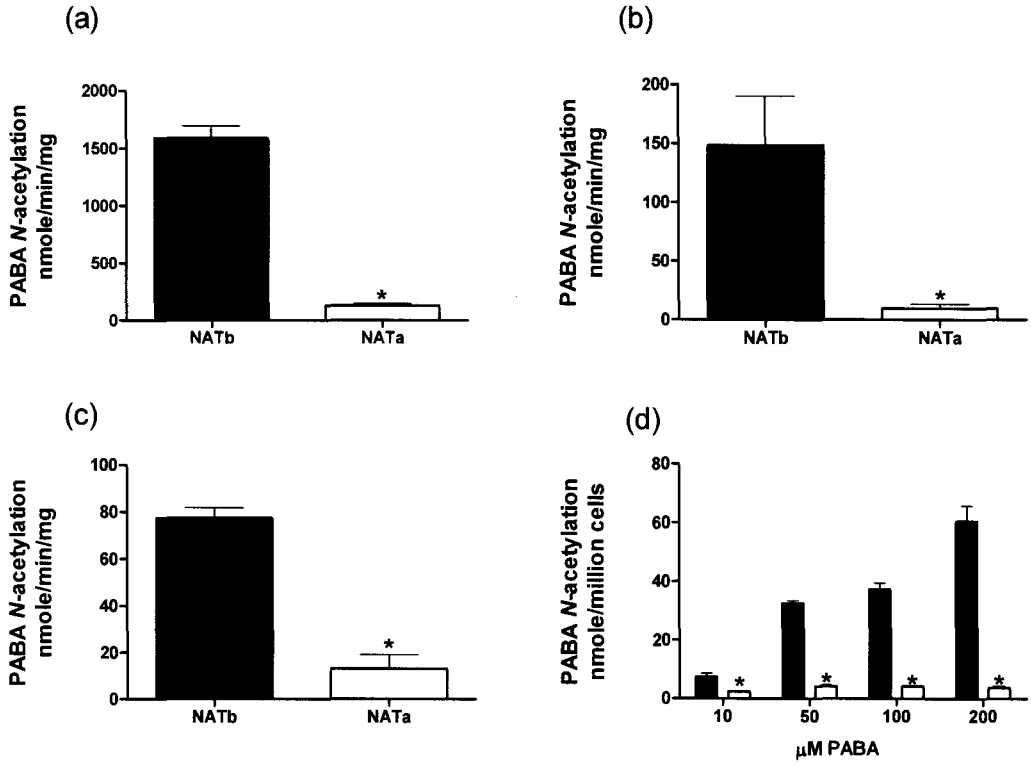

Figure 2-2: NATb and NATa *N*-acetylation of PABA

N-acetylation of PABA in UV5/1A1 cells expressing *CYP1A1* and NATb/*NAT1*4* (solid bars) or NATa/*NAT1*4* (open bars). (a) PABA *N*-acetylation activity following transient transfection with pcDNA5/FRT; (b) PABA NAT1 catalytic activity following stable transfection with pcDNA5/FRT of 3 different clones of each NATb/*NAT1*4* and NATa/*NAT1*4*; (c) PABA *N*-acetylation activity following transient transfection with pEF1/V5-His; (d) PABA *N*-acetylation *in situ* following stable transfection of pcDNA5/FRT. Each bar represents mean ± S.E.M. for three transient transfections (a, c), 3 separate collections of 3 clones (b) or 3 separate collections of 1 clone (d). Asterisks (*) represent a significant difference ($p<0.05$) (a, b, d) or ($p<0.0001$) (c) following a student's t-test.

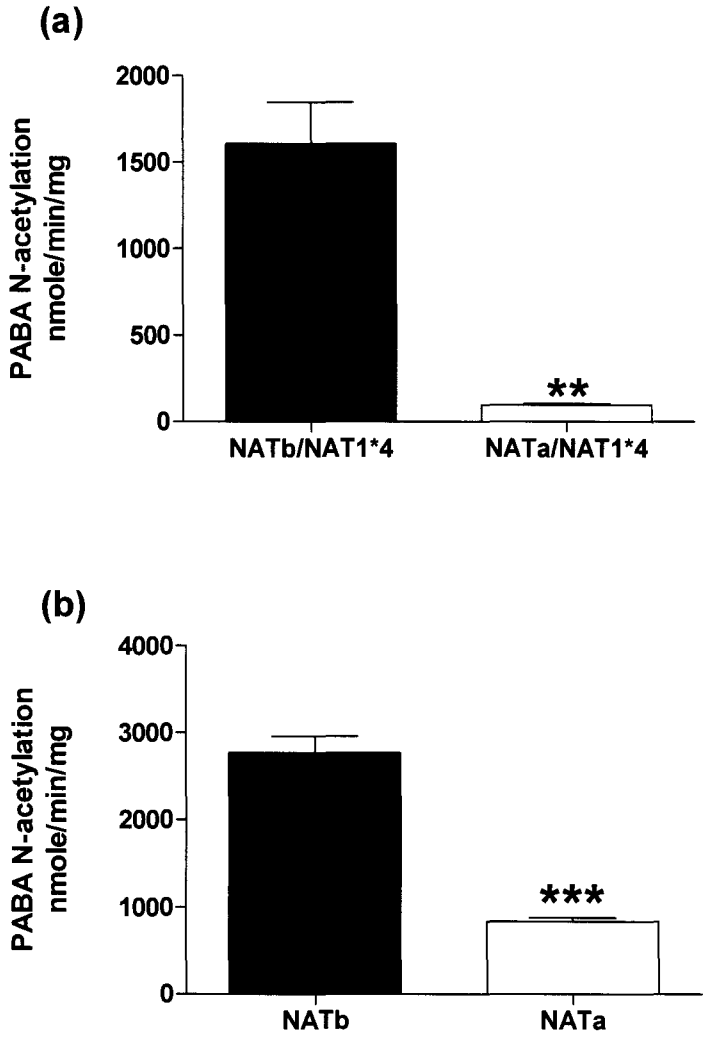

Figure 2-3: NATb and NATa N-acetylation of PABA in COS-1 cells

N-acetylation of PABA in COS-1 cells transiently transfected with (a) pcDNA5/FRT or pEF1/V5-His (b) containing NATb/*NAT1*4* or NATa/*NAT1*4*. Each bar represents mean ± S.E.M. for three transient transfections. Asterisks represent a significant difference either ($p<.005$) (a) or ($p<.0001$) (b) following a student's t-test.

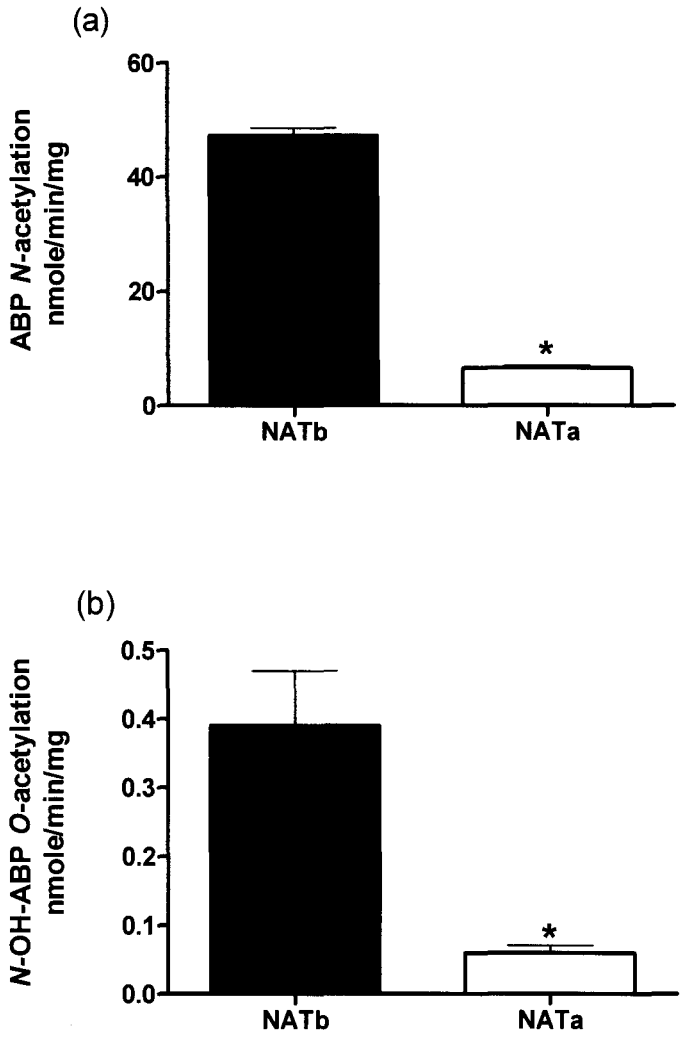

Figure 2-4: NATb and NATa *N*- and *O*-acetylation of ABP

(a) *N*-acetylation of ABP and (b) *O*-acetylation of *N*-hydroxy-ABP in UV5/1A1 cells stably expressing *CYP1A1* and either NATb/*NAT1*4* (solid bars) or NATa/*NAT1*4* (open bars) in pcDNA5/FRT. Each bar represents mean ± S.E.M. for three separate collections. Asterisks (*) represent a significant difference ($p<0.0001$) (a) or ($p<0.05$) (b) following a student's t-test.

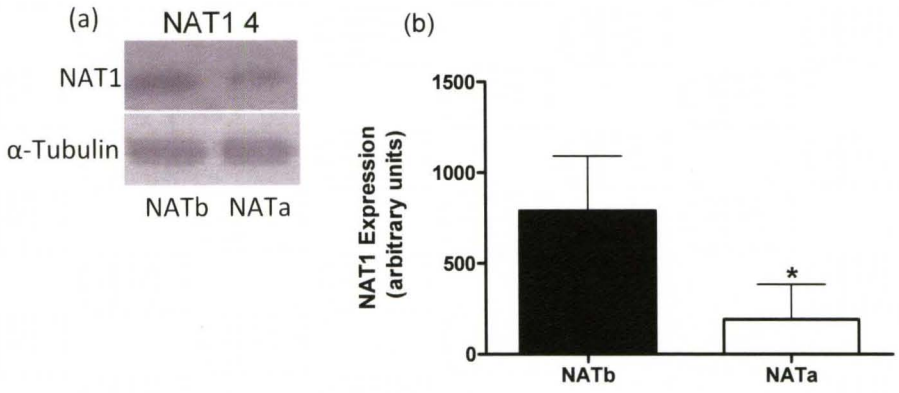

Figure 2-5: NATb and NATa protein expression

NAT1 protein expression in UV5/1A1 cells stably expressing *CYP1A1* and NATb/*NAT1*4* (solid bars) or NATa/*NAT1*4* (open bars) in pcDNA5/FRT. (a) Representative western blot of 20 µg of total protein loaded; (b) Percent intensity units (NATb defined as 100%) of densitometric analysis perfomed on three independent Western blots. Asterisks (*) represent a significant difference ($p<0.05$) following a student's t-test.

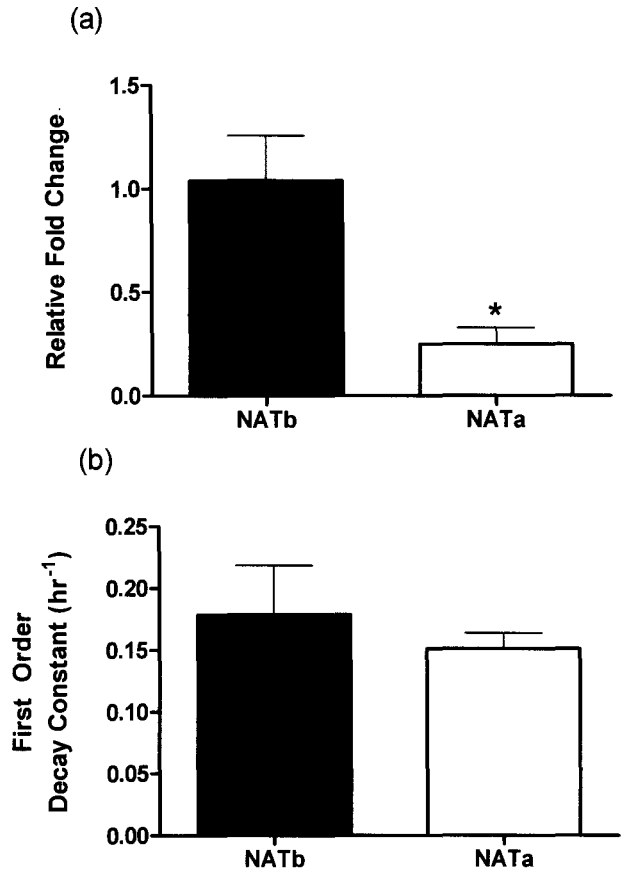

Figure 2-6: NATb and NATa mRNA levels

(a) NAT1 mRNA expression levels; (b) mRNA stability in UV5/1A1 cells stably expressing *CYP1A1* and NATb/*NAT1*4* (solid bars) or NATa/*NAT1*4* (open bars) in pcDNA5/FRT. Each bar represents mean ± S.E.M. for (a) three or (b) nine determinations. Asterisks (*) represent a significant difference ($p<0.05$) following a student's t-test.

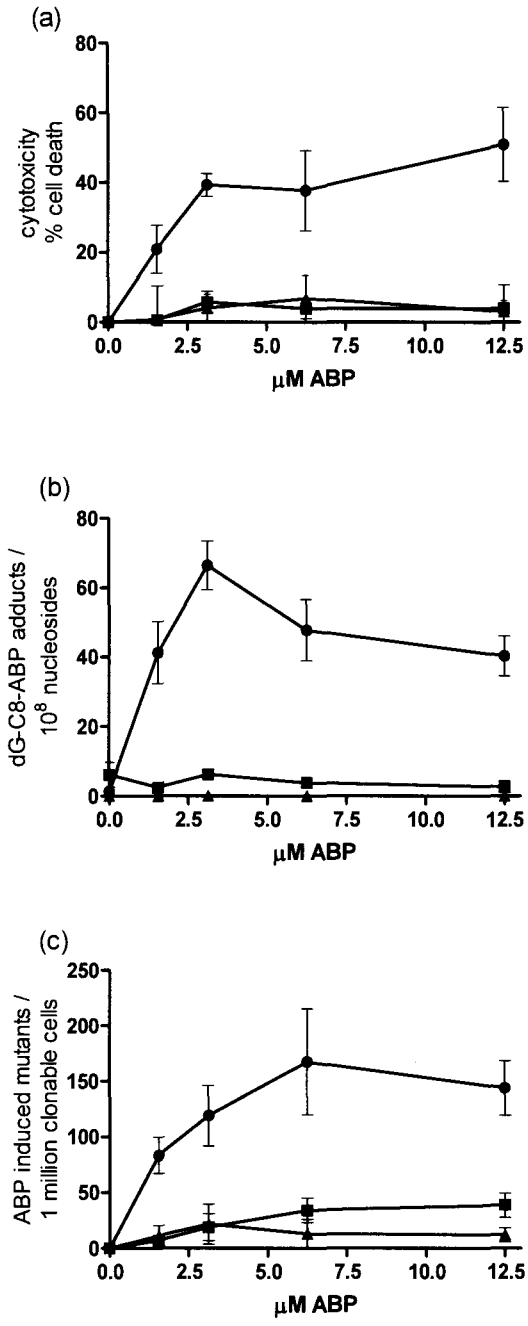

Figure 2-7: ABP-induced cytoxicity, mutagenesis and DNA adducts

ABP-induced cytotoxicity, mutagenesis, and DNA adduct formation in CHO cells stably expressing *CYP1A1* only (triangles) and NATb/*NAT1*4* (circles) or NATa/*NAT1*4* (squares) in pcDNA5/FRT. Each data point represents mean ± S.E.M. for three determinations. (a) ABP-induced cytotoxicity; (b) ABP-induced dG-C8-ABP adducts/10^8 nucleosides; (c) ABP-induced *hprt* mutant levels.

DISCUSSION

As outlined in the introduction, numerous studies report that *NAT1* genetic polymorphisms increase cancer risk following exposure to heterocyclic and aromatic amines. Due to the large variability in NAT1 activity that has been reported within a single genotype, it is becoming increasingly more apparent that factors other than genetic polymorphisms are affecting gene expression and cancer risk. One such factor is the use of alternative promoters to produce mRNAs with distinct 5'-UTRs. Recent studies have shown that between 30-50% of all human genes utilize alternative promoters (Cooper et al., 2006; Takeda et al., 2007) to allow for cell, tissue and disease specific expression. *NAT1* has two promoters, NATa and NATb, which differ in promoter strength and tissue specificity (Barker et al., 2006; Husain et al., 2007). Transcripts derived from NATa are found primarily in liver, lung, trachea and kidney, while transcripts derived from NATb are found in all tissues studied to date (Barker et al., 2006; Husain et al., 2007). It is possible that NATa transcripts are expressed in a wider range of tissues, but only when the cell is under specific environmental stress or disease states. For example, expression of NATa transcripts has recently been reported in several ER-positive breast cancer cell lines (Wakefield et al., 2008). NATa transcripts may be selectively up-regulated following certain environmental exposures or in specific tissues, such as breast, during certain disease states.

In the current study, two referent *NAT1*4* constructs were cloned to mimic the most common transcripts originating from each of the two alternative *NAT1* promoters, NATa and NATb (Figure 3-1a). Beginning with frequently used transcription start sites, the constructs include all exons found in the most common *NAT1* transcripts originating at the NATa or NATb promoters and represent Type Ia or Type IIa transcripts (Barker et al., 2006; Butcher et al., 2005; Husain et al., 2004). The NATa/*NAT1*4* and

NATb/*NAT1*4* constructs have identical open reading frames (ORFs) and 3'-UTRs. Both constructs include the entire ORF comprised of 870 nucleotides and 888 nucleotides of the 3'-UTR. The only difference between the two constructs is the 5'-UTR. The NATb 5'-UTR contains 117 nts and includes exon 4 and exon 8 while the NATa 5'-UTR contains 371 nts and includes exons 1, 2, 3, and 8 (Figure 3-1b, c).

Two constitutive promoters, the CMV and the EF1α promoter, were used to drive transcription of either the NATb/*NAT1*4* or NATa/*NAT1*4* full length transcripts to examine regulatory control located in the 5'-UTRs. In this study, we report that cells transfected with NATb/*NAT1*4* had approximately 4-times greater NAT1 expression than cells transfected with NATa/*NAT1*4*. A 4-fold difference in NAT1 mRNA expression also was observed, suggesting that transcriptional control is largely responsible for the functional differences observed between NATb/*NAT1*4* and NATa/*NAT1*4*. Recent studies have elucidated a large number of tissue- and cell-type specific isoforms of transcription factors and cis-acting factors. Alternative 5'-UTRs contribute to this intricate control of transcription allowing for very specific altered expression in tissues, cells and even disease states (Davuluri et al., 2008). The differences we observed were not caused by a specific interaction between the promoter and one of the 5'-UTRs because results were confirmed using two different constitutive promoters, CMV and EF1α.

There are many regulatory mechanisms that could be responsible for the observed differences in expression and functional effects including polymerase pausing, microRNA binding, and the presence of upstream open reading frames and stem loops. A recent genome wide study has provided evidence that many genes are controlled after transcription initiation has occurred (Nechaev et al., 2010) and another such study

reveals that polymerase pausing may be a widespread genetic control of gene expression (Core et al., 2008). Elongation of transcription is known to be non-uniform and RNA polymerases are prone to transient pausing that is sequence dependent (Adelman et al., 2002). Polymerase pausing could be examined in the NATa- and NATb-transfected cell lines by nuclear run-on or RIP-chip assays. A second possible mechanism of regulation is microRNA (miRNA) binding which regulates gene expression by catalyzing mRNA cleavage (Ambros, 2004; Doench and Sharp, 2004). MicroInspector (miRNA target software) predicted only 2 miRNA binding sites in the NATb 5'-UTR located at positions 7 (has-miR-3937) and 46 (has-miR-198) while 54 miRNA binding sites were predicted throughout the NATa 5'-UTR. Regulation by these miRNAs could be analyzed by such methods as northern hybridization or microarray analysis. A third possible mechanism is regulation by upstream open reading frames (uORFs) which have been shown to reduce protein and mRNA expression (Calvo et al., 2009). Both NATa and NATb 5'-UTRs were examined for uORFs by the NCBI ORF Finder. The NATa 5'-UTR was predicted to have 2 uORFs, while the NATb 5'-UTR was predicted to have none. Studies including a luciferase reporter assay could be conducted to determine the transcriptional effects on the NATa 5'-UTR due to uORFs. Lastly, differential regulation of the NATa and NATb 5'-UTRs could be due to the presence of stem-loops (Malys and McCarthy, 2011). NATa and NATb 5'-UTRs were both examined for the presence of stem-loops by OligoCalc (Northwestern University, Evanston, IL) with a constraint of 5 base pair minimum. The NATa 5'-UTR has 42 potential stem-loop structures while the NATb 5'-UTR has only 7 potential stem-loop structures. Real time observation of transcription initiation and elongation (Larson et al., 2011) could be useful to determine the mechanism of the differential regulation observed between NATa and NATb 5'-UTRs.

Significantly more NAT1 activity, protein, mRNA, ABP-induced cytoxicity, DNA adducts and mutagenesis were detected in cells stably transfected with NATb/*NAT1*4* than in cells transfected with NATa/*NAT1*4* ($p<0.05$). DNA adduct and mutant levels following exposure to ABP are biological endpoints that are very relevant to cancer risk. The findings that ABP-mediated DNA adduct and mutant levels were significantly higher in cells transfected with elevated NAT1 catalytic activity emphasizes the relative importance of NAT1-catalyzed *O*-acetylation of *N*-hydroxy-ABP in cancer risk. Associations between higher N-acetyltransferase 2 catalytic activity with higher ABP-mediated cytoxicity, DNA adduct formation, and mutagenesis also were recently reported (Bendaly et al., 2009). The finding that these cancer risk indicators were higher in cells transfected with NATb/*NAT1*4* than cells transfected with NATa/*NAT1*4* suggest that differential regulation in the *NAT1* 5'-UTR also may modify ABP-mediated cancer risk. Because NATb transcripts are expressed ubiquitously, the minor transcript, NATa, may be expressed following environmental exposures or under certain disease states resulting in increased mutagenesis, enhanced tumor growth, and decreased chemotherapeutic sensitivity. For example, expression of NATa transcripts have recently been reported in several ER-positive breast cancer cell lines (Wakefield et al., 2008).

The findings of this study are significant due to their relevance to ABP-mediated carcinogenesis. However, translation of our results obtained in cell culture to human subjects will require additional studies to investigate tissue specificity. Although our study focused only on the referent allele, *NAT1*4,* future studies should investigate 5'-UTR control with other *NAT1* alleles, particularly those associated with increased cancer risk. Future investigations to determine mechanism(s) and location(s) of the differential regulation in the NAT1 5'-UTR also are needed.

CHAPTER 3

PHENOTYPE OF THE MOST COMMON "SLOW ACETYLATOR" ARYLAMINE *N*-ACETYLTRANSFERASE 1 GENETIC VARIANT (*NAT1*14B*) IS SUBSTRATE DEPENDENT

INTRODUCTION

Human arylamine *N*-acetyltransferase 1 (NAT1) is a phase II cytosolic enzyme responsible for the biotransformation of many arylamine compounds including pharmaceuticals and environmental carcinogens (Hein et al., 2000). NAT1 catalyzes both arylamine *N*-acetylation and *O*-acetylation. Genetic polymorphisms in NAT1 can alter the amount of NAT1 protein and result in modified enzymatic activity. In addition to bioactivation of arylamines, recent studies have provided evidence that NAT1 is involved in density dependent cell growth and survival. Studies have shown that overexpression of NAT1 increased density dependent cell proliferation, whereas knock-down of NAT1 resulted in marked change in cell morphology, an increase in cell-cell contact inhibition and a loss of cell viability at confluence (Adam et al., 2003; Tiang et al., 2011). Molecular epidemiological studies have reported associations between NAT1 genetic polymorphisms and altered risk for developing several types of cancer including urinary bladder (Gago-Dominguez et al., 2003), breast (Ambrosone et al., 2007; Millikan et al., 1998; Zheng et al., 1999), colorectal (Bell et al., 1995b; Lilla et al., 2006), lung (Wikman et al., 2001), non-Hodgkin lymphoma (Morton et al., 2006) and pancreatic (Li et al., 2006). The only known endogenous NAT1 substrate is p-aminobenzoylglutamate

(PABG), a catabolite of folate. late (Wakefield et al., 2007). *NAT1* has been associated with various birth defects (Jensen et al., 2005; Lammer et al., 2004) that may be related to deficiencies in folate metabolism. The most common NAT1 variant allele associated with reduced acetylator phenotype is *NAT1*14B.* The allelic frequency for *NAT1*14*B in the Lebanese population was determined to be 23.8% (Dhaini and Levy, 2000). *NAT1*14B* is likely to be very prevalent in other countries in the middle east, however allelic frequencies for many of those populations are not available. *NAT1*14B* has been associated with an increased risk of smoking-induced lung cancer (Bouchardy et al., 1998).

*NAT1*14B* is characterized by a single nucleotide polymorphism (SNP) G560A (rs4986782) located in the open reading frame (ORF). G560A results in an amino acid substitution R187Q. Computational homology modeling based on the NAT1 crystal structure indicate that the side chain of R187 is partially exposed to the domain II beta barrel, the protein surface, and the active site pocket (Walraven et al., 2008). Interactions with these domains serve to stabilize the protein and help shape the active site pocket. The substitution of arginine for glutamine results in at least partial loss of these stabilizing hydrogen bonds resulting in destabilization of the NAT1 structure. Therefore, homology modeling predicts that NAT1 binding of acetyl coenzyme A (AcCoA), active site acetylation, substrate specificity and catalytic activity could be affected by the R187Q substitution (Walraven et al., 2008).

Previous studies have reported *NAT1*14B* to be associated with a reduced *N*-acetylation phenotype. For example, in peripheral blood mononuclear cells, NAT1 14B was reported to result in reduced *N*-acetyltransferase activities and protein levels (Hughes et al., 1998). Recombinant NAT1 14B expression in yeast demonstrated reduced *N*- and *O*-acetylation, protein levels and increased proteasomal degradation (Butcher et al., 2004; Fretland et al., 2001; Fretland et al., 2002). NAT1 14 expressed in

mammalian cells also resulted in decreased in reduced V_{max} but increased substrate K_m towards p-aminobenzoic acid (PABA).

Modifications in NAT1 protein activity are biologically relevant because formation of DNA adducts, tumor growth and drug resistance could be altered by differences in enzymatic activity. This study reports findings in constructs that completely mimic NAT1 mRNA by including the 5'- and 3'-UTRs and ORF of the referent, *NAT1*4,* and of the most common allele associated with reduced acetylation, *NAT1*14B*. This report describes NAT1 14B *N*- and *O*-acetylation of the urinary bladder carcinogen 4-aminobiphenyl (ABP). Initial pilot experiments were conducted following recombinant expression in yeast (*Schizosaccaromyces pombe*) followed by more detailed studies utilizing recombinant expression in Chinese hamster ovary (CHO) cells. ABP is a confirmed bladder carcinogen (Feng et al., 2002) and strict federal regulations have banned industrial uses of ABP (IARC, 1987). However, ABP can still be found as a contaminant in color additives, paints, food colors, leather, textile dyes, diesel-exhaust particles, cooking oil fumes and commercial hair dyes (Nauwelaers et al., 2011). Mainstream cigarette smoke has been reported to contain up to 23 ng per cigarette and sidestream smoke has been reported to contain up to 140 ng per cigarette (Hoffmann et al., 1997).

METHODS

Experiments in Yeast

In situ N-acetylation following recombinant expression of human NAT1 in yeast

The ORFs of *NAT1*14B* and *NAT1*4* were recombinantly expressed in the pESP-3 yeast (*Schizosaccaromyces pombe*) expression system (Stratagene, La Jolla, CA). They were cultured in YES media (Teknova, Hollister, CA, 0.5% yeast extract, 3.0% glucose, 0.0225% adenine, 0.0225% histidine, 0.0225% leucine, 0.0225% uracil, and 0.0225% lysine) and grown to an optical density (OD) of 0.40. Aliquots (10 mL) from both the *NAT1*4* and *NAT1*14B* expressing cultures were each treated with ABP to make total volume concentrations of 10, 50 and 100 µM ABP. Samples (100 µl) were collected following 30 minute incubation with ABP.

Acetyl-ABP was separated and quantitated by HPLC as described previously (Hein et al., 2006).

Experiments in CHO cells

Polyadenylation site removal

The bovine growth hormone (BGH) polyadenylation site from the pcDNA5/FRT (Invitrogen, Carlsbad, CA) vector was removed to allow the endogenous *NAT1* polyadenylation sites to be active. This was accomplished by digestion of pcDNA5/FRT at 37°C with restriction endonucleases, ApaI and SphI (New England Biolabs, Ipswich, MA), followed by overhang digestion with T4 DNA polymerase (New England Biolabs) and ligation with T4 Ligase (New England Biolabs).

Preparation of NATb/*NAT1*4* construct

NATb/*NAT1*4* construct was created utilizing gene splicing via overlap extension (Horton et al., 1989) by amplifying the 5'-UTR and the coding region/3'-UTR separately

and then fusing the two regions together. Beginning with a frequently used transcription start site of the NATb promoter, the 5'-UTR (Barker et al., 2006; Husain et al., 2004) was amplified from cDNA prepared from RNA isolated from homozygous *NAT1*4* HepG2 cells. All primer sequences used are shown in Table 1. The primers used to amplify the NATb 5'-UTR region were Lkm40P1 and NAT1 (3') ORF Rev. The coding region and 3'-UTR were amplified as one piece from *NAT1*4* human genomic DNA with *NAT1*4/NAT1*4* genotype. The forward primer used to amplify the coding region/3'-UTR was NAT1 (3') ORF Forward while the reverse primer was pcDNA5distal Reverse. The two sections, the 5'-UTR and the coding region/3'UTR, were fused together via overlap extention and amplification of the entire product using nested primers. The forward nested primer was P1 Fwd Inr NheI and the reverse nested primer was NAT1 Kpn Rev. The forward nested primer included the KpnI endonuclease restriction site and the reverse nested primer contained the NheI endonuclease restriction site to facilitate cloning. The pcDNA5/FRT vector and NATb/*NAT1*4* allelic segments were digested at 37^0C with restriction endonucleases KpnI and NheI (New England Biolabs). The NATb/*NAT1*4* construct was then ligated into pcDNA5/FRT using T4 ligase (New England Biolabs).

Preparation of NATb/*NAT1*14B*

To construct the NATb/*NAT1*14B* pcDNA5/FRT plasmid, the NATb/*NAT1*4* pcDNA5/FRT and a previously constucted *NAT1*14B* allelic contruct expressed in a yeast vector, pESP-3 (Stratagene, La Jolla, CA) (Fretland et al., 2001), were both incubated at 37^0 with restriction enzymes, SbfI and AflII (NEB). Following restriction digestion, the NATb/*NAT1*4* pcDNA5/FRT and the 476 bp segment of *NAT1*14B* (including G560A) were gel purified and ligated utilizing T4 ligase (New England Biolabs). All constructs were sequenced to ensure integrity of allelic segments and

junction sites. These constructs that contain NATb 5'-UTR, coding region of *NAT1*4* or *NAT1*14B*, and 3'-UTR are illustrated in Figure 3-1 and referred to as *NAT1*4* and *NAT1*14B* throughout this manuscript.

Cell culture

UV5-CHO cells, a nuclease excision repair (NER)-deficient derivative of AA8 which are hypersensitive to bulky DNA lesions, were obtained from the ATCC (catalog number: CRL-1865). Unless otherwise noted, cells were incubated at 37^0C in 5% CO_2 in complete alpha-modified minimal essential medium (α-MEM, Lonza, Walkersville, MD) without L-glutamine, ribosides, and deoxyribosides supplemented with 10% fetal bovine serum (Hyclone, Logan, UT), 100 units/mL penicillin (Lonza), 100 µg/mL streptomycin (Lonza), and 2 mM L-glutamine (Lonza). The UV5/CHO cells used in this study were previously stably transfected with a single Flp Recombination Target (FRT) integration site (Metry et al., 2007). The FRT site allowed stable transfections to utilize the Flp-In System (Invitrogen). When co-transfected with pOG44 (Invitrogen), a Flp recombinase expression plasmid, a site-specific, conserved recombination event of pcDNA5/FRT (containing either NATa/*NAT1*4* or NATb/*NAT1*4)* occurs at the FRT site. The FRT site allows recombination to occur immediately downstream of the hygromycin resistance gene, allowing for hygromycin selectivity only after Flp-recombinase mediated integration. The UV5/FRT cells were further modified by stable integration of human *CYP1A1* and NADPH-cytochrome P450 reductase gene (*POR*) (Metry et al., 2007). They are referred to in this manuscript as UV5/*1A1* cells.

Stable transfections

Stable transfections were carried out using the Flp-In System (Invitrogen) into UV5/*1A1* cells that were previously stably transfected with a FRT site (as noted above). The pcDNA5/FRT plasmids containing human NATb/*NAT1*4* or NATb/*NAT1*14B* were co-transfected with pOG44 (Invitrogen), a Flp recombinase expression plasmid. UV5/*1A1* cells were stably transfected with pcDNA5/FRT containing NATb/*NAT1*4* and NATb/*NAT1*14B* constructs using Effectene transfection reagent (Qiagen, Valencia, CA) following the manufacturer's recommendations. Since the pcDNA5/FRT vector contains a hygromycin resistance cassette, cells were passaged in complete α-MEM containing 600 μg/mL hygromycin (Invitrogen) to select for cells containing the pcDNA5/FRT plasmid. Hygromycin resistant colonies were selected approximately 10 days after transfection and isolated with cloning cylinders.

Determination of *in vitro* (in-solution biochemistry) kinetic parameters of *N*-acetylation for NAT1 4 and NAT1 14B

Lysate was prepared by centrifuging the cells and resuspending pellet in homogenization buffer (20 mM $NaPO_4$ pH 7.4, 1 mM EDTA, 1 mM DTT, 0.1 mM PMSF, 2 μg/mL aprotinin and 2 mM pepstatin A). The resuspended cell pellet was subjected to 3 rounds of freezing at -80°C and thawing at 37°C and then centrifuged at 15,000xg for 10 min. *In vitro* assays using PABA or ABP were conducted and acetylated products were separated utilizing HPLC as previously described (Hein et al., 2006). Preliminary studies optimized reactions with respect to linearity of time and protein concentration. PABA and ABP kinetic constants were determined at a fixed concentration of 100 μM acetyl coenzyme A (AcCoA). PABA kinetic constants were determined using varying PABA concentrations between 11.7 – 3000 μM. ABP kinetic constants were determined

using varying ABP concentrations between 11.7 – 3000 μM. Reactions containing substrate, AcCoA and enzyme were incubated at 37°C for 10 min. Reactions were terminated by the addition of 1/10 volume of 1M acetic acid and centrifuged at 15,000Xg for 10 min. Measurements were adjusted according to baseline measurements using lysates of the UV5/*CYP1A1* cell line and normalized by the amount of total protein. Protein concentrations were measured using the method of Bradford (Bio-Rad, Hercules, CA). V_{max}, K_m, and K_{cat} were determined by fitting substrate concentration and velocity data to the hyperbolic Michaelis-Menten model. All calculations were determined using GraphPad Prism Software (Graphpad Software, La Jolla, California).

Determination of *in situ* (whole-cell assay) kinetic parameters of NAT1 4 and NAT1 14B

In situ kinetic parameters were determined by in a whole cell assay using media spiked with varying concentrations of PABA or ABP. PABA kinetic constants were determined using varying PABA concentrations between 2.25 – 300 μM. ABP kinetic constants were determined using varying ABP concentrations between 0.19 and 25 μM. The cells were incubated at 37°C and media was collected after 1 h (PABA) or 22 min (ABP), 1/10 volume of 1M acetic acid was added, and the mixture was centrifuged at 13,000xg for 10 min. Values were normalized to the amount of cells present at time of media removal. The supernatant was injected into the reverse phase HPLC column and *N*-acetyl-PABA was separated and quantitated as described above. V_{max} and K_m were determined as described above.

Determination of *in vitro* kinetic parameters of *O*-acetylation for NAT1 4 and NAT1 14B

N-hydroxy-4-aminobiphenyl (*N*-OH-ABP) *O*-acetyltransferase assays were conducted and product was separated from substrate using HPLC as previously described (Metry et al., 2007). Assays containing 50 μg total protein, *N*-OH-ABP,

AcCoA, and 1 mg/mL deoxyguanosine (dG) were incubated at 37°C for 10 min. *N*-OH-ABP kinetic constants were determined at a fixed concentration of 100 µM AcCoA and *N*-OH-ABP concentrations between 0.78 and 200 µM. Reactions were stopped with the addition of 100 µL of water saturated ethyl acetate and centrifuged at 13,000xg for 10 min. The organic phase was removed, evaporated to dryness, redissolved in 100 µL of 10% ACN and injected onto the HPLC. V_{max}, K_m, and K_{cat} were determined as described above.

Measurement of NAT1 Protein

The amount of NAT1 produced in UV5*1A1* cells stably transfected with *NAT1*4* or *NAT1*14B* was determined by western blot. Cell lysates were isolated as described above. Varying amounts of lysate were mixed 1:1 with 5% β-mercaptoethanol in Laemmli buffer (Bio-Rad), boiled for 5 min, and resolved by 12% SDS-PAGE. The proteins were then transferred by semi-dry electroblotting to polyvinylidene fluoride (PVDF) membranes. The membranes were probed with G5, a monoclonal mouse anti-NAT1(1:200) Santa Cruz Biotechnology, Santa Cruz, CA) and with horseradish peroxidase (HRP)-conjugated secondary donkey anti-mouse IgG antibody (1:2,000) (Santa Cruz). Supersignal West Pico Chemiluminescent Substrate was used for detection (Pierce). To determine a quantitative amount of NAT1 protein in lysate collected from cells stably transfected with *NAT1*4* or *NAT1*14B*, a standard curve was obtained from loading 0.14 µg – 1.09 ng of purified NAT1 (Abnova, Taipei, Taiwan). Intensities of varying amounts of lysate (55, 28, and 14 µg) from NAT1 4 and NAT1 14B were compared to intensities of the standard curve to determine the amount of NAT1 protein in the lysate. Kinetic properties of the NAT1 antibody binding of the purified protein and to NAT1 from sample lysate were assumed to be the same. Densitometric analysis was performed using Quantity One Software (Bio-Rad).

DNA Isolation and dG-C8-ABP Quantitation

DNA was isolated and dG-C8-ABP adducts were quantitated with modifications to a previously described method (Metry et al., 2007). Stably transfected cells grown to approximately 80% confluency in 15 cm dishes were incubated in complete α-MEM media containing 1.56, 3.13, 6.25, 12.5 μM ABP or vehicle alone (0.5% DMSO) at 37°C. The cells were collected following 24 h of treatment, centrifuged for 5 min at 260xg, and the pellet was resuspended in 2 volumes of homogenization buffer (20 mM sodium phosphate pH 7.4, 1 mM EDTA), 0.1 volumes of 10% SDS and 0.1 volume of 20 mg/mL Proteinase K and allowed to incubate overnight at 37°C. The DNA was extracted using phenol/chloroform:isoamyl alcohol and precipitated with isopropanol. The pellet was dried and resuspended in 500 μL of DNA adduct buffer (5 mM Tris pH 7.4, 1 mM $CaCl_2$, 1 mM $ZnCl_2$, and 10 mM $MgCl_2$). The DNA was quantitated by spectrophotometry at A_{260}. Five hundred pg of internal standard (dG-C8-ABP-d5, Toronto Research Chemicals, North York, Ontario, Canada) was added to 30 μg of sample DNA, treated with 10 units *DNase I* (Sigma) for 1 h at 37°C followed by treatment with 10 units nuclease P1 (Sigma) for 6 h. The reactions were then treated with 10 units of alkaline phosphatase (Sigma) overnight at 37°C. The samples were then loaded onto PepClean C-18 Spin Columns (Thermo Fisher Scientific), washed with 10% acetonitrile (ACN), eluted with 50% ACN by centrifugation at 2000xg and dried. The samples were reconstituted with 25 μL 5% ACN in 2.5 mM NH_4HCO_3 just before analysis and 10 μL of the sample was analyzed by Accela LC System (Thermo Scientific, San Jose, CA) coupled with a LTQ-Orbitrap XL mass spectrometer (Thermo Scientific, San Jose, CA). Samples were loaded onto a 30 × 1mm × 1.9 μm Hypersil GOLD column (Thermo Scientific, San Jose, CA) and eluted with a 12.5 min binary solvent gradient (Solvent A: 5% ACN/0.1% formic acid and Solvent B: 95% ACN/0.1% formic acid) at 50 μl/min. The

gradient started from 5% Solvent B, increased linearly to 75% Solvent B in 10 min, and then remained at 75% B for 2.5 min. The eluates were ionized by electrospray isonization and dG-C8-ABP and dG-C8-ABP-d5 were detected with linear ion trap and detected by multiple reaction monitoring using the transitions of m/z 435.2 to m/z 319.2 (dG-C8-ABP) and m/z 440.2 to m/z 324.2 (dG-C8-ABP-d5). Concentrations of dG-C8-ABP were calculated from peak areas of dG-C8-ABP and dG-C8-ABP-d5 with a calibration curve from synthetic dG-C8-ABP and dG-C8-ABP-d5.

Measurement of Cytotoxicity

Assays for cell cytoxicity were carried as previously described (Wu et al., 1997) with slight modifications. Cells were grown in HAT medium (30 mM hypoxanthine, 0.1 mM aminopterin, and 30 mM thymidine) for 12 doublings. Cells ($1x10^6$) were plated, allowed to grow for 24 h and were then treated with 1.56, 3.13, 6.25 or 12.5 μM ABP (Sigma) or vehicle alone (0.5% DMSO) in media. After 48 h, cells were plated to determine survival following exposure to ABP. To determine cloning efficiency following each dose of ABP, 100 cells were plated in triplicate in 6 well-plates and allowed to grow for 7 days in non-selective media. Colonies were counted and expressed as percent of vehicle control.

RESULTS

Initial experiments performed in yeast (*in situ*) resulted in higher NAT1 14B *N*-acetylation at 10 μM ($p<0.001$) and 50 μM ABP ($p<0.05$) compared to NAT1 4. There was no difference in *N*-acetylation between NAT1 14B and NAT1 4 following exposure to 100 μM ABP (Figure 3-2). The results of subsequent experiments performed in CHO cells are described below.

Kinetic parameters of the referent, NAT1 4, and the variant, NAT1 14B *in vitro* (per mg total protein in-solution biochemistry) are shown in Table 3-2. The apparent K_m of NAT1 14B was higher for PABA ($p<0.0001$) compared to NAT1 4 whereas the apparent K_m of NAT1 14B was lower for ABP ($p<0.0001$) and *N*-OH-ABP ($p<0.0001$) when compared to NAT1 4. The apparent V_{max} of NAT1 14B was lower for PABA ($p<0.0001$), ABP ($p<.0001$), and *N*-OH-ABP ($p<0.0001$) when compared to NAT1 4. The apparent V_{max}/K_m of NAT1 14B was lower for PABA ($p<0.0001$), higher for *N*-OH-ABP ($p<0.0001$), and not significantly different for ABP ($p>0.05$) when compared to NAT1 4.

The kinetic parameters, apparent K_m and K_{cat} also were determined *in vitro* (per mg NAT1 protein in solution biochemistry) for the referent, NAT1 4 and the variant, NAT1 14B (Table 3-2). The apparent K_{cat} of NAT1 14B was lower for PABA ($p<0.0001$) but higher for *N*-OH-ABP ($p<0.0001$) when compared to NAT1 4. There was no significant difference in apparent K_{cat} for ABP between NAT1 14B and NAT1 4 ($p>0.05$). The apparent K_{cat}/K_m of NAT1 14B was lower for PABA ($p<0.0001$) but higher for ABP ($p<0.05$) and N-OH-ABP ($p<0.0001$) when compared to NAT1 4.

Apparent K_m and V_{max} for PABA and ABP also were determined *in situ* (per million cells in a whole cell based assay) for the referent, NAT1 4, and the variant, NAT1 14B (Table 3-3). The apparent K_m of NAT1 14B was not significantly different for PABA ($p>0.05$) but was significantly lower for ABP ($p<0.0001$) when compared to NAT1 4. The apparent V_{max} of NAT1 14B was lower for PABA ($p<0.05$) and ABP ($p<0.0001$) when

compared to NAT1 4. The apparent V_{max}/K_m of NAT1 14B for PABA was significantly less ($p<0.05$) but was significantly higher for ABP ($p<0.05$) when compared to NAT1 4.

Expression of NAT1 14B and NAT1 4 was determined by western blot (Figure 3-3). Based on intensities determined from the standard curve, after loading 55, 28, or 14 µg of total protein lysate, there were 154, 77, and 38 ng of NAT1 4 protein and 38, 19, and 10 ng of NAT1 14B protein. Overall, NAT1 14B resulted in a 4-fold reduction in NAT1 protein compared to NAT1 4 ($p<0.001$).

ABP-induced cytotoxicity was also determined in cells stably transfected with *NAT1*4* and *NAT1*14B* (Figure 3-4a). Significantly more ABP-induced cytotoxicity was observed in *NAT1*14B* transfected cells following exposures to each ABP concentration. ABP-induced dG-C8-ABP adducts in cells stably transfected with *NAT1*4* and *NAT1*14B* were determined (Figure 3-4b). Significantly more dG-C8-ABP adducts were observed following exposures between 1.56 – 12.5 µM ABP in cells transfected with *NAT1*14B* than in cells transfected with *NAT1*4.*

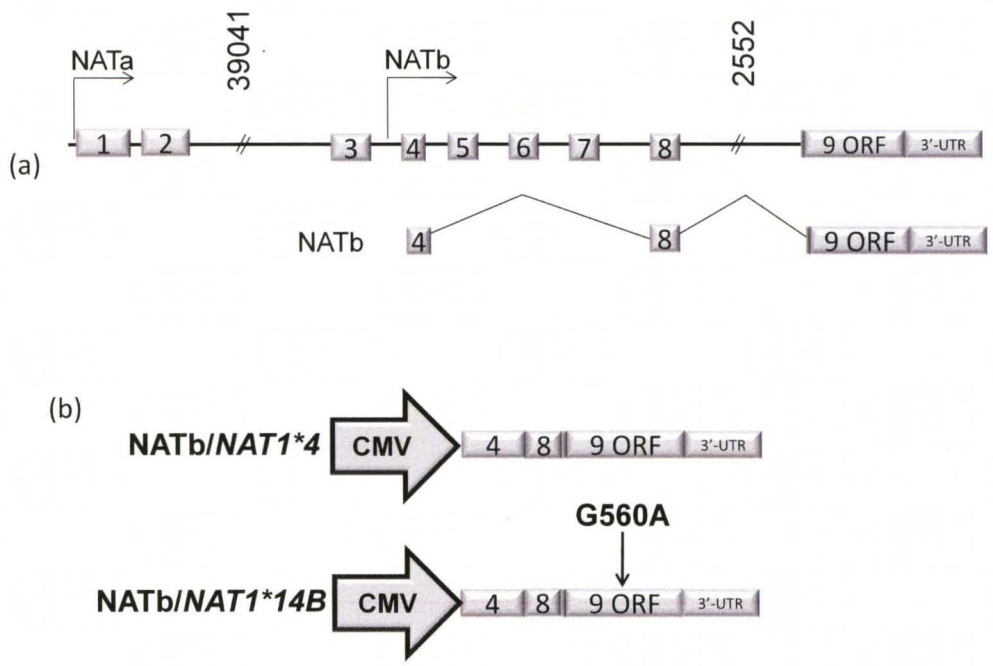

Figure 3-1: NATb/*NAT1*4* and NATb/*NAT1*14B* constructs

(a) Schematic of NAT1 genomic structure and most common RNA transcribed by the NATb promoter. (b) Constructs including 5'-UTR, open reading frame (exon 9) and the 3'-UTR.

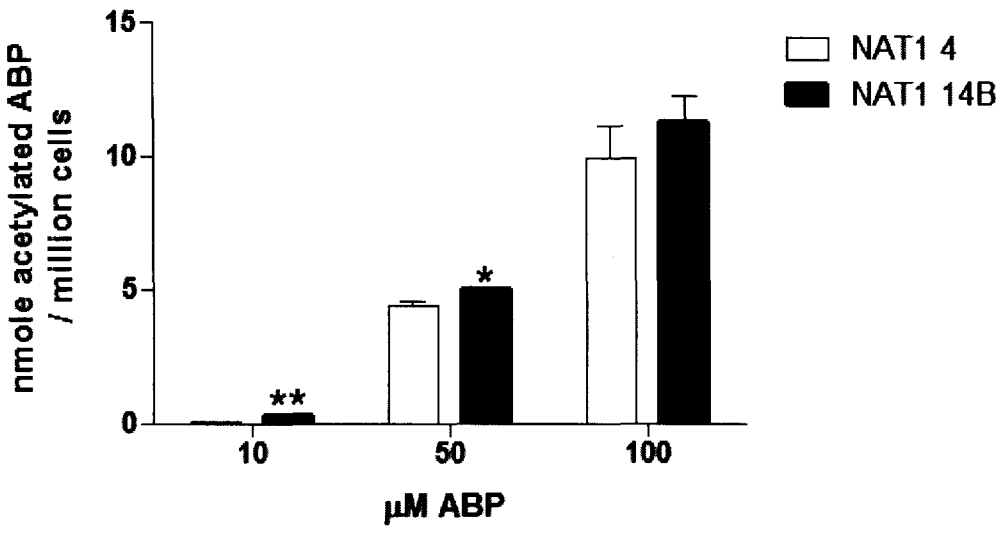

Figure 3-2: ABP *N*-acetylation by NAT1 4 and NAT1 14B expressed in yeast

In situ ABP *N*-acetylation assay of yeast cultures recombinantly expressing*NAT1*4* and *NAT1*14B* per million cells. Error bars represent mean of 3 separate collections ± SEM. Difference determined following a Student's t-test and significance denoted by **p<0.001 and *p<.05.

Primer Name	Use	Sequence
Lkm40P1	NATb 5-'UTR forward specific PCR	5'-GGCCGCGGCATTCAGTCTAGTTCCTGGTTGCC-3'
P1 Fwd Inr NheI	NATb 5'-UTR forward specific nested PCR	5'-TTTAAAGCTAGCATTCAGTCTAGTCTAGTTCCTGGTTGCCGGCT-3'
NAT1 (3') ORF Rev	NATa/NATb 5'-UTR reverse PCR	5'-TTCCTCACTCAGAGTCTTGAACTCTATT-3'
NAT1 (3') ORF For	NAT1 coding region forward PCR	5'-AGACATCTCCATCATCTGTGTTTACTAGT-3'
pcDNA5 FRTdistal Rev	NAT1 3'-UTR reverse PCR	5'-CGTGGGGATACCCCCTAGA-3'
NAT1 KPN-Rev	NAT1 3'-UTR reverse nested PCR	5'-ATAGTAGGTACCTCTGAATTATAGATAAGCAAAGATTCAGATTCT-3'

Table 3-1: Primers used to amplify NATb/*NAT1*4* construct

Allele	Substrate	$K_{m(app)}$	$V_{max(app)}$	V_{max}/K_m	$K_{cat(app)}$	K_{cat}/K_m
		μM	nmole min^{-1} mg^{-1}	mL min^{-1} mg^{-1}	min^{-1}	min^{-1} μM^{-1}
*NAT1*4*	PABA	42.9±3.3	116±3	2.72±0.21	2399±57	56.5±4.3
*NAT1*14B*		430±1 [a]	18.5±1.5 [b]	0.043±0.002 [b]	1552±97 [b]	3.61±0.20 [b]
*NAT1*4*	ABP	273±46	57.7±5.8	0.218±0.018	1200±122	4.52±0.38
*NAT1*14B*		65.6±3.9 [b]	18.0±4.3 [b]	0.280±.031	1760±128	22.9±0.23 [c]
*NAT1*4*	*N*-OH-ABP	141±1.1	2.97±0.19	0.0211±0.0014	35.1±68	0.250±0.02
*NAT1*14B*		46.8±1.3 [b]	1.76±0.03 [b]	0.038±0.001 [c]	147±7 [a]	3.15±0.23 [c]
*NAT1*4*	AcCoA	6.23±0.75	1.25±0.04	0.204±0.019	25.9±0.7	4.24±0.38
*NAT1*14B*		16.8±2.2 [c]	1.50±0.29	0.087±0.005 [b]	126±24 [c]	7.31±0.45 [a]

Table 3-2: NAT1 4 and NAT1 14B kinetic constants determined *in vitro*

NAT1 4 and NAT1 14B kinetic constants determined *in vitro* (per mg total protein). PABA, ABP, and *N*-OH-ABP constants were determined at a fixed concentration of 100 μM AcCoA. AcCoA kinetic constants were determined at a fixed concentration of 100 μM *N*-OH-ABP. Table values represent mean ± SEM for 3-6 individual determinations. Differences were tested for significance by Student's t-test. [a]significantly higher than NAT1 4 ($p<0.0001$); [b]significantly lower than NAT1 4 ($p<0.0001$); [c]significantly higher than NAT1 4 ($p<0.05$).

Allele	Substrate	$K_{m(app)}$	$V_{max(app)}$	V_{max}/K_m
		μM	**nmole min^{-1} million $cells^{-1}$**	**nmole min^{-1} million $cells^{-1}$ μM^{-1}**
*NAT1*4*	PABA	95.5±1.1	0.16±0.01	1.71±0.08
*NAT1*14B*		72.1±11.1	0.101±0.018[a]	1.1±0.09[a]
*NAT1*4*	ABP	10.5±0.6	0.024±.0007	2.4±0.1
*NAT1*14B*		2.3±0.2[b]	0.0063±0.0005[b]	2.9±0.1[c]

Table 3-3: NAT1 4 and NAT1 14B kinetic constants determined *in situ*

NAT1 4 and NAT1 14B kinetic constants determined *in situ* (per million cells). Table values represent mean ± SEM for 3-6 individual determinations. Differences were tested for significance by Student's t-test. [a]significantly lower than NAT1 4 ($p<0.05$); [b]significantly lower than NAT1 4 ($p<0.0001$); [c]significantly higher than NAT1 4 ($p<0.05$).

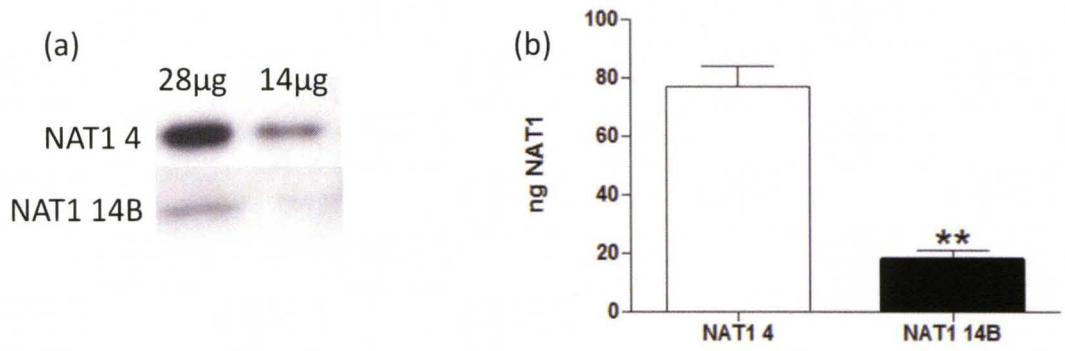

Figure 3-3: NAT1 4 and NAT1 14B protein expression

Western blot to determine relative protein expression of NAT1 4 and NAT1 14B. (a) representative western blot and (b) densitometric analysis. Loading either 28 or 14 µg of total protein from lysate, NAT1 14B resulted in approximately 4-fold less NAT1 protein than NAT1 4. In 28 µg of total protein from lysate, 77 µg of NAT1 4 and 18 µg of NAT1 14B protein were detected ($p<0.001$). One clone stably expressing *NAT1*4* and two clones stably expressing *NAT1*14B* were evaluated. Bars represent mean ± SEM for 3 western blots and significance was determined by Student's t-test.

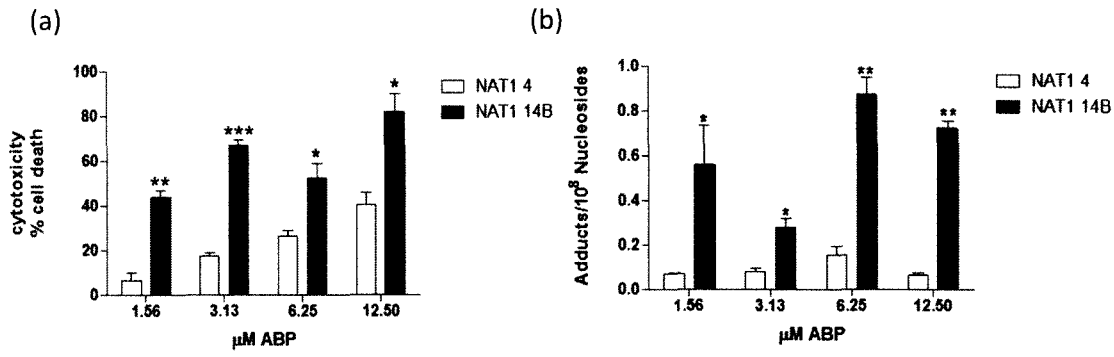

Figure 3-4: ABP-induced cytotoxicity and DNA adducts

ABP-induced cytotoxicity (a) and dG-C8-ABP adducts (b) in cells stably transfected with *NAT1*4* and *NAT1*14B*. Significantly more cytotoxicity was observed for NAT1 14B than NAT1 4 following all ABP exposures between 1.56 – 12.5 µM. Significantly more adducts were observed following all exposures examined in cells expressing NAT1 14B than in cells expressing NAT1 4. Values were adjusted for baseline values of UV5/*1A1* cells. Bars represent mean ± SEM for 3 determinations and significance was determined by Student's t-test. (*) $p<0.05$, (**) $p<0.001$, and (***) $p<0.0001$.

DISCUSSION

Smokers possessing *NAT1*14B* have been associated with increased risk for lung cancer compared to individuals possessing *NAT1*4* (Bouchardy et al., 1998). Previous studies have reported that *NAT1*14B* is associated with reduced *N*- and *O*-acetylation of various substrates including PABA, *p*-aminosalisylic acid, and various arylamine carcinogens (Fretland et al., 2001; Fretland et al., 2002; Hughes et al., 1998; Zhu and Hein, 2008). Recombinant NAT1 14B expression in yeast demonstrated lower *N*- and *O*-acetylation, NAT1-specific protein levels and increased NAT1 proteasomal degradation (Butcher et al., 2004; Fretland et al., 2001; Fretland et al., 2002). Similarly, NAT1 14B expressed in COS-1 cells also resulted in less NAT1 *N*- and *O*-acetylation, NAT1 protein level, and NAT1 $V_{max,}$ but higher PABA K_m when compared to the referent, NAT1 4 (Zhu and Hein, 2008). Our kinetic constant determinations performed in CHO cells confirmed that NAT1 14B results in a lower apparent V_{max} (both *in vitro* and *in situ*) for PABA when compared to the referent, NAT1 4. We also confirmed the higher PABA apparent K_m in NAT1 14B determined *in vitro* when compared to NAT1 4. In addition to PABA acetylation, we also report on *N*- and *O*-acetylation of ABP and *N*-OH-ABP. ABP is a human urinary bladder carcinogen found as a contaminant in cigarette smoke, food dyes, paints, textile dyes, engine exhaust, and commercial hair dyes (Nauwelaers et al., 2011).

The arylamine substrate K_m of NAT1 is dependent on the AcCoA concentration because acetylation proceeds via a 'ping-pong bi-bi' reaction (Weber and Hein, 1985). Because AcCoA concentrations have been measured *in vivo* in the low micromolar range (Reeves et al., 1988), we chose an *in vitro* AcCoA concentration of 100 μM. In order to better mimic NAT1 catalyzed acetylation *in vivo*, kinetic constants were determined *in situ* (when possible) allowing the concentration of AcCoA to be provided by the cell.

Studies performed *in situ* using NAT1 14B and NAT1 4 produced in yeast did not result in lowered NAT1 14B *N*-acetylation of ABP (Figure 4-2) as previous studies had shown *in vitro* (Fretland et al., 2002). This result was surprising as previous studies reported NAT1 14B activity and protein expression to be lower than NAT1 4. To further explore the NAT1 14B acetylation status, studies were conducted in stably transfected CHO cells.

When comparing apparent V_{max} (*in vitro*), the NAT1 14B apparent V_{max} was lower than the NAT1 4 for all substrates studied. The apparent V_{max} describes the maximum enzyme velocity extrapolated to maximum substrate concentrations. The lower apparent V_{max} for PABA, ABP, and *N*-OH-ABP indicate that at high substrate concentrations, NAT1 14B has a decreased ability to metabolize the substrate when compared to NAT1 4. The apparent V_{max}/K_m, or intrinsic clearance, describes an enzyme's ability to metabolize a substrate at substrate concentrations well below the K_m and has also been shown to correlate well to human liver clearance (Chen et al., 2011; Northrop, 1999). Although there are limitations in using V_{max}/K_m as a comparator of two enzymes, we determined apparent V_{max} for comparison at high substrate concentrations and apparent V_{max}/K_m for comparison at low substrate concentrations (Eisenthal et al., 2007). For PABA, the NAT1 14B apparent V_{max}/K_m was lower than NAT1 4. In contrast, no significant difference was observed between NAT1 14B and NAT1 4 apparent V_{max}/K_m towards the *N*-acetylation of ABP. Surprisingly, the NAT1 14B apparent V_{max}/K_m for the O-acetylation of *N*-OH-ABP was higher in *NAT1*14B* CHO cells compared to *NAT1*4*. This indicates that the status of NAT1 14B intrinsic clearance compared to NAT1 4 intrinsic clearance is substrate dependent.

Transfection of *NAT1*14B* resulted in approximately a 4-fold less NAT1 protein expression compared to *NAT1*4*. When the amount of NAT1 protein was used to calculate apparent K_{cat} (determined *in vitro*), the results suggested that the lower NAT1

14B apparent V_{max} for these substrates is due to a reduction in NAT1 protein, not a reduction in the acetylation rate of the NAT1 14B enzyme. For example, although the NAT1 14B apparent V_{max} for *N*-OH-ABP was lower than the NAT1 4, the NAT1 14B apparent K_{cat} for *N*-OH-ABP was higher than NAT1 4. This difference in V_{max} compared to K_{cat} indicates that the lowered NAT1 14B apparent V_{max} is caused by a reduction in protein expression. Butcher et. al (2004) reported that NAT1 14B and other NAT1 genetic variants associated with reduced enzymatic activity have reduced ability to be acetylated which resulted in an unstable NAT1 protein. Therefore, NAT1 14B was reported to be less stable and have increased proteasomal degradation compared to NAT1 4 (Butcher et al., 2004). Our study confirmed that NAT1 14B resulted in reduction of NAT1 protein.

Because determination of kinetic parameters is dependent upon AcCoA concentration, acetylation was measured *in situ* to allow the concentration of AcCoA to be provided by the cell. When comparing V_{max} (*in situ*), the NAT1 14B apparent V_{max} was lower than the NAT1 14B for all substrates studied. When evaluated *in situ,* PABA NAT1 14B apparent V_{max}/K_m or intrinsic clearance was lower when compared to NAT1 4. In contrast, for ABP, the *in situ* NAT1 14B apparent V_{max}/K_m was higher when compared to NAT1 4. Because kinetic parameters of *N*-OH-ABP could not be determined *in situ*, an *in vitro* determination was performed. Like ABP, the NAT1 14B apparent V_{max}/K_m for *N*-OH-ABP was higher compared to NAT1 4. These findings indicate that differences in apparent V_{max}/K_m between NAT1 14B and NAT1 4 are substrate dependent. Risk for individuals possessing *NAT1*14B* is also likely exposure dependent. Increased apparent V_{max}/K_m indicates that NAT1 14B has an increased ability to metabolize ABP and *N*-OH-ABP at low substrate concentrations compared to NAT1 4 (Northrop, 1999). Since low substrate concentrations are relevant *in vivo*, the higher NAT1 14B apparent V_{max}/K_m suggests that differences between NAT1 14B and NAT1 4 catalyzed ABP

acetylation should be observed *in vivo*. Therefore, risk for individuals possessing *NAT1*14B* is dependent on exposure type and can also be altered depending on exposure level.

NAT1 homology modeling predicted that the R187Q could affect NAT1 active site acetylation and enzymatic activity (Walraven et al., 2008). Because changes in binding of AcCoA and substrate specificity are likely altered due to the R187Q, it is not surprising that differences in intrinsic clearance between NAT1 14B and NAT1 4 were observed. We confirmed that R187Q modifies substrate affinity, albeit in opposite directions depending on substrate. Further epidemiological studies are necessary to determine which carcinogen exposures result in increased risk for individuals possessing *NAT1*14B*. Exposure dependent risk has been previously reported for an *N*-acetyltransferase 2 (NAT2) (Hickman et al., 1995; Zang et al., 2007). The *NAT2*7B* allozyme exhibits altered kinetic parameters of substrates including sulfamethazine and dapsone but not for other substrates such as 2-aminofluorene and isoniazid when compared to the referent, *NAT2*4* (Hickman et al., 1995; Zang et al., 2007). Our study is the first report of exposure dependent behavior for a variant of NAT1.

In addition to higher apparent V_{max}/K_m for NAT1 14B towards ABP and *N*-OH-ABP when compared to NAT1 4, ABP-induced DNA-adducts and cytoxicity were higher for NAT1 14B compared to NAT1 4. Measurement of DNA adduct levels following exposure to ABP is a biological endpoint very relevant to cancer risk. Because NAT1 14B resulted in increased ABP-induced DNA adducts, our results suggest that individuals possessing the *NAT1*14B* allele likely have increased risk compared to those who are homozygous for *NAT1*4* following low (environmental) dose exposure to ABP. NAT1 14B is not simply associated with "slow acetylation" but rather is substrate dependent, since NAT1 14B exhibits lower *N*-acetylation catalytic efficiency of PABA but

higher *N*- and *O*-acetylation catalytic efficiency as well as DNA adducts following exposure to the human carcinogen ABP.

CHAPTER 4

FUNCTIONAL ANALYSIS OF *NAT1*10* VS *NAT1*4* IN COMPLETE NATb AND NATa mRNA CONSTRUCTS

INTRODUCTION

Human arylamine N-acetyltransferase 1 (NAT1) is a phase II cytosolic isozyme responsible for the biotransformation of many arylamine compounds including pharmaceuticals and environmental carcinogens (Hein et al., 2000). NAT1 has been implicated in several types of cancer due to its role in metabolic activation of arylamine carcinogens, and recent findings report NAT1 may be important for cell growth and survival of cancer cells (Tiang et al., 2011) NAT1 has been found in nearly all tissues studied including fetal tissue (Boukouvala and Sim, 2005; Grant et al., 1989; Pacifici et al., 1986). NAT1 is capable of both *N*-acetylation and *O*-acetylation. Following *N*-acetylation (inactivation) the innocuous acetylated compounds can be excreted from the body. However, following *O*-acetylation (activation) the compound forms an unstable *N*-acetoxyarylamine which undergoes heterolytic cleavage to yield a highly reactive nitrenium ion. These nitrenium ions are highly electrophilic and can react with proteins or DNA to form adducts. Therefore, following exposure to arylamine carcinogens, the acetylator phenotype may modulate individual susceptibility to cancer.

NAT1 and NAT2 are known to be highly polymorphic with over 20 alleles identified for each. Polymorphic variations of NAT1 and NAT2 can result in altered acetylation capacity. The functional effects of NAT2 polymorphisms have been well characterized in relationship to their phenotype, but the functional effects of NAT1

polymorphisms remain poorly understood. The most common NAT1 polymorphisms are located in the region 3' to the open reading frame; however conflicting results about their effect on acetylation capacity have been reported. *NAT1*10* is the most common NAT1 variant allele in many populations and is characterized by two SNPs in the 3'-UTR, $T^{1088}A$ (rs1057126) and $C^{1095}A$ (rs15561). One study suggested that *NAT1*10* has higher acetylation capacity than the referent allele, *NAT1*4*, (Bell et al., 1995a), while another have reported no difference (de Leon et al., 2000). There are no amino acid changes due to these polymorphisms, but the $T^{1088}A$ causes a change in the second consensus polyadenylation signal (AATAAA – AAAAAA). It has been speculated that this change in polyadenylation signal may give rise to a difference in mRNA stability and modulated acetylation activity of NAT1 10 (Bell et al., 1995a). The 3'-UTR of a gene contains binding sites for important translational regulatory elements that include microRNAs, proteins or protein complexes, cytoplasmic polyadenylation elements (CPE) and polyadenylation signals (AAUAAA) (Mishra et al., 2008). It has been shown that SNPs in 3'-UTRs of dihydrofolate reductase (DHFR), thrombin and resistin genes cause functional affects and alter disease risk (Gehring et al., 2001; Mishra et al., 2008; Pizzuti et al., 2002).

In addition to the high allelic frequency in many populations, *NAT1*10* is also of great interest because it has been associated with increased risk of so many different forms of cancer. *NAT1*10* heterozygous genotype is associated with increased odds ratios for non-Hodgkin lymphoma (Morton et al., 2006), gastric adenocarcinoma (Boissy et al., 2000), prostate cancer (Hein et al., 2002) and breast cancer (Stephenson et al., 2010) when compared to the homozygous *NAT1*4* genotype. It has also been reported that cancer risk associated with *NAT1*10* is further modulated by exposure to environmental carcinogens found in cigarette smoke, meats cooked at high

temperatures, and the use of hair dye. For example, frequent consumption of red meat in combination with *NAT1*10* is associated with an increased odds ratio for colorectal cancer (Lilla et al., 2006) and the use of dark, permanent hair dye in combination with *NAT1*10* is associated with an increased risk for non-Hodgkin lymphoma (Morton et al., 2007). Heavy smokers possessing the *NAT1*10* allele have an increased risk for developing pancreatic cancer compared to non-smokers (Li et al., 2006) and for developing breast cancer (Zheng et al., 1999). The contribution of *NAT1*10* to increased cancer risk is not well understood. It is imperative that the phenotype of *NAT1*10* be clearly defined in order to resolve the association of *NAT1*10* genotype with increased cancer risk.

The NAT1 gene is located on the small arm of chromosome 8 (Blum et al., 1990) and spans 53 kb. NAT1 is encoded by a single intronless coding exon containing an open reading frame (ORF) of 870 base pairs (bp). Several NAT1 transcripts have been identified containing various combinations of the 9 noncoding 5'-untranslated region (UTR) exons and are known to originate from two distinct promoters, NATa and NATb. NATa originates 51.5 kb upstream of the single NAT1 ORF while NATb originates 11.8 kb upstream of the NAT1 ORF (Barker et al., 2006; Boukouvala and Sim, 2005; Husain et al., 2004). The reason for the two promoters and the resulting distinct transcripts remains unclear. However, there is tissue specific expression between transcripts derived from the two major promoters. NATb transcripts are expressed in all tissues studied, while NATa transcripts are located in kidney, liver, lung and trachea (Barker et al., 2006). Because the NATa transcripts are found only in areas of high environmental exposure, differences in transcriptional regulation may necessitate two separate promoters.

Differences in transcripts derived from the NATb and NATa promoters have been reported both in translation and transcription (Butcher et al., 2005; Millner, 2011). Transcripts derived from the NATb promoter are translated more efficiently than transcripts derived from the NATa promoter (Butcher et al., 2005). Chinese hamster ovary cells stably transfected with *Cytochrome p450 1A1* and NATb/*NAT1*4* (mRNA type/allele) resulted in lower NAT1 protein, mRNA as wells as *N*- and *O*- acetylation compared to cells transfected with NATa/*NAT1*4* (Millner, 2011). Following treatment with 4-aminobiphenyl, NATb/*NAT1*4* transfected cells also resulted in higher DNA adducts, cytotoxicity and mutants compared to NATa/*NAT1*4* transfected cells (Millner, 2011).

In addition to polymorphic variation, it may be necessary to consider transcriptional and translational regulation to further understand the variation associated with *NAT1*10* acetylation activity and effect on cancer risk. In contrast to previous studies which included only the *NAT1* open reading frame (ORF), this study employs constructs that mimic the most common transcripts originating from the NATb and the NATa promoters. In this study, the constructs are referred to as NATb/*NAT1*X* or NATa/*NAT1*X*. NATb or NATa refers to the 5' non-coding exons (NCEs) while *NAT1*X* refers to the specific allele. The constructs contain the ORF, the 3'-UTR and all 5' NCEs found in the most common *NAT1* transcripts originating at the NATb and NATa promoter (Figure 4-1) (Barker et al., 2006; Husain et al., 2004; Husain et al., 2007). The NATb/*NAT1*X* construct contains exons 4 and 8 (5' NCEs) and exon 9 (ORF) which has been termed transcript Type IIA by Butcher et al., 2005. The NATa/*NAT1*X* construct contains exons 1, 2, 3, 8 (5' NCEs) and 9 (ORF) which has been termed transcript Type 1A by Butcher et al., 2005. In addition to the 5' NCEs and the ORF, the NATb/*NAT1*X* and NATa/*NAT1*X* constructs also contain 888 nucleotides of the 3'-UTR. The

NATb/*NAT1*X* and NATa/*NAT1*X* constructs were employed to provide a more comprehensive model of *in vivo* metabolism and to study any allele specific interactions between the 5'-UTR and *NAT1*10* polymorphisms. These constructs were utilized to determine *N*- and *O*- acetylation, mRNA levels, protein levels, and polyadenylation patterns between cells transfected with NATb/*NAT1*4* and NATa/*NAT1*4* as well as variants of *NAT1*10* in both mRNA constructs.

METHODS

Polyadenylation site removal

The bovine growth hormone (BGH) polyadenylation site from the pcDNA5/FRT (Invitrogen, Carlsbad, CA) vector was removed to allow the endogenous *NAT1* polyadenylation sites to be active. This was accomplished by digestion of pcDNA5/FRT at 37°C with restriction endonucleases, ApaI and SphI (New England Biolabs, Ipswich, MA), followed by overhang digestion with T4 DNA polymerase (New England Biolabs) and ligation with T4 Ligase (New England Biolabs).

NATb/*NAT1*4*, NATb/*NAT1*10* NATb/*NAT1*10B*, NATa/*NAT1*4,* NATa/*NAT1*10*, and NATa/*NAT1*10B* construct

The constructs were created utilizing gene splicing via overlap extension (Horton et al., 1989) by amplifying the 5'-UTR and the coding region/3'-UTR separately and then fusing the two regions together. Beginning with frequently used transcription start sites (Barker et al., 2006; Husain et al., 2004), the 5'-UTRs were amplified from cDNA prepared from RNA isolated from homozygous *NAT1*4* HepG2 cells. All primer sequences used are shown in Table 1. The primers used to amplify the NATb 5'-UTR region were Lkm40P1 and NAT1 (3') ORF Rev while the primers used to amplify the NATa 5'-UTR region were Lkm41P1 and NAT1 (3') ORF Rev. The coding region and 3'-UTR were amplified as one piece from homozygous *NAT1*4* or homozygous *NAT1*10* human genomic DNA. The forward primer used to amplify the coding region/3'-UTR was NAT1 (3') ORF Forward while the reverse primer was pcDNA5distal Reverse. The two sections, the 5'-UTR and the coding region/3'UTR, were fused together via overlap and amplification of the entire product using nested primers. The forward nested primer for NATb was P1 Fwd Inr NheI while the forward nested primer for NATa was P3 Fwd Inr

NheI. The reverse nested primer for both NATa and NATb constructs was NAT1 Kpn Rev (*NAT1*4* and *NAT1*10*) or NAT1 Kpn Rev 10B (*NAT1*10B*). Both forward nested primers included the *Nhe1* endonuclease restriction site and both reverse nested primers contained the *Kpn1* endonuclease restriction site to facilitate cloning. The pcDNA5/FRT vector and NATa/*NAT1*4* and NATb/*NAT1*4* allelic segments were digested at 37^0C with restriction endonucleases *KpnI* and *NheI* (New England Biolabs). The *NAT1* constructs were then ligated into pcDNA5/FRT using T4 ligase (Invitrogen). All constructs were sequenced to ensure integrity of allelic segments and junction sites.

NATb/*NAT1*10* Construction

NATb/*NAT1*10* constructs were created using the same NATb 5'-UTRs amplified from cDNA prepared from *NAT1*4* homozygous RNA isolated from HepG2 cells, while the ORF (open reading frame) and region 3' to the ORF were amplified as one piece from *NAT1*10/NAT1*10* homozygous human genomic DNA. These two sections, the 5' UTR and the ORF/region 3' to the ORF were fused together using nested primers. Upon sequencing to ensure allelic and junction site integrity, it was discovered that one of the *NAT1*10* clones had 4 additional polymorphisms located in the region 3' to the ORF including 1571T>C, 1642A>C, 1647 ΔCT, and 1716C>T (Table 1). The presence of these polymorphisms in *NAT1* was verified against NCBI databases. This study refers to this allele as NATb/*NAT1*10B* and was used to compare *N*-acetylation activity along with NATb/*NAT1*10* and NATb/*NAT1*4*.

Cell culture

UV5-CHO cells, a nuclease excision repair (NER)-deficient derivative of AA8 which are hypersensitive to bulky DNA lesions, were obtained from the ATCC (catalog number: CRL-1865). Unless otherwise noted, cells were incubated at 37^0C in 5% CO_2 in complete alpha-modified minimal essential medium (α-MEM, Lonza, Walkersville, MD) without L-glutamine, ribosides, and deoxyribosides supplemented with 10% fetal bovine serum (Hyclone, Logan, UT), 100 units/mL penicillin (Lonza), 100 µg/mL streptomycin (Lonza), and 2 mM L-glutamine (Lonza). The UV5/CHO cells used in this study were previously stably transfected with a single Flp Recombination Target (FRT) integration site (Metry et al., 2007). The FRT site allowed stable transfections to utilize the Flp-In System (Invitrogen). When co-transfected with pOG44 (Invitrogen), a Flp recombinase expression plasmid, a site-specific, conserved recombination event of pcDNA5/FRT (containing either NATa/*NAT1*4* or NATb/*NAT1*4)* occurs at the FRT site. The FRT site allows recombination to occur immediately downstream of the hygromycin resistance gene, allowing for hygromycin selectivity only after Flp-recombinase mediated integration. The UV5/FRT cells were further modified by stable integration of human *CYP1A1* and NADPH-cytochrome P450 reductase gene (*POR*) (Metry et al., 2007). They are referred to in this manuscript as UV5/*1A1* cells.

Transient Transfection

UV5/*1A1* cells were transiently transfected with pcDNA5/FRT (Invitrogen) or pEF1/V5-His (Invitrogen) containing NATb/*NAT1*4,* NATb/*NAT1*10,* and NATb/*NAT1*10B* constructs using Lipofectamine reagent (Invitrogen) following the manufacturer's recommendations. UV5/1A1 cells were co-transfected with pCMV-SPORT-βgal (β-galactosidase transfection control plasmid, Invitrogen). The cells were harvested the next day. Lysate was prepared by centrifuging the cells and resuspending

pellet in lysis buffer (0.2% triton-X 100, 20 mM $NaPO_4$ pH 7.4, 1 mM EDTA, 1 mM DTT, 0.1 mM PMSF, 2 µg/mL aprotinin and 2 mM pepstatin A). The resuspended cell pellet was centrifuged at 13,000xg for 10 min. The supernatant was used to measure *N*-acetyltransferase activity and β-galactosidase activity.

Stable transfections

Stable transfections were carried out using the Flp-In System (Invitrogen) into UV5/*1A1* cells that were previously stably transfected with a FRT site (as noted above). The pcDNA5/FRT plasmids containing human NATb/*NAT1*X* and NATa/*NAT1*X* were co-transfected with pOG44 (Invitrogen), a Flp recombinase expression plasmid. UV5/*1A1* cells were stably transfected with pcDNA5/FRT containing NATb/*NAT1*4* and NATb/*NAT1*14B* constructs using Effectene transfection reagent (Qiagen, Valencia, CA) following the manufacturer's recommendations. Since the pcDNA5/FRT vector contains a hygromycin resistance cassette, cells were passaged in complete α-MEM containing 600 µg/mL hygromycin (Invitrogen) to select for cells containing the pcDNA5/FRT plasmid. Hygromycin resistant colonies were selected approximately 10 days after transfection and isolated with cloning cylinders.

Determination of *in vitro N*-acetylation for NAT1 4, NAT1 10, and NAT1 10B

Lysate was prepared as described above. *In vitro* assays using the NAT1 specific substrate para-aminobenzoic acid (PABA, 300 µM) or 4-aminobiphenyl (ABP, 100 µM) were conducted and acetylated products were separated utilizing HPLC as previously described (Hein et al., 2006). *N*-acetylation activity was determined at a fixed concentration of 1 mM acetyl coenzyme A (AcCoA). Reactions containing substrate, AcCoA and enzyme were incubated at 37˚C for 10 min. Reactions were terminated by

the addition of 1/10 volume of 1M acetic acid and centrifuged at 15,000Xg for 10 min. Measurements were adjusted according to baseline measurements using lysates of the UV5/*CYP1A1* cell line and normalized by the amount of total protein. Protein concentrations were measured using the method of Bradford (Bio-Rad, Hercules, CA). All calculations were determined using GraphPad Prism Software (Graphpad Software, La Jolla, California).

In situ N-acetylation by NAT1 4, NAT1 10, and NAT1 10B

In situ N-acetylation activities were determined by a whole cell assay using media spiked with varying concentrations of PABA or ABP. *N*-acetylation activities were determined using varying concentrations of PABA and ABP between 10 and 300 µM. The cells were incubated at 37°C and media was collected after 1 h (PABA) or 22 min (ABP), 1/10 volume of 1M acetic acid was added, and the mixture was centrifuged at 13,000xg for 10 min. Values were normalized to the amount of cells present at time of media removal. The supernatant was injected into the reverse phase HPLC column and *N*-acetyl-PABA or *N*-acetyl-ABP was separated and quantitated as described above.

Determination of *in vitro O*-acetylation for NAT1 4 and NAT1 10 and NAT1 10B

N-hydroxy-4-aminobiphenyl (*N*-OH-ABP) *O*-acetyltransferase assays were conducted and product was separated from substrate using HPLC as previously described (Metry et al., 2007). Assays containing 50 µg total protein, *N*-OH-ABP (100 µM), AcCoA (1 mM), and 1 mg/mL deoxyguanosine (dG) were incubated at 37°C for 10 min. Reactions were stopped with the addition of 100 µL of water saturated ethyl acetate and centrifuged at 13,000xg for 10 min. The organic phase was removed, evaporated to dryness, redissolved in 100 µL of 10% ACN and injected onto the HPLC.

Measurement of NAT1 Protein

The amount of NAT1 produced in UV5/*1A1* cells stably transfected with NATb/*NAT1*X* or NATa/*NAT1*X* was determined by western blot. Cell lysates were isolated as described above. Varying amounts of lysate were mixed 1:1 with 5% β-mercaptoethanol in Laemmli buffer (Bio-Rad), boiled for 5 min, and resolved by 12% SDS-PAGE. The proteins were then transferred by semi-dry electroblotting to polyvinylidene fluoride (PVDF) membranes. The membranes were probed with G5, a monoclonal mouse anti-NAT1(1:200) Santa Cruz Biotechnology, Santa Cruz, CA) and with horseradish peroxidase (HRP)-conjugated secondary donkey anti-mouse IgG antibody (1:2,000) (Santa Cruz). Supersignal West Pico Chemiluminescent Substrate was used for detection (Pierce). Densitometric analysis was performed using Quantity One Software (Bio-Rad).

Measurement of NAT1 mRNA

Total RNA was isolated from cells using the RNeasy kit (Qiagen) followed by removal of contaminating DNA by treatment with TurboDNase Free (Ambion, Austin, TX). Synthesis of cDNA was performed using qScript cDNA Synthesis Kit (Quanta Biosciences, Gaithersburg, MD) using 1 µg of total RNA in a 20 µL reaction per the manufacturer's protocol. Quantitative RT-PCR (qRT-PCR) assays were used to assess the relative amount of *NAT1* mRNA in cells stably transfected cells. The Step One Plus (Applied Biosystems, Foster City, CA) was used to perform qRT-PCR in reactions containing 1x final concentration of qScript One-Step Fast mix (Quanta Biosciences), 300 nM of each primer and 100 nM of probe in a total volume of 20 µL. For qRT-PCR of *NAT1* mRNA, a TaqMan probe was used with NAT1 Total Splice Forward and NAT1 Total Splice Reverse primers (Table 2) designed using Primer Express 1.5 software (Applied Biosystems). An initial incubation at 50°C was carried out for 2 minutes and at

94°C for 10 minutes followed by 40 cycles of 95°C for 15 seconds and 60°C for 1 minute. TaqMan® Ribosomal RNA Control Reagents for quantitation of the endogenous control, 18S rRNA, (Applied Biosystems) were used to determine ΔCt (*NAT1* Ct –18S rRNA Ct). ΔΔCt was determined by subtraction of the smallest ΔCt and relative amounts of *NAT1* mRNA were calculated using $2^{-\Delta\Delta Ct}$ as previously described (Barker et al., 2006).

RNase Protection Assay

Biotinylated RNA probes were constructed to span the region 3' to the NAT1 ORF using the MAXIscript *In Vitro* Transcription kit (Applied Biosystems/Ambion, Austin, TX). RNase Protection Assays (RNAPs) were carried out using RPAIII Kits (Applied Biosystems/Ambion) according to the manufacturer's protocols. Briefly, total RNA was collected from transiently transfected cells CHO cells and treated with Turbo DNase Free kit (Applied Biosystems/Ambion). Five μg of total RNA was allowed to hybridize overnight in molar excess of biotinylated RNA probes. The resulting RNA-probe mixture was treated with RNase A/TI (kit) to degrade any non-hybridized RNA and any remaining probe. The RNased hybridized mixture was then separated on a polyacrylamide gel and transferred to a nitrocellulose membrane. The membrane was detected with Chemiluminescent Nucleic Acid Detection Module (ThermoScientific) and exposed to x-ray film to visualize.

Measurement of Cytotoxicity and Mutagenesis

Assays for cell cytoxicity and mutagenesis were carried as previously described (Wu et al., 1997) with slight modifications. Cells were grown in HAT medium (30 mM

hypoxanthine, 0.1 mM aminopterin, and 30 mM thymidine) for 12 doublings. Cells ($1x10^6$) were plated, allowed to grow for 24 h and were then treated with 1.56, 3.13, 6.25 or 12.5 μM ABP (Sigma) or vehicle alone (0.5% DMSO) in media. After 48 h, cells were plated to determine survival and mutagenic response to ABP. To determine cloning efficiency following each dose of ABP, 100 cells were plated in triplicate in 6 well-plates and allowed to grow for 7 days in non-selective media. Colonies were counted and expressed as percent of vehicle control. To determine mutagenic response following ABP exposure, $5x10^5$ cells were plated and sub-cultured for 7 days and then seeded with $1x10^5$ cells/100 x 20 mm dish (10 replicates) in complete DMEM containing 40 μM 6-thioguanine (Sigma). Mutant *hprt* cells were allowed to grow for 7 days and colonies were counted to determine ABP-induced mutants and corrected by cloning efficiency.

Removal of the SV40 polyadenylation signal from NATa and NATb *NAT1*10B* Constructs

The SV40 polyadenylation signal was removed from the NATa and NATb *NAT1*10B* pcDNA5/FRT constructs by incubation at 37° with restriction enzymes, SacII and SapI. The overhangs were filled in using T4 DNA polymerase (New England Biolabs) and then ligated back together using T4 DNA ligase (New England Biolabs). Transient transfections and PABA *in vitro N*-acetylation assays were performed as described above.

Statistical Analysis

Statistical differences were determined using either an unpaired Student's t-test or one-way ANOVA using Prism Software by Graphpad (La Jolla, CA).

RESULTS

Upon sequencing two sources of *NAT1*10* genomic DNA used to create the *NAT1*10* constructs, 4 additional polymorphisms were found in the 3'-UTR of one of the sources (Table 1). In addition to T1088A (rs1057126), C1095A (rs15561), and G1191T (rs4986993), A1642C (rs8190865) a deletion ΔCT1647, and C1716T (rs8190870) and A1735T. These were validated by their inclusion in the NCBI dbSNP database.

NATb/*NAT1* enzymatic activity was examined with PABA, ABP, or *N*-OH-ABP. Significantly more *N*-acetylation activity towards PABA (Figure 4-2) and ABP (Figure 4-3) was detected in NATb/*NAT1*10* and NATb/*NAT1*10B* than in NATb/*NAT1*4* ($p<0.05$) in transiently and stably transfected cells. Significantly more *O*-acetylation of *N*-OH-ABP was detected in NATb/*NAT1*10* and NATb/*NAT1*10B* than in NATb/*NAT1*4* ($p<0.05$) in stably transfected UV5/1A1 cells (Figure 4-3). NATa/*NAT1* activity was also examined using PABA, ABP and *N*-OH-ABP. Significantly more NATa/*NAT1*10B N*-acetylation of PABA (Figure 4-4), ABP (Figure 4-5), and *O*-acetylation of *N*-OH-ABP (Figure 5) was observed when compared to NATa/*NAT1*4* ($p<0.05$) both *in vitro* and *in situ.* No difference was observed between NATa/*NAT1*10* and NATa/*NAT1*4* stably transfected cells towards the N-acetylation of PABA (Figure 4-4), ABP (Figure 4-5) or the *O*-acetylation of *N*-OH-ABP (Figure 4-5).

The pcDNA5/FRT (Invitrogen) utilized in these experiments contained an SV40 polyadenylation signal for the hygromycin cassette. To ensure there was no artifactual use of the SV40 polyadenylation signal, it was removed to ensure that the presence of NATa and NATb *NAT1*10B* transcripts beyond the 3rd probe was not vector induced. Following removal of the SV40 polyadenylation site from the pcDNA5/FRT, no difference was observed in PABA *N*-acetylation between *NAT1*10B* and *NAT1*10B ΔSV40*

polyadenylation site in NATb (Figure 4-6a) or NATa (Figure 4-6b) transiently transfected UV5/1A1 cells.

Western blots were performed to examine NAT1 protein expression in stably transfected UV5/1A1 cells (Figure 4-7). Equal amounts of total protein were loaded and densitometric analysis was performed using Quantity One 1-D Analysis Software (Bio Rad). Significantly more protein ($p<0.05$) was detected in NATb/*NAT1*10* and NATb/*NAT1*10B* than in NATb/*NAT1*4* transfected cells (Figure 4-7b). Significantly more protein was observed in NATa/*NAT1*10B* when compared to NATa/*NAT1*4* ($p<0.05$) stably transfected cells (Figure 4-7c). No difference in protein ($p>0.05$) was observed between NATa/*NAT1*10* and NATa/*NAT1*4* stably transfected cells (Figure 4-7c).

mRNA levels in stably transfected CHO cells were determined by RT-PCR (Figure 4-8). Significantly more mRNA was observed in NATb/*NAT1*10* and NATb/*NAT1*10B* than NATb/*NAT1*4* transfected cells (Figure 4-8b). Significantly more mRNA was observed in NATa/*NAT1*10B* but not NATa/*NAT1*10* when compared to NATa/*NAT1*4* stably transfected cells.

Stable transfection of NATb/*NAT1*4* and NATb/*NAT1*10* increased ABP-induced cytotoxicity (Figure 4-9a) and *hprt* mutants (Figure 4-9b) compared to non-transfected cells. Significant differences between NATb/*NAT1*4* and *NATb/NAT1*10* were not observed, although, NATb/*NAT1*10* ABP-induced *hprt* mutants were higher than NATb/*NAT1*4* (Figure 4-9b).

Three biotinylated RNA probes were used to determine the polyadenylation pattern of *NAT1*4*, *NAT1*10*, and *NAT1*10B* (NATa and NATb constructs) in transiently transfected UV5/1A1 cells in an RNase Protection assay (Figure 4-10). RNase

Protection assays detected no difference in polyadenylation site usage between RNA isolated from CHO cells transfected with NATb/*NAT1*4 or* NATb/*NAT1*10* (Figure 4-10 b-d). Bands were detected that correspond to mRNAs utilizing polyadenylation signals located at positions 1028, 1088, 1209, 1248, and 1613 nts. As expected, bands corresponding to PolyA Signal 1 located at position 1028 (215 nucleotides), PolyA Signal 2 located at position 1088 (284 nucleotides), PolyA Signal 3 located at position 1209 (118 nucleotides), PolyA Signal 4 located at position 1248 (163 nucleotides) and PolyA Signal 5 located at position 1613 (252 nucleotides) were observed for all constructs. Full length probe 1 (371 nucleotides) and full length probe 2 (388 nucleotides) was observed for *NAT1*4*, *NAT1*10*, and *NAT1*10*B (NATa and NATb) (Figure 4-10 b, c). Full length protection of probe 3 was observed only in *NAT1*10B* (NATa and NATb constructs) transfected cells (369 nucleotides) (Figure 4-10d). No band was observed in the lane with Yeast RNA (negative control) for any probe.

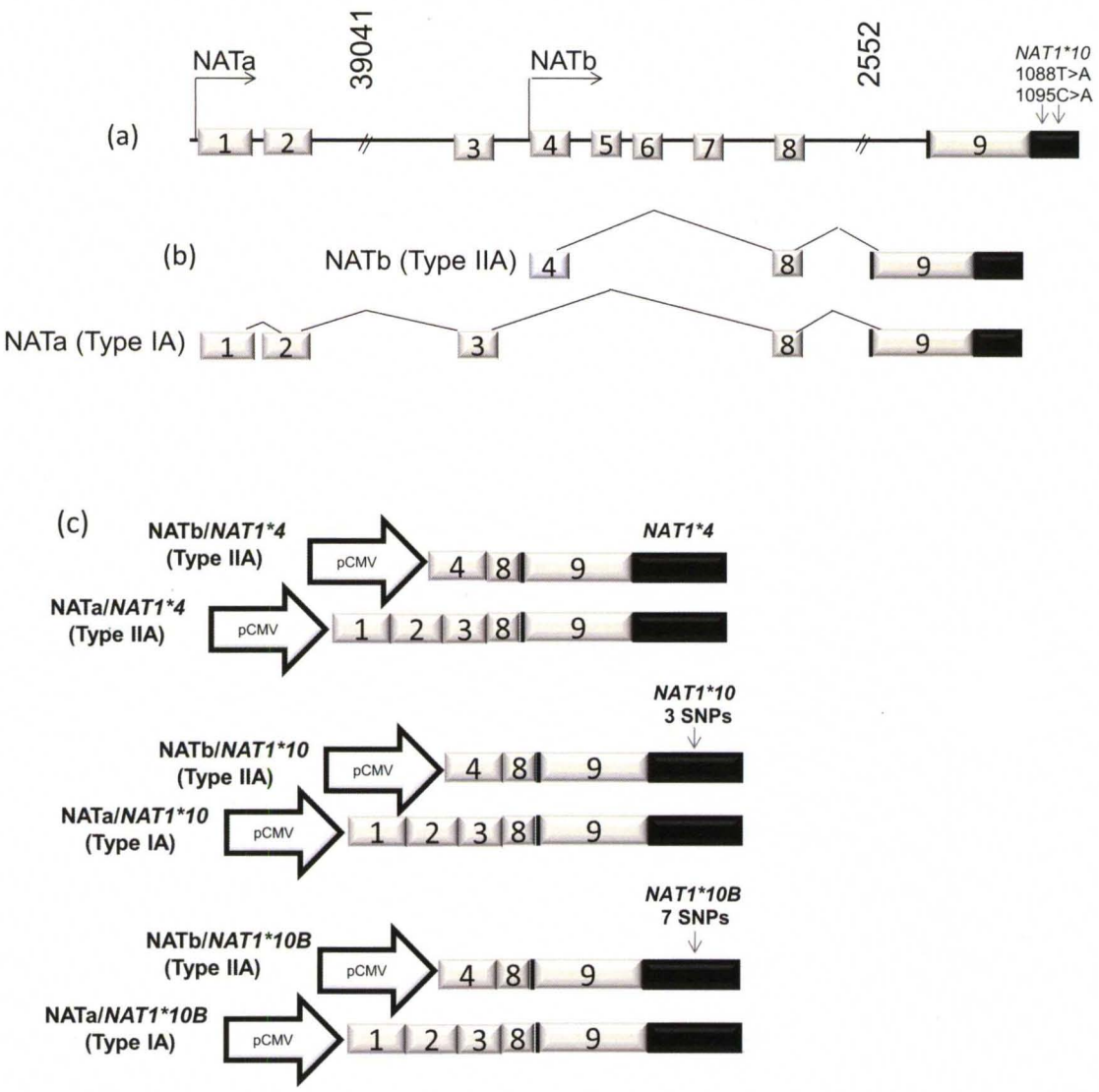

Figure 4-1 Genomic organization of NAT1 gene

(a) Genomic organization of NAT1 gene (b) Type I and Type II NAT1 transcripts (c) NATb and NATa *NAT1*4*, *NAT1*10,* and *NAT1*10B* constructs. (Adapted from Butcher et al., 2005). *NAT1*10* SNPs include T1088A, C1095A, and T1191G. Additional *NAT1*10B* polymorphisms include A1642C, ΔCT1647, C1716T and A1735T.

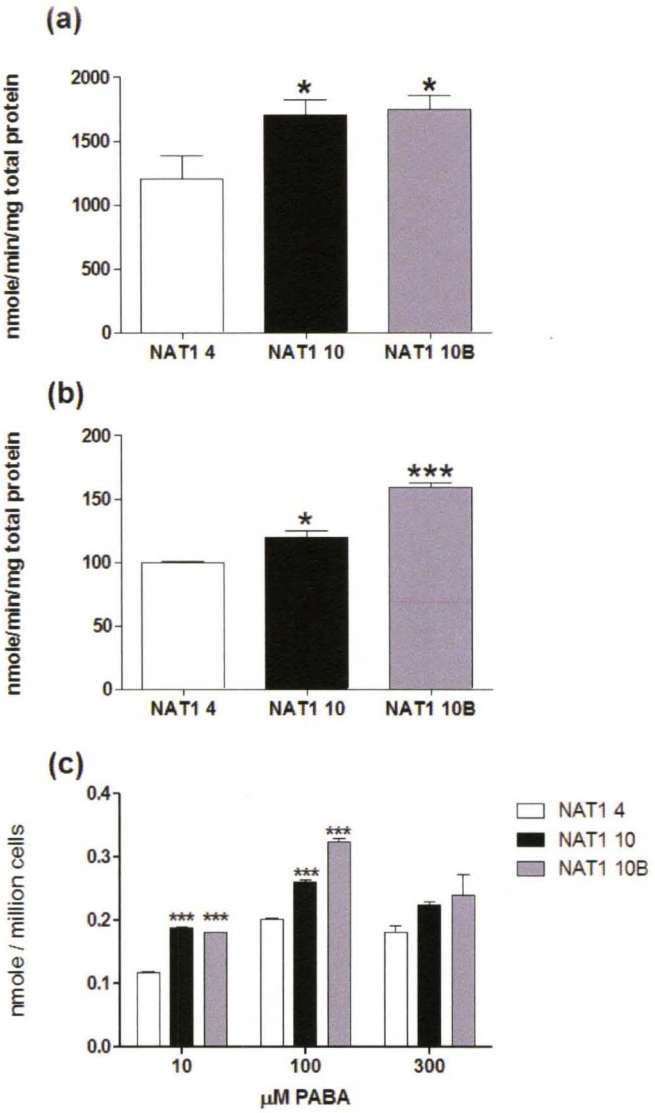

Figure 4-2: *N*-acetylation of PABA by NAT1 4 and NAT1 10 in NATb constructs

NATb activity. *N*-acetylation of PABA in UV5/1A1 cells expressing *NAT1*4* (open bars), *NAT1*10* (closed bars) and *NAT1*10B* (grey bars). (a) PABA *N*-acetylation (*in vitro*) activity following transient transfection with pcDNA5/FRT; (b) PABA *N*-acetylation activity (*in vitro*) following stable transfection with pcDNA5/FRT; (c) PABA *N*-acetylation (*in situ)* following stable transfection with pcDNA5/FRT. Each bar represents mean ± S.E.M. for three transient transfections (a) or three separate collections performed in triplicate (b and c) Significantly higher than NAT1 4 denoted by *$p<0.05$ and ***$p<0.0001$ following analysis with one-way ANOVA.

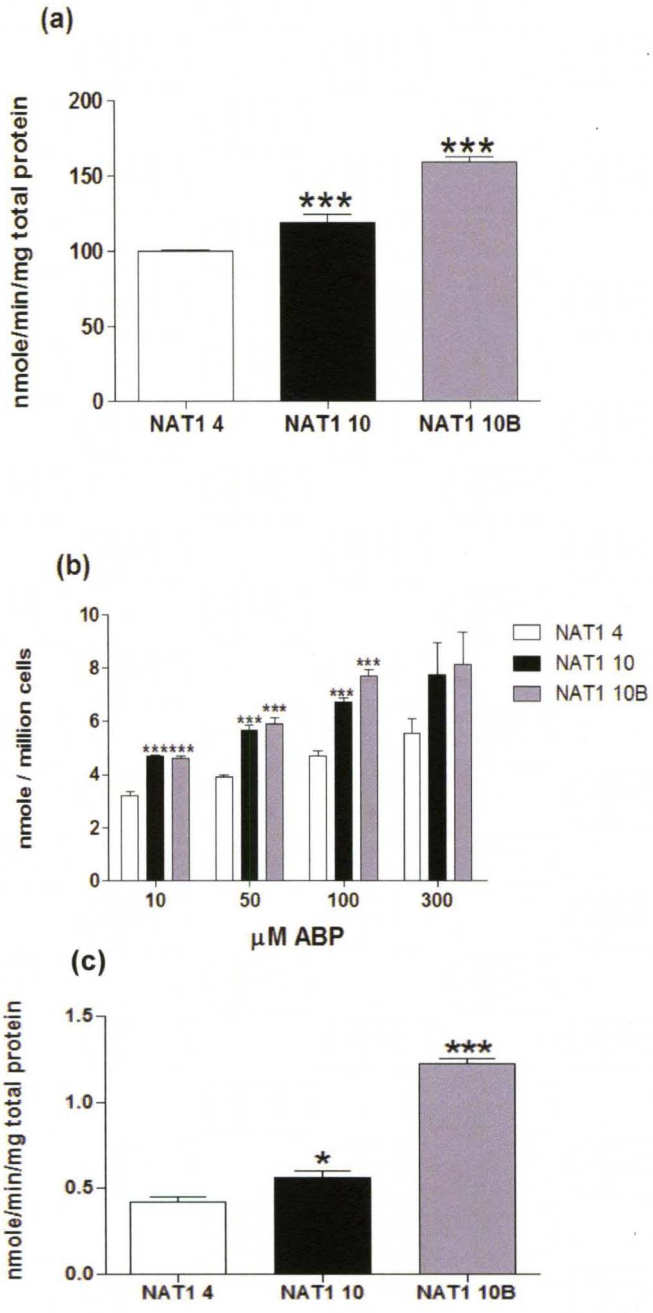

Figure 4-3: *N*- and *O*- ABP acetylation by NAT1 4 and NAT1 10 in NATb constructs

NATb activity. *N*- and *O*-acetylation of ABP and *N*-OH-ABP following stable transfection in UV5/1A1 cells transfected with *NAT1*4* (open bars), *NAT1*10* (closed bars) and *NAT1*10B* (grey bars) in NATb constructs. (a) ABP *N*-acetylation activity (*in vitro*); (b) ABP *N*-acetylation (*in situ*); (c) *O*-acetylation of *N*-OH-ABP (*in vitro*). Each bar represents mean ± S.E.M. for three separate collections performed in triplicate. Significantly higher than NAT1 4 denoted by *$p<0.05$ and ***$p<0.0001$ following analysis with one-way ANOVA.

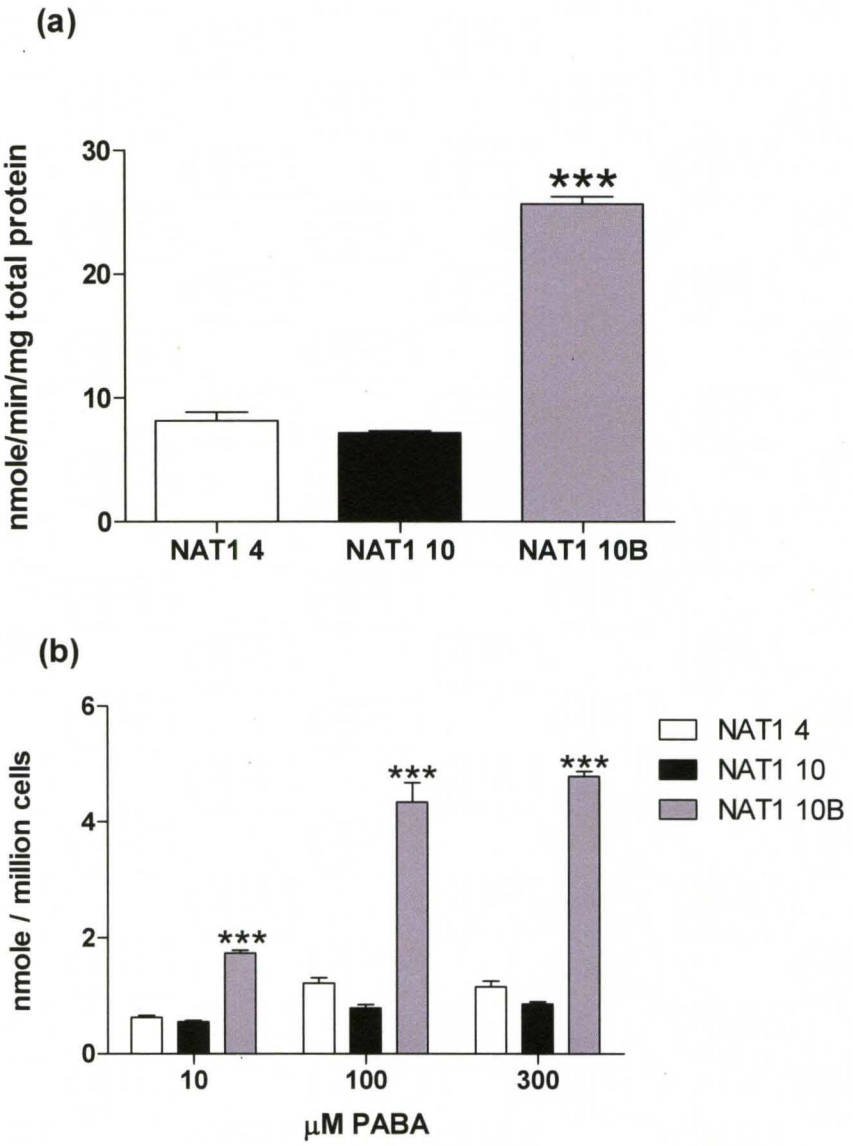

Figure 4-4: *N*-acetylation by NAT1 4 and NAT1 10 in NATa constructs

NATa activity. *N*-acetylation of PABA UV5/1A1 cells stably transfected with *NAT1*4* (open bars), *NAT1*10* (closed bars) and *NAT1*10B* (grey bars) in NATa. (a) PABA *N*-acetylation activity (*in vitro*) and (b) PABA *N*-acetylation (*in situ*). Each bar represents mean ± S.E.M. for three separate collections performed in triplicate. Significantly higher than NAT1 4 denoted by ***p<0.0001 following analysis with one-way ANOVA.

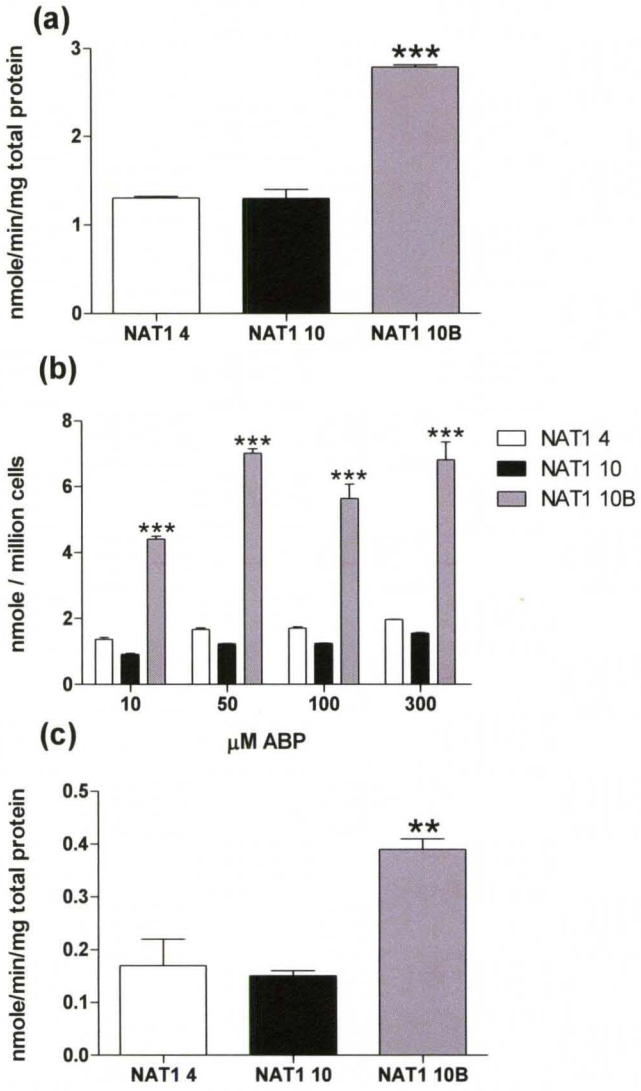

Figure 4-5: *N*- and *O*- ABP acetylation by NAT1 4 and NAT1 10 in NATa constructs

NATa activity. *N*- and *O*-acetylation of ABP and *N*-OH-ABP following stable transfection in UV5/1A1 cells transfected with *NAT1*4* (open bars), *NAT1*10* (closed bars) and *NAT1*10B* (grey bars) in NATa constructs. (a) ABP *N*-acetylation activity (*in vitro*); (b) ABP *N*-acetylation (*in situ*); (c) *O*-acetylation of *N*-OH-ABP (*in vitro*). Each bar represents mean ± S.E.M. for three separate collections performed in triplicate. Significantly higher than NAT1 4 denoted by *p<0.05 and ***p<0.0001 following analysis with one-way ANOVA.

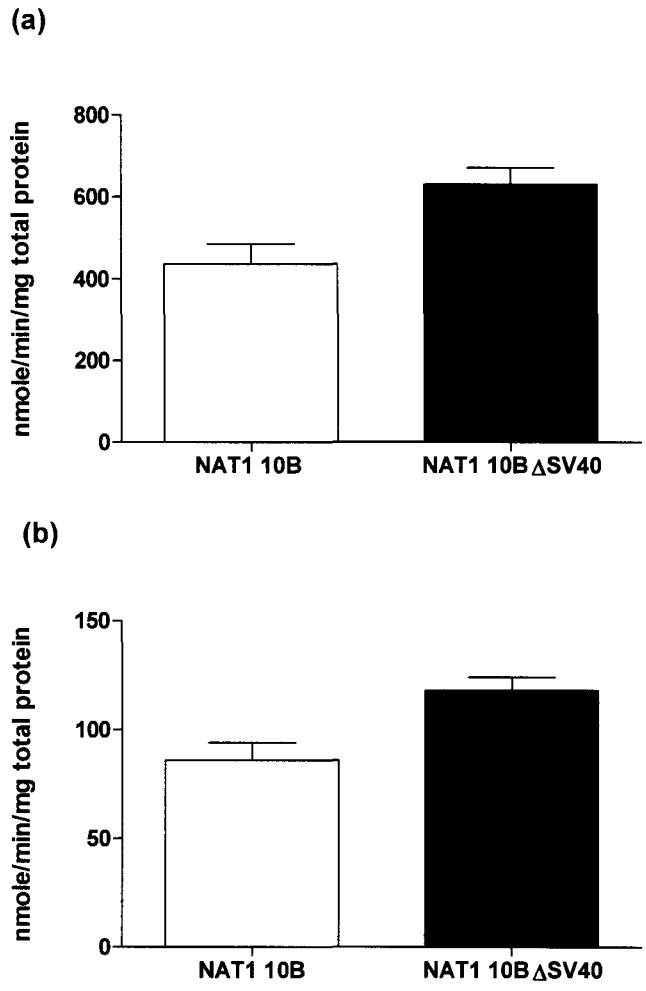

Figure 4-6: NAT1 10BΔSV40 *N*-acetylation in transiently transfected cells

PABA *N*-acetylation *in vitro* of UV5/1A1 cells transiently transfected with *NAT1*10B* (open bars) or *NAT1*10B* ΔSV40 polyadenylation site (closed bars) in NATb constructs (a) or NATa constructs (b). Error bars represent one collection performed in triplicate and significance testing was done using a student's t-test.

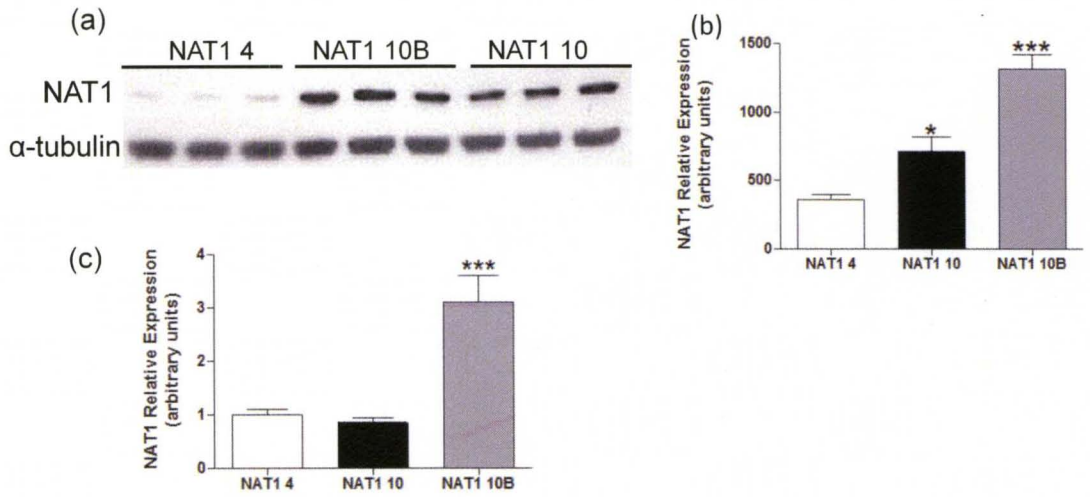

Figure 4-7: NAT1 protein expression of NAT1 4 and NAT1 10

Representative western blot of NAT1 4, NAT1 10, and NAT1 10B expression in NATb constructs (a) and densitometric analysis of NATb constructs (b) and NATa constructs (c). Each bar represents mean ± SEM of 1 or 2 western blots performed in triplicate. Analysis done with Quantity One software (BioRad). Significantly higher than NAT1 4 denoted by *$p<0.05$ and ***$p<0.0001$ following analysis with one-way ANOVA.

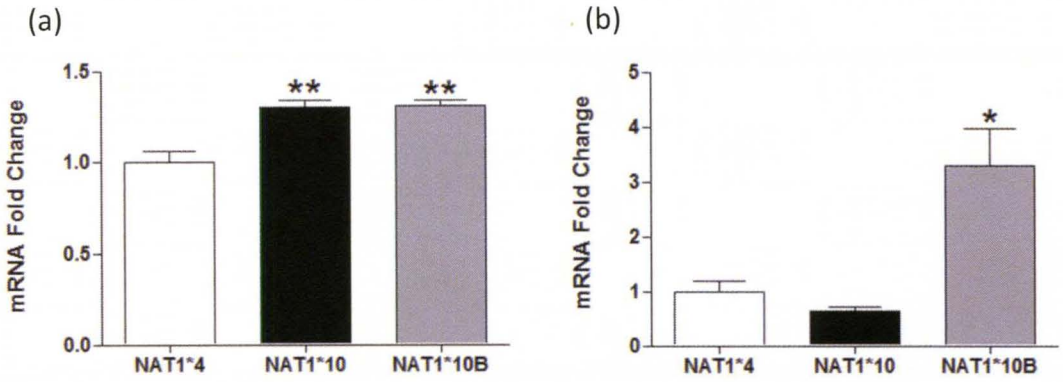

Figure 4-8: NAT1 mRNA levels of *NAT1*4* and *NAT1*10*

NAT1 mRNA expression levels of UV5/1A1 cells stably transfected with *NAT1*4* (open bars), *NAT1*10* (closed bars) or *NAT1*10B* (grey bars) in NATb (a) or in NATa (b) constructs. Each bar represents mean ± S.E.M. for 3 determinations. Significantly higher than NAT1 4 denoted by *$p<0.05$ or **$p<0.001$ following analysis by one-way ANOVA.

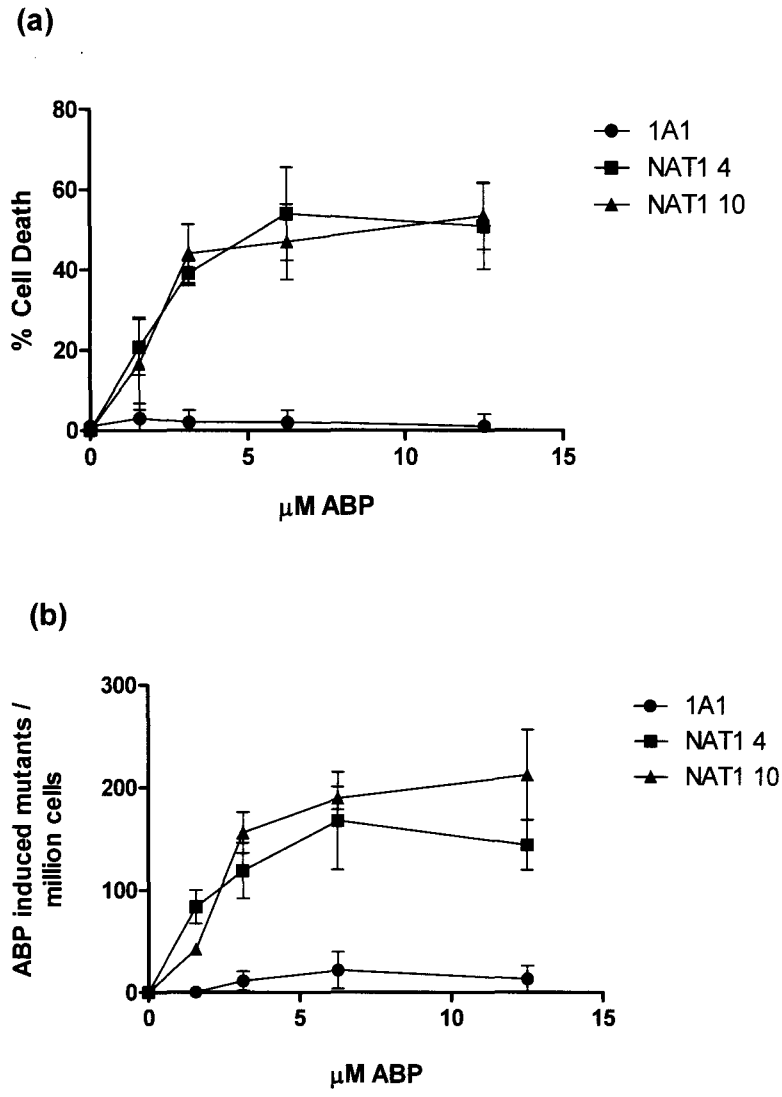

Figure 4-9: ABP-induced cytotoxicity and mutants

(a) ABP-induced cytotoxicity and (b) ABP-induced *hprt* mutants per million cells in UV5/1A1 cells stably expressing *CYP1A1 only* (●), *CYP1A1/NAT1*4* (■), and *CYP1A1 /NAT1*10* (▲) in NATb constructs. Each data point represents mean ± S.E.M. for three determinations.

(a)

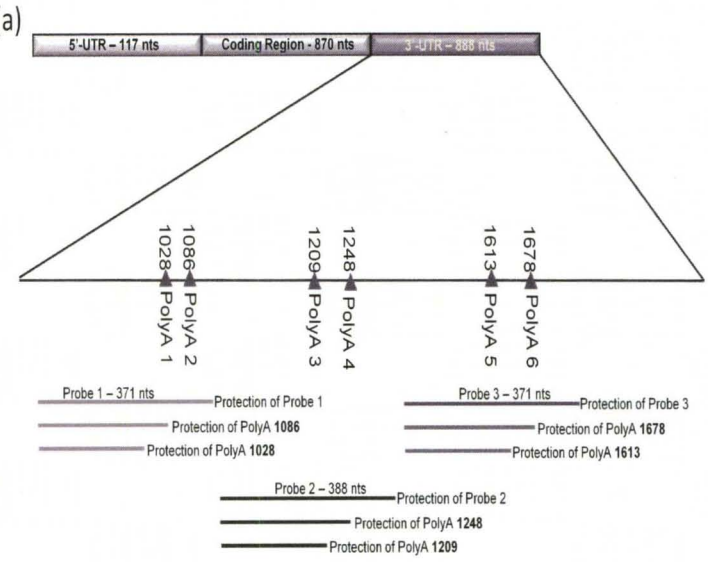
5'-UTR – 117 nts
Coding Region - 870 nts
3'-UTR – 888 nts
1028
1086
1209
1248
1613
1678
PolyA 1
PolyA 2
PolyA 3
PolyA 4
PolyA 5
PolyA 6
Probe 1 – 371 nts
Protection of Probe 1
Protection of PolyA 1086
Protection of PolyA 1028
Probe 3 – 371 nts
Protection of Probe 3
Protection of PolyA 1678
Protection of PolyA 1613
Probe 2 – 388 nts
Protection of Probe 2
Protection of PolyA 1248
Protection of PolyA 1209

(b)

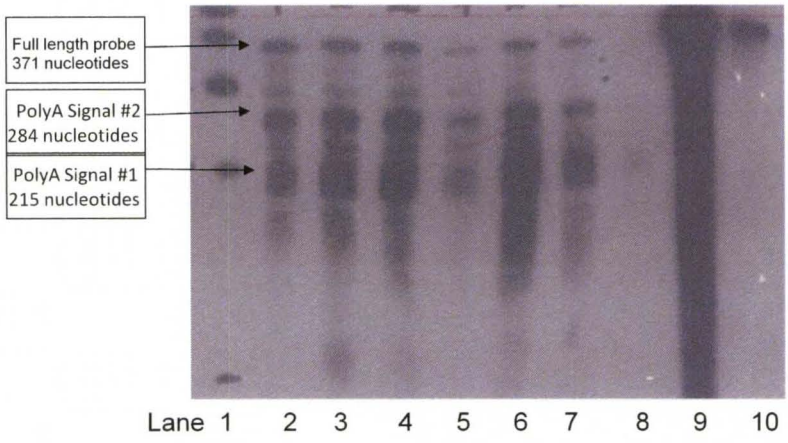
Full length probe
371 nucleotides
PolyA Signal #2
284 nucleotides
PolyA Signal #1
215 nucleotides
Lane 1 2 3 4 5 6 7 8 9 10

(c)

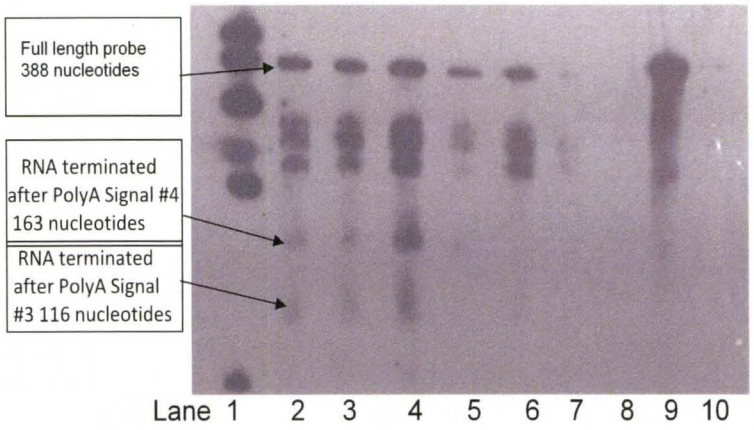

(d)

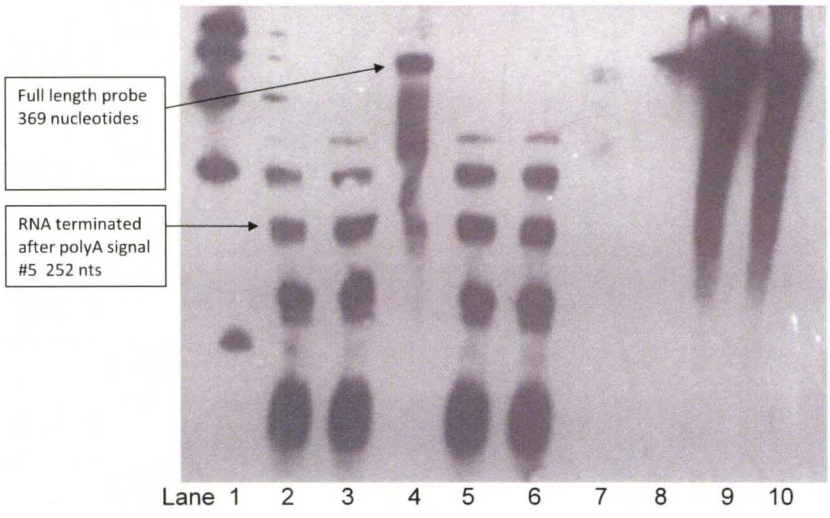

Figure 4-10: RNase protection assay of *NAT1*4*, *NAT1*10*, and *NAT1*10B*

An RNase protection assay examining pattern of polyadenylation usage. (a) Schematic representation of NAT1 3'-UTR and the probes used for the RNase protection assay. Lane 1 contains a biotinylated marker, lane 2 contains RNA isolated from transiently transfected with lane 2 *NAT1*4*, lane 3 *NAT1*10*, lane 4 *NAT1*10B* in NATb constructs, lane 5 with *NAT1*4*, lane 6 with *NAT1*10*, and lane 7 with *NAT1*10B* in NATa constructs. Lanes 8-10 are control lanes; lane 8 contains yeast (no target) RNA, lane 9 contains no RNase and lane 10 is probe alone. Lanes 2 – 8 were all hybridized to probe and treated with RNAse. (b) The 1st and 2nd polyadenylation sites were mapped with probe 1. (c) The 3rd and 4th polyadenylation sites were mapped with probe 2. (d) The 5th and 6th polyadenylation sites were mapped with probe 3.

Table 4-1: *NAT1*10* and *NAT1*10B* Polymorphisms

	Nucleotide Position						
Allele	1088	1095	1191	1642	1647	1716	1735
*NAT1*4*	T	C	G	A	CT	C	A
*NAT1*10*	A	A	T	A	CT	C	A
*NAT1*10B*	A	A	T	C	ΔCT	T	T

Primer	Use	Sequence
Lkm40P1	NATb 5-'UTR forward specific PCR	5'-GGCCGCGGCATTCAGTCTAGTTCCTGGTTGCC-3'
P1 Fwd Inr NheI	NATb 5'-UTR forward specific nested PCR	5'TTTAAAGCTAGCATTCAGTCTAGTCTAGTTCCTGGTTGCCGGCT-3'
Lkm41P3	NATa 5'-UTR forward specifc PCR	5'-GGCCGCGGAACACATTCTGCTCAAATAAGCCT-3'
P3 Fwd Inr NheI	NATa 5'-UTR forward specific nested PCR	5'TTAATGCTAGCAACACATTCTGCTCAAATAAAGCCTAGG-3'
NAT1 (3') ORF Rev	NATa/NATb 5'-UTR reverse PCR	5'-TTCCTCACTCAGAGTCTTGAACTCTATT-3'
NAT1 (3') ORF For	NAT1 coding region forward PCR	5'-AGACATCTCCATCATCTGTGTTTACTAGT-3'
pcDNA5 FRTdistal Rev	NAT1 3'-UTR reverse PCR	5'-CGTGGGGATACCCCCTAGA
NAT1 KPN-Rev	NAT1 3'-UTR reverse nested PCR	5'-ATAGTAGGTACCTCTGAATTATAGATAAGCAAAGATTCAGATTCT-3'
NAT1 KPN-Rev*10B	NAT1 3'-UTR reverse nested PCR	5'-ATAGTAGGTACCTCTGAATTATAGATAAGCAAAGATACAGATTCT-3'
NAT1 total spliced Forward	NAT1 specific forward q-RT-PCR	5'-GAATTCAAGCCAGGAAGAAGCA-3'
NAT1 total spliced Reverse	NAT1 specific reverse q-RT-PCR	5'-TCCAAGTCCAATTTGTTCCTAGACT-3'
NAT1 TAQMAN probe	TAQMAN probe for NAT1 total splice	6FAM-5'-CAATCTGTCTTCTGGATTAA-3'MGBNFQ

Table 4-2: Primers used to construct *NAT1*4*, *NAT1*10*, and *NAT1*10B*

Primers used to construct *NAT1*4*, *NAT1*10*, and *NAT1*10B* in NATa and NATb Type transcript constructs and for RT-PCR. These allelic constructs were then ligated into pcDNA5/FRT expression vectors.

DISCUSSION

*NAT1*10* has been associated with higher risk for many different forms of cancer including breast, colorectal, prostate and urinary bladder cancers, gastric adenocarcinoma, and non-Hodgkins lymphoma. Several studies suggest that *NAT1*10* has higher acetylation capacity than the referent allele, *NAT1*4*, (Bell et al., 1995a), while others have reported no difference (de Leon et al., 2000). Increased *O*-acetylation activity could result in an increased amount of unstable intermediates able to form DNA adducts. Because *NAT1*10* has a high allelic frequency in so many populations (Cascorbi et al., 2001; Lo-Guidice et al., 2000; Vaziri et al., 2001; Zhangwei et al., 2006), it is important to identify the risk that is associated with *NAT1*10*. To better understand the risk associated with *NAT1*10* and cancer, *NAT1*10* acetylation activity was studied (*in vitro* and *in situ*) using complete NATb and NATa mRNA constructs to better mimic *in vivo* acetylation.

Differences between the referent protein, NAT1 4, and the variants, NAT1 10 and NAT1 10B, have been studied in UV5/1A1 CHO cells transiently and stably transfected with NATb and NATa type mRNA. The effect that *NAT1*10* polymorphisms exert on mRNA and protein expression and enzymatic activity appears to be transcript dependent. We have shown increased *N*- and *O*- acetylation and increased mRNA and protein expression for NAT1 10 and NAT1 10B when compared to NAT1 4 in cells transfected in the NATb type mRNA. This was observed in both transiently and stably transfected cells. In contrast, no significant difference was observed between NAT1 10 and NAT1 4 in cells transfected with the NATa type mRNA. However, a significant difference was observed between NAT1 4 and NAT1 10B in cells transfected with the NATa mRNA. This effect of mRNA type on *NAT1*10* polymorphisms is a novel finding. It is possible that mRNA type may be partly responsible for discrepancies concerning

*NAT1*10* phenotype. Studies have reported allele-specific differences in transcription factor binding levels (McDaniell et al., 2010). It is possible that allele specific transcription differences could be dependent on transcript type as well.

In addition to importance of transcript type on *NAT1*10* phenotype, we also report on additional polymorphisms located in the 3'-UTR in an allele referred to in this dissertation as *NAT1*10B. NAT1*10B* has 4 polymorphisms in addition to the T>A1088, C>A1095 and G>T1191 that characterize *NAT1*10. NAT1*10B* also includes A>C1642, ΔCT1647, C>1716, and A>T1735. Cells transfected with *NAT1*10B* resulted in increased enzymatic activity, mRNA and protein expression compared to *NAT1*10.* Because the additional polymorphisms found in *NAT1*10B* are not routinely screened for, it is possible that some of the discrepancies concerning *NAT1*10* phenotype could also be attributed to misidentification of *NAT1*10B* as *NAT1*10.*

There are 6 potential polyadenylation signals located in the region 3' to the NAT1 ORF. NAT1 transcripts have been identified that utilize the first 5 of the 6 potential polyadenylation signals using dbSNP. The $T^{1088}A$ SNP present in *NAT1*10* alters the 2nd polyadenylation signal (AATAAA – AAAAAA). It has been suggested (Boukouvala and Sim, 2005) that this change in polyadenylation signal may increase the stability of the *NAT1*10* RNA which could be responsible for any differences seen between *NAT1*10* and *NAT1*4* in acetylation capacity. To examine the *NAT1*10* polyadenylation pattern, RNase Protection Assays (RNAP) were conducted. RNAP assays were carried out in cells transfected with *NAT1*4*, *NAT1*10*, and *NAT1*10B* in both NATb and NATa constructs. Bands were observed corresponding to the first 5 potential polyadenylation signals and no qualitative differences were observed between *NAT1*4* and *NAT1*10* in either the NATb or NATa construct. However, there was a difference in *NAT1*10B* in both NATb and NATa constructs using probe 3. Full length protection of probe 3 was

observed for *NAT1*10B* but not for *NAT1*10* or *NAT1*4* in cells transfected with both NATb and NATa constructs. This indicates the presence of *NAT1*10B* transcripts that extend beyond probe 3. Other bands present may be due to either RNA cruciform structures or probe-probe interactions. While there were no quantitative differences observed, there could be some quantitative differences that were not large enough to be detected by RNAP.

To ensure that differences in *NAT1*10*B activity compared to *NAT1*4* and *NAT1*10* were not caused by the presence of the strong SV40 polyadenylation signal in the pcDNA5/FRT expression vector, it was removed from the vector and then ligated together. Transient transfections confirmed that there were no differences in *NAT1*10B* with or without the presence of the SV40 polyadenylation signal.

Because the *NAT1*10* allele has high allelic frequency in many populations, clearly defining the *NAT1*10* phenotype would allow cancer risk and other toxicities related to environmental arylamine exposure to be better understood. We have shown that NATb/*NAT1*10* has higher enzymatic activity and mRNA and protein expression compared to NATb/*NAT1*4*. *NAT1*10* has been associated with increased risk for many cancers. This higher activity could be partly responsible for the increased risk associated for individuals possessing *NAT1*10*. Butcher et al. suggests that there may be cell-type specific expression of an RNA-binding protein that would allow increased mRNA stability in some cell types (Butcher et al., 2008). It has also been suggested that *NAT1*10* transcripts have enhanced stability compared to *NAT1*4* in some cell lines and not in others. This could be reflective of cell-type specific expression of RNA-binding proteins that affect stability of the NAT1 transcript. Cell-type may also be important for differences between 5'-UTR and allele interactions. Therefore, cell-type may play an important role in *NAT1*10* expression and activity. Future studies should be done to

determine in what cell types *NAT1*10* has higher levels of steady-state mRNA, protein and activity. Interaction of RNA-binding protein is also likely to be different between NATa and NATb transcripts so cell-types expressing both transcript types likely have complicated *NAT1*10* regulation.

CHAPTER 5: GENERAL DISCUSSION

Previous studies have failed to elucidate a clear correlation between genotype and phenotype of NAT1 alleles. The experiments in this dissertation have examined the phenotype of NAT1 variant alleles, *NAT1*10, NAT1*10B* and *NAT1*14B* compared to the referent, *NAT1*4*. This was accomplished utilizing constructs that mimic full length NAT1 mRNA including the 5'-UTR, ORF, and 3'-UTR. In contrast to utilizing constructs that contain only the ORF, the experiments in this dissertation have allowed natural mRNA folding and stability to occur by utilizing full length mRNA constructs.

Differences in NATa and NATb transcripts containing the referent allele, *NAT1*4*, were observed. Transient and stable transfections of NATb/*NAT1*4* resulted in significantly more *N*- and *O*- acetylation, protein and mRNA expression, ABP-induced DNA adducts and ABP-induced *hprt* mutants. Following studies comparing the two mRNA of *NAT1*4*, variant alleles were studied in the same NATa and NATb constructs.

Differences in *NAT1*10* compared to *NAT1*4* were mRNA-type dependent. In the NATb mRNA, *NAT1*10* and *NAT1*10B* both had higher *N*- and *O*- acetylation, protein and mRNA expression than *NAT1*4*. In the NATa mRNA, *NAT1*10B* had higher *N*- and *O*- acetylation, protein and mRNA expression than *NAT1*10* and *NAT1*4*. There was no difference between *NAT1*10* and *NAT1*4* in the NATa mRNA. This finding emphasizes the importance of studying each allele in combination with full length mRNA. Failure to study mRNA type in combination with alleles may have contributed to some of the ambiguous results of *NAT1*10* phenotype in previous literature. Also, the additional

polymorphisms included in the *NAT1*10B* genotype may further complicate *NAT1*10* phenotype. To comprehensively study the correlation between *NAT1*10* genotype and phenotype, the studies in this dissertation reveal the need to genotype additional polymorphisms in the *NAT1*10* 3'-UTR.

Differences between *NAT1*4* and *NAT1*14B* were observed in NATb mRNA. Lower V_{max} for NAT1 14B toward all substrates was observed when compared with NAT1 4. This indicates that at high substrate concentrations, NAT1 14B has lowered acetylation capacity compared to NAT1 4. Lower V_{max}/K_m (catalytic efficiency) for NAT1 14B toward PABA was observed when compared to NAT1 4. In contrast, higher V_{max}/K_m for NAT1 14B toward ABP and *N*-OH-ABP was observed when compared to NAT1 4. This indicates that at low substrate concentrations (concentrations well below K_m) NAT1 14B has higher acetylation capacity compared to NAT1 4. These studies revealed that *NAT1*14B* acetylator phenotype is dependent on both substrate and substrate concentration. Because NAT1 14B resulted in increased ABP-induced DNA adducts, our results suggest that individuals possessing the *NAT1*14B* allele likely have increased risk compared to those who are homozygous for *NAT1*4* following low (environmental) dose exposure to ABP. NAT1 14B is not simply associated with "slow acetylation" but rather is substrate dependent, since NAT1 14B exhibits lower *N*-acetylation catalytic efficiency of PABA but higher *N*- and *O*-acetylation catalytic efficiency as well as DNA adducts following exposure to the human carcinogen ABP.

Limitations and recommended future studies

The UV5 cell line is a good model for many reasons. It is a mammalian cell line, appropriate for studying DNA damage due to its nucleotide excision repair deficiency and does not endogenously express NAT1 or NAT2. However, because the 5'-UTR regulation reported here could be cell type specific, this regulation should be studied in human cell lines. Also, real-time RT-PCR on human cell lines and human tissues should be utilized to determine relative amounts of NATa and NATb type transcripts. This should be done in healthy and cancerous tissue to determine if NATa transcripts are upregulated differentially from NATb transcripts. This would be a start to determining the role of two types of transcripts.

Efficient *N*-acetyltransferase purification methods would permit a more complete evaluation of human enzyme kinetics. All kinetic studies described in this dissertation were carried out with whole cell lysate. The ability to purify the NAT1 protein would result in more accurate characterizations. *NAT1*14B* studies were only conducted in NATb mRNA. Future studies should be performed using *NAT1*14B* expressed in NATa mRNA.

The only known NAT1 substrate is para-aminobenzoylglutamate (PABG), which is a catabolite of folate. It has been suggested that NAT1 polymorphisms are associated with birth defects due to the metabolism of PABG. Kinetic parameters of PABG were not able to be determined using current methods of HPLC separation. More sensitive methods of measurement are required to determine NAT1 PABG acetylation by NAT1 expressed in UV5/1A1 cells. A colorimetric assay such as the serotonin *N*-acetyltransferase (De Angelis et al., 1998) could be adapted or developed for this purpose. NAT1 4 and NAT1 14B kinetic parameters for PABG should be determined as well as NAT1 10 and NAT1 10B PABG acetylation.

The *in vitro* kinetics were determined at 100 μM acetyl CoA. The cellular concentration of acetyl CoA should be determined to better mimic *in vivo* kinetic behavior. This could be examined using an indirect detection method such as conversion of acetyl CoA to CoA and then reacting the CoA to NADH which can then react with a fluorescent probe (Abnova, Tapei, Taiwan).

The RNase protection assays were performed with RNA from transiently transfected cells. More assays should be performed using stably transfected cells and RNA from other sources, including human tissue. Although miRNA binding sites were not predicted to be located on any *NAT1*10* SNPs using predictive software, miRNA regulation of *NAT1*10* should still be examined. Regulation by miRNA could be analyzed by northern hybridization (Lim et al., 2003), microarray analysis (Krichevsky et al., 2003; Liu et al., 2004) or stem-loop RT-PCR (Chen et al., 2005).

Transcription factors associated with each transcript should also be examined. Because transcription factors have been shown to be allele specific (McDaniell et al., 2010), differences in transcription factors should be examined for each allele and in each transcript form. This study used NATb (type IIA) and NATa (type IA) only. Future studies should examine other NAT1 mRNA types in combination with variant alleles. Future studies should also genotype for *NAT1*10B* separately from *NAT1*10*. Because the *NAT1*10B* SNPs occur with linkage disequilibrium, this could be accomplished by designing an RT-PCR assay to detect C1642A as a flag SNP.

REFERENCES

Adam, P.J., Berry, J., Loader, J.A., Tyson, K.L., Craggs, G., Smith, P., De Belin, J., Steers, G., Pezzella, F., Sachsenmeir, K.F., *et al.* (2003). Arylamine N-acetyltransferase-1 is highly expressed in breast cancers and conveys enhanced growth and resistance to etoposide in vitro. Mol Cancer Res *1*, 826-835.

Adelman, K., La Porta, A., Santangelo, T.J., Lis, J.T., Roberts, J.W., and Wang, M.D. (2002). Single molecule analysis of RNA polymerase elongation reveals uniform kinetic behavior. Proc Natl Acad Sci U S A *99*, 13538-13543.

Aida, M., Chen, Y., Nakajima, K., Yamaguchi, Y., Wada, T., and Handa, H. (2006). Transcriptional pausing caused by NELF plays a dual role in regulating immediate-early expression of the junB gene. Mol Cell Biol *26*, 6094-6104.

Ambros, V. (2004). The functions of animal microRNAs. Nature *431*, 350-355.

Ambrosone, C.B., Abrams, S.M., Gorlewska-Roberts, K., and Kadlubar, F.F. (2007). Hair dye use, meat intake, and tobacco exposure and presence of carcinogen-DNA adducts in exfoliated breast ductal epithelial cells. Arch Biochem Biophys *464*, 169-175.

Badawi, A.F., Hirvonen, A., Bell, D.A., Lang, N.P., and Kadlubar, F.F. (1995). Role of aromatic amine acetyltransferases, NAT1 and NAT2, in carcinogen-DNA adduct formation in the human urinary bladder. Cancer Res *55*, 5230-5237.

Barker, D.F., Husain, A., Neale, J.R., Martini, B.D., Zhang, X., Doll, M.A., States, J.C., and Hein, D.W. (2006). Functional properties of an alternative, tissue-specific promoter for human arylamine N-acetyltransferase 1. Pharmacogenet Genomics *16*, 515-525.

Bell, D.A., Badawi, A.F., Lang, N.P., Ilett, K.F., Kadlubar, F.F., and Hirvonen, A. (1995a). Polymorphism in the N-acetyltransferase 1 (NAT1) polyadenylation signal: association of NAT1*10 allele with higher N-acetylation activity in bladder and colon tissue. Cancer Res *55*, 5226-5229.

Bell, D.A., Stephens, E.A., Castranio, T., Umbach, D.M., Watson, M., Deakin, M., Elder, J., Hendrickse, C., Duncan, H., and Strange, R.C. (1995b). Polyadenylation

polymorphism in the acetyltransferase 1 gene (NAT1) increases risk of colorectal cancer. Cancer Res *55*, 3537-3542.

Bendaly, J., Doll, M.A., Millner, L.M., Metry, K.J., Smith, N.B., Pierce, W.M., Jr., and Hein, D.W. (2009). Differences between human slow N-acetyltransferase 2 alleles in levels of 4-aminobiphenyl-induced DNA adducts and mutations. Mutat Res *671*, 13-19.

Biehl, J.P., and Sklavem, J.H. (1953). Toxicity of isoniazid. Am Rev Tuberc *68*, 296-297.

Blum, M., Grant, D.M., McBride, W., Heim, M., and Meyer, U.A. (1990). Human arylamine N-acetyltransferase genes: isolation, chromosomal localization, and functional expression. DNA Cell Biol *9*, 193-203.

Boissy, R.J., Watson, M.A., Umbach, D.M., Deakin, M., Elder, J., Strange, R.C., and Bell, D.A. (2000). A pilot study investigating the role of NAT1 and NAT2 polymorphisms in gastric adenocarcinoma. Int J Cancer *87*, 507-511.

Bouchardy, C., Mitrunen, K., Wikman, H., Husgafvel-Pursiainen, K., Dayer, P., Benhamou, S., and Hirvonen, A. (1998). N-acetyltransferase NAT1 and NAT2 genotypes and lung cancer risk. Pharmacogenetics *8*, 291-298.

Boukouvala, S., and Fakis, G. (2005). Arylamine N-acetyltransferases: what we learn from genes and genomes. Drug Metab Rev *37*, 511-564.

Boukouvala, S., and Sim, E. (2005). Structural analysis of the genes for human arylamine N-acetyltransferases and characterisation of alternative transcripts. Basic Clin Pharmacol Toxicol *96*, 343-351.

Butcher, N.J., Arulpragasam, A., Goh, H.L., Davey, T., and Minchin, R.F. (2005). Genomic organization of human arylamine N-acetyltransferase Type I reveals alternative promoters that generate different 5'-UTR splice variants with altered translational activities. Biochem J *387*, 119-127.

Butcher, N.J., Arulpragasam, A., and Minchin, R.F. (2004). Proteasomal degradation of N-acetyltransferase 1 is prevented by acetylation of the active site cysteine: a mechanism for the slow acetylator phenotype and substrate-dependent down-regulation. J Biol Chem *279*, 22131-22137.

Butcher, N.J., Tiang, J., and Minchin, R.F. (2008). Regulation of arylamine N-acetyltransferases. Curr Drug Metab *9*, 498-504.

Calvo, S.E., Pagliarini, D.J., and Mootha, V.K. (2009). Upstream open reading frames cause widespread reduction of protein expression and are polymorphic among humans. Proc Natl Acad Sci U S A *106*, 7507-7512.

Carmichael, S.L., Shaw, G.M., Yang, W., Iovannisci, D.M., and Lammer, E. (2006). Risk of limb deficiency defects associated with NAT1, NAT2, GSTT1, GSTM1, and NOS3 genetic variants, maternal smoking, and vitamin supplement intake. Am J Med Genet A *140*, 1915-1922.

Cascorbi, I., Roots, I., and Brockmoller, J. (2001). Association of NAT1 and NAT2 polymorphisms to urinary bladder cancer: significantly reduced risk in subjects with NAT1*10. Cancer Res *61*, 5051-5056.

Chen, C., Ridzon, D.A., Broomer, A.J., Zhou, Z., Lee, D.H., Nguyen, J.T., Barbisin, M., Xu, N.L., Mahuvakar, V.R., Andersen, M.R., *et al.* (2005). Real-time quantification of microRNAs by stem-loop RT-PCR. Nucleic Acids Res *33*, e179.

Chen, Y., Liu, L., Nguyen, K., and Fretland, A.J. (2011). Utility of intersystem extrapolation factors in early reaction phenotyping and the quantitative extrapolation of human liver microsomal intrinsic clearance using recombinant cytochromes P450. Drug Metab Dispos *39*, 373-382.

Clark, D.W. (1985). Genetically determined variability in acetylation and oxidation. Therapeutic implications. Drugs *29*, 342-375.

Cooper, S.J., Trinklein, N.D., Anton, E.D., Nguyen, L., and Myers, R.M. (2006). Comprehensive analysis of transcriptional promoter structure and function in 1% of the human genome. Genome Res *16*, 1-10.

Core, L.J., Waterfall, J.J., and Lis, J.T. (2008). Nascent RNA sequencing reveals widespread pausing and divergent initiation at human promoters. Science *322*, 1845-1848.

Davuluri, R.V., Suzuki, Y., Sugano, S., Plass, C., and Huang, T.H. (2008). The functional consequences of alternative promoter use in mammalian genomes. Trends Genet *24*, 167-177.

De Angelis, J., Gastel, J., Klein, D.C., and Cole, P.A. (1998). Kinetic analysis of the catalytic mechanism of serotonin N-acetyltransferase (EC 2.3.1.87). J Biol Chem *273*, 3045-3050.

de Leon, J.H., Vatsis, K.P., and Weber, W.W. (2000). Characterization of naturally occurring and recombinant human N-acetyltransferase variants encoded by NAT1. Mol Pharmacol *58*, 288-299.

Dhaini, H.R., and Levy, G.N. (2000). Arylamine N-acetyltransferase 1 (NAT1) genotypes in a Lebanese population. Pharmacogenetics *10*, 79-83.

Doench, J.G., and Sharp, P.A. (2004). Specificity of microRNA target selection in translational repression. Genes Dev *18*, 504-511.

Drapkin, R., Reardon, J.T., Ansari, A., Huang, J.C., Zawel, L., Ahn, K., Sancar, A., and Reinberg, D. (1994). Dual role of TFIIH in DNA excision repair and in transcription by RNA polymerase II. Nature *368*, 769-772.

Eisenthal, R., Danson, M.J., and Hough, D.W. (2007). Catalytic efficiency and kcat/KM: a useful comparator? Trends Biotechnol *25*, 247-249.

Evans, D.A., Manley, K.A., and Mc, K.V. (1960). Genetic control of isoniazid metabolism in man. Br Med J *2*, 485-491.

Feng, Z., Hu, W., Rom, W.N., Beland, F.A., and Tang, M.S. (2002). 4-aminobiphenyl is a major etiological agent of human bladder cancer: evidence from its DNA binding spectrum in human p53 gene. Carcinogenesis *23*, 1721-1727.

Fretland, A.J., Doll, M.A., Leff, M.A., and Hein, D.W. (2001). Functional characterization of nucleotide polymorphisms in the coding region of N-acetyltransferase 1. Pharmacogenetics *11*, 511-520.

Fretland, A.J., Doll, M.A., Zhu, Y., Smith, L., Leff, M.A., and Hein, D.W. (2002). Effect of nucleotide substitutions in N-acetyltransferase-1 on N-acetylation (deactivation) and O-acetylation (activation) of arylamine carcinogens: implications for cancer predisposition. Cancer Detect Prev *26*, 10-14.

Gago-Dominguez, M., Bell, D.A., Watson, M.A., Yuan, J.M., Castelao, J.E., Hein, D.W., Chan, K.K., Coetzee, G.A., Ross, R.K., and Yu, M.C. (2003). Permanent hair dyes and bladder cancer: risk modification by cytochrome P4501A2 and N-acetyltransferases 1 and 2. Carcinogenesis *24*, 483-489.

Gehring, N.H., Frede, U., Neu-Yilik, G., Hundsdoerfer, P., Vetter, B., Hentze, M.W., and Kulozik, A.E. (2001). Increased efficiency of mRNA 3' end formation: a new genetic mechanism contributing to hereditary thrombophilia. Nat Genet *28*, 389-392.

Ghoshal, A., Davis, C.D., Schut, H.A., and Snyderwine, E.G. (1995). Possible mechanisms for PhIP-DNA adduct formation in the mammary gland of female Sprague-Dawley rats. Carcinogenesis *16*, 2725-2731.

Grant, D.M., Hughes, N.C., Janezic, S.A., Goodfellow, G.H., Chen, H.J., Gaedigk, A., Yu, V.L., and Grewal, R. (1997). Human acetyltransferase polymorphisms. Mutat Res *376*, 61-70.

Grant, D.M., Lottspeich, F., and Meyer, U.A. (1989). Evidence for two closely related isozymes of arylamine N-acetyltransferase in human liver. FEBS Lett *244*, 203-207.

Guzzo, T.J., Bivalacqua, T.J., and Schoenberg, M.P. (2008). Bladder cancer and the aluminium industry: a review. BJU Int *102*, 1058-1060.

Hein, D.W., Doll, M.A., Fretland, A.J., Leff, M.A., Webb, S.J., Xiao, G.H., Devanaboyina, U.S., Nangju, N.A., and Feng, Y. (2000). Molecular genetics and epidemiology of the NAT1 and NAT2 acetylation polymorphisms. Cancer Epidemiol Biomarkers Prev *9*, 29-42.

Hein, D.W., Doll, M.A., Nerland, D.E., and Fretland, A.J. (2006). Tissue distribution of N-acetyltransferase 1 and 2 catalyzing the N-acetylation of 4-aminobiphenyl and O-acetylation of N-hydroxy-4-aminobiphenyl in the congenic rapid and slow acetylator Syrian hamster. Mol Carcinog *45*, 230-238.

Hein, D.W., Doll, M.A., Rustan, T.D., Gray, K., Feng, Y., Ferguson, R.J., and Grant, D.M. (1993). Metabolic activation and deactivation of arylamine carcinogens by recombinant human NAT1 and polymorphic NAT2 acetyltransferases. Carcinogenesis *14*, 1633-1638.

Hein, D.W., Leff, M.A., Ishibe, N., Sinha, R., Frazier, H.A., Doll, M.A., Xiao, G.H., Weinrich, M.C., and Caporaso, N.E. (2002). Association of prostate cancer with rapid N-acetyltransferase 1 (NAT1*10) in combination with slow N-acetyltransferase 2 acetylator genotypes in a pilot case-control study. Environ Mol Mutagen *40*, 161-167.

Hickman, D., Palamanda, J.R., Unadkat, J.D., and Sim, E. (1995). Enzyme kinetic properties of human recombinant arylamine N-acetyltransferase 2 allotypic variants expressed in Escherichia coli. Biochem Pharmacol *50*, 697-703.

Hoffmann, D., Djordjevic, M.V., and Hoffmann, I. (1997). The changing cigarette. Prev Med *26*, 427-434.

Horton, R.M., Hunt, H.D., Ho, S.N., Pullen, J.K., and Pease, L.R. (1989). Engineering hybrid genes without the use of restriction enzymes: gene splicing by overlap extension. Gene *77*, 61-68.

Hughes, N.C., Janezic, S.A., McQueen, K.L., Jewett, M.A., Castranio, T., Bell, D.A., and Grant, D.M. (1998). Identification and characterization of variant alleles of human acetyltransferase NAT1 with defective function using p-aminosalicylate as an in-vivo and in-vitro probe. Pharmacogenetics *8*, 55-66.

Husain, A., Barker, D.F., States, J.C., Doll, M.A., and Hein, D.W. (2004). Identification of the major promoter and non-coding exons of the human arylamine N-acetyltransferase 1 gene (NAT1). Pharmacogenetics *14*, 397-406.

Husain, A., Zhang, X., Doll, M.A., States, J.C., Barker, D.F., and Hein, D.W. (2007). Functional analysis of the human N-acetyltransferase 1 major promoter: quantitation of tissue expression and identification of critical sequence elements. Drug Metab Dispos *35*, 1649-1656.

IARC (1987). Overall Evaluations of Carcinogenicity. Lyon, France: International Agency for Research on Cancer. 440 pp. IARC Monographs on the Evaluation of Carcinogenic Risk ofChemicals to Humans *1-42, suppl 7.*

International Agency for Research on Cancer, Lyon, France: (1987). Overall evaluation of carcinogenicity: an update of IARC monographs. Monographs on the evaluation of carcinogenic risk to humans *1-42, suppl 7.*

Jensen, L.E., Hoess, K., Mitchell, L.E., and Whitehead, A.S. (2006). Loss of function polymorphisms in NAT1 protect against spina bifida. Hum Genet *120*, 52-57.

Jensen, L.E., Hoess, K., Whitehead, A.S., and Mitchell, L.E. (2005). The NAT1 C1095A polymorphism, maternal multivitamin use and smoking, and the risk of spina bifida. Birth Defects Res A Clin Mol Teratol *73*, 512-516.

Keating, G.A., and Bogen, K.T. (2004). Estimates of heterocyclic amine intake in the US population. J Chromatogr B Analyt Technol Biomed Life Sci *802*, 127-133.

Kidd, L.R., Hein, D.W., Woodson, K., Taylor, P.R., Albanes, D., Virtamo, J., and Tangrea, J.A. (2011). Lack of association of the N-acetyltransferase NAT1*10 allele with prostate cancer incidence, grade, or stage among smokers in Finland. Biochem Genet *49*, 73-82.

Kilfoy, B.A., Zheng, T., Lan, Q., Han, X., Holford, T., Hein, D.W., Qin, Q., Leaderer, B., Morton, L.M., Yeager, M., *et al.* (2010). Genetic variation in N-acetyltransferases 1 and

2, cigarette smoking, and risk of non-Hodgkin lymphoma. Cancer Causes Control *21*, 127-133.

Krichevsky, A.M., King, K.S., Donahue, C.P., Khrapko, K., and Kosik, K.S. (2003). A microRNA array reveals extensive regulation of microRNAs during brain development. RNA *9*, 1274-1281.

Lammer, E.J., Shaw, G.M., Iovannisci, D.M., Van Waes, J., and Finnell, R.H. (2004). Maternal smoking and the risk of orofacial clefts: Susceptibility with NAT1 and NAT2 polymorphisms. Epidemiology *15*, 150-156.

Larson, D.R., Zenklusen, D., Wu, B., Chao, J.A., and Singer, R.H. (2011). Real-time observation of transcription initiation and elongation on an endogenous yeast gene. Science *332*, 475-478.

Li, D., Jiao, L., Li, Y., Doll, M.A., Hein, D.W., Bondy, M.L., Evans, D.B., Wolff, R.A., Lenzi, R., Pisters, P.W., *et al.* (2006). Polymorphisms of cytochrome P4501A2 and N-acetyltransferase genes, smoking, and risk of pancreatic cancer. Carcinogenesis *27*, 103-111.

Lilla, C., Verla-Tebit, E., Risch, A., Jager, B., Hoffmeister, M., Brenner, H., and Chang-Claude, J. (2006). Effect of NAT1 and NAT2 genetic polymorphisms on colorectal cancer risk associated with exposure to tobacco smoke and meat consumption. Cancer Epidemiol Biomarkers Prev *15*, 99-107.

Lim, L.P., Glasner, M.E., Yekta, S., Burge, C.B., and Bartel, D.P. (2003). Vertebrate microRNA genes. Science *299*, 1540.

Liu, C.G., Calin, G.A., Meloon, B., Gamliel, N., Sevignani, C., Ferracin, M., Dumitru, C.D., Shimizu, M., Zupo, S., Dono, M., *et al.* (2004). An oligonucleotide microchip for genome-wide microRNA profiling in human and mouse tissues. Proc Natl Acad Sci U S A *101*, 9740-9744.

Lo-Guidice, J.M., Allorge, D., Chevalier, D., Debuysere, H., Fazio, F., Lafitte, L.J., and Broly, F. (2000). Molecular analysis of the N-acetyltransferase 1 gene (NAT1*) using polymerase chain reaction-restriction fragment-single strand conformation polymorphism assay. Pharmacogenetics *10*, 293-300.

Malys, N., and McCarthy, J.E. (2011). Translation initiation: variations in the mechanism can be anticipated. Cell Mol Life Sci *68*, 991-1003.

McDaniell, R., Lee, B.K., Song, L., Liu, Z., Boyle, A.P., Erdos, M.R., Scott, L.J., Morken, M.A., Kucera, K.S., Battenhouse, A., *et al.* (2010). Heritable individual-specific and allele-specific chromatin signatures in humans. Science *328*, 235-239.

McGrath, M., Michaud, D., and De Vivo, I. (2006). Polymorphisms in GSTT1, GSTM1, NAT1 and NAT2 genes and bladder cancer risk in men and women. BMC Cancer *6*, 239.

Metry, K.J., Zhao, S., Neale, J.R., Doll, M.A., States, J.C., McGregor, W.G., Pierce, W.M., Jr., and Hein, D.W. (2007). 2-amino-1-methyl-6-phenylimidazo [4,5-b] pyridine-induced DNA adducts and genotoxicity in chinese hamster ovary (CHO) cells expressing human CYP1A2 and rapid or slow acetylator N-acetyltransferase 2. Mol Carcinog *46*, 553-563.

Millikan, R.C., Pittman, G.S., Newman, B., Tse, C.K., Selmin, O., Rockhill, B., Savitz, D., Moorman, P.G., and Bell, D.A. (1998). Cigarette smoking, N-acetyltransferases 1 and 2, and breast cancer risk. Cancer Epidemiol Biomarkers Prev *7*, 371-378.

Millner, L.M., Doll, M.A., Cai, J., States, J.C. and Hein, D.W. (2011). NATb/NAT1*4 promotes greater N-acetyltransferase 1 mediated DNA adducts and mutations than NATa/NAT1*4 following exposure to 4-aminobiphenyl. Mol Carcinog *In press.*

Minchin, R.F., Hanna, P.E., Dupret, J.M., Wagner, C.R., Rodrigues-Lima, F., and Butcher, N.J. (2007). Arylamine N-acetyltransferase I. Int J Biochem Cell Biol *39*, 1999-2005.

Mishra, P.J., Banerjee, D., and Bertino, J.R. (2008). MiRSNPs or MiR-polymorphisms, new players in microRNA mediated regulation of the cell: Introducing microRNA pharmacogenomics. Cell Cycle *7*, 853-858.

Morton, L.M., Schenk, M., Hein, D.W., Davis, S., Zahm, S.H., Cozen, W., Cerhan, J.R., Hartge, P., Welch, R., Chanock, S.J., *et al.* (2006). Genetic variation in N-acetyltransferase 1 (NAT1) and 2 (NAT2) and risk of non-Hodgkin lymphoma. Pharmacogenet Genomics *16*, 537-545.

Nauwelaers, G., Bessette, E.E., Gu, D., Tang, Y., Rageul, J., Fessard, V., Yuan, J.M., Yu, M.C., Langouet, S., and Turesky, R.J. (2011). DNA Adduct Formation of 4-Aminobiphenyl and Heterocyclic Aromatic Amines in Human Hepatocytes. Chem Res Toxicol.

Nechaev, S., Fargo, D.C., dos Santos, G., Liu, L., Gao, Y., and Adelman, K. (2010). Global analysis of short RNAs reveals widespread promoter-proximal stalling and arrest of Pol II in Drosophila. Science *327*, 335-338.

Northrop, D.B. (1999). Rethinking fundamentals of enzyme action. Adv Enzymol Relat Areas Mol Biol *73*, 25-55.

Pacifici, G.M., Bencini, C., and Rane, A. (1986). Acetyltransferase in humans: development and tissue distribution. Pharmacology *32*, 283-291.

Pizzuti, A., Argiolas, A., Di Paola, R., Baratta, R., Rauseo, A., Bozzali, M., Vigneri, R., Dallapiccola, B., Trischitta, V., and Frittitta, L. (2002). An ATG repeat in the 3'-untranslated region of the human resistin gene is associated with a decreased risk of insulin resistance. J Clin Endocrinol Metab *87*, 4403-4406.

Ragunathan, N., Dairou, J., Pluvinage, B., Martins, M., Petit, E., Janel, N., Dupret, J.M., and Rodrigues-Lima, F. (2008). Identification of the xenobiotic-metabolizing enzyme arylamine N-acetyltransferase 1 as a new target of cisplatin in breast cancer cells: molecular and cellular mechanisms of inhibition. Mol Pharmacol *73*, 1761-1768.

Reeves, P.T., Minchin, R.F., and Ilett, K.F. (1988). Induction of sulfamethazine acetylation by hydrocortisone in the rabbit. Drug Metab Dispos *16*, 110-115.

Ring, B.Z., Seitz, R.S., Beck, R., Shasteen, W.J., Tarr, S.M., Cheang, M.C., Yoder, B.J., Budd, G.T., Nielsen, T.O., Hicks, D.G., *et al.* (2006). Novel prognostic immunohistochemical biomarker panel for estrogen receptor-positive breast cancer. J Clin Oncol *24*, 3039-3047.

Sanderson, S., Salanti, G., and Higgins, J. (2007). Joint effects of the N-acetyltransferase 1 and 2 (NAT1 and NAT2) genes and smoking on bladder carcinogenesis: a literature-based systematic HuGE review and evidence synthesis. Am J Epidemiol *166*, 741-751.

Schaeffer, L., Moncollin, V., Roy, R., Staub, A., Mezzina, M., Sarasin, A., Weeda, G., Hoeijmakers, J.H., and Egly, J.M. (1994). The ERCC2/DNA repair protein is associated with the class II BTF2/TFIIH transcription factor. EMBO J *13*, 2388-2392.

Schut, H.A., and Snyderwine, E.G. (1999). DNA adducts of heterocyclic amine food mutagens: implications for mutagenesis and carcinogenesis. Carcinogenesis *20*, 353-368.

Seyler, T.H., Reyes, L.R., and Bernert, J.T. (2010). Analysis of 4-aminobiphenyl hemoglobin adducts in smokers and nonsmokers by pseudo capillary on-column gas chromatography- tandem mass spectrometry. J Anal Toxicol *34*, 304-311.

Shin, A., Shrubsole, M.J., Rice, J.M., Cai, Q., Doll, M.A., Long, J., Smalley, W.E., Shyr, Y., Sinha, R., Ness, R.M., *et al.* (2008). Meat intake, heterocyclic amine exposure, and metabolizing enzyme polymorphisms in relation to colorectal polyp risk. Cancer Epidemiol Biomarkers Prev *17*, 320-329.

Sim, E., Payton, M., Noble, M., and Minchin, R. (2000). An update on genetic, structural and functional studies of arylamine N-acetyltransferases in eucaryotes and procaryotes. Hum Mol Genet *9*, 2435-2441.

Smale, S.T. (1997). Transcription initiation from TATA-less promoters within eukaryotic protein-coding genes. Biochim Biophys Acta *1351*, 73-88.

Stanley, L.A., Coroneos, E., Cuff, R., Hickman, D., Ward, A., and Sim, E. (1996). Immunochemical detection of arylamine N-acetyltransferase in normal and neoplastic bladder. J Histochem Cytochem *44*, 1059-1067.

Stephenson, N., Beckmann, L., and Chang-Claude, J. (2010). Carcinogen metabolism, cigarette smoking, and breast cancer risk: a Bayes model averaging approach. Epidemiol Perspect Innov *7*, 10.

Suzuki, H., Morris, J.S., Li, Y., Doll, M.A., Hein, D.W., Liu, J., Jiao, L., Hassan, M.M., Day, R.S., Bondy, M.L., *et al.* (2008). Interaction of the cytochrome P4501A2, SULT1A1 and NAT gene polymorphisms with smoking and dietary mutagen intake in modification of the risk of pancreatic cancer. Carcinogenesis *29*, 1184-1191.

Takeda, J., Suzuki, Y., Nakao, M., Kuroda, T., Sugano, S., Gojobori, T., and Imanishi, T. (2007). H-DBAS: alternative splicing database of completely sequenced and manually annotated full-length cDNAs based on H-Invitational. Nucleic Acids Res *35*, D104-109.

Tiang, J.M., Butcher, N.J., Cullinane, C., Humbert, P.O., and Minchin, R.F. (2011). RNAi-Mediated Knock-Down of Arylamine N-acetyltransferase-1 Expression Induces E-cadherin Up-Regulation and Cell-Cell Contact Growth Inhibition. PLoS One *6*, e17031.

Vatsis, K.P., and Weber, W.W. (1993). Structural heterogeneity of Caucasian N-acetyltransferase at the NAT1 gene locus. Arch Biochem Biophys *301*, 71-76.

Vaziri, S.A., Hughes, N.C., Sampson, H., Darlington, G., Jewett, M.A., and Grant, D.M. (2001). Variation in enzymes of arylamine procarcinogen biotransformation among bladder cancer patients and control subjects. Pharmacogenetics *11*, 7-20.

Wakefield, L., Cornish, V., Long, H., Griffiths, W.J., and Sim, E. (2007). Deletion of a xenobiotic metabolizing gene in mice affects folate metabolism. Biochem Biophys Res Commun *364*, 556-560.

Wakefield, L., Robinson, J., Long, H., Ibbitt, J.C., Cooke, S., Hurst, H.C., and Sim, E. (2008). Arylamine N-acetyltransferase 1 expression in breast cancer cell lines: a potential marker in estrogen receptor-positive tumors. Genes Chromosomes Cancer *47*, 118-126.

Walraven, J.M., Trent, J.O., and Hein, D.W. (2008). Structure-function analyses of single nucleotide polymorphisms in human N-acetyltransferase 1. Drug Metab Rev *40*, 169-184.

Weber, W.W., and Hein, D.W. (1985). N-acetylation pharmacogenetics. Pharmacol Rev *37*, 25-79.

Wideroff, L., Vaughan, T.L., Farin, F.M., Gammon, M.D., Risch, H., Stanford, J.L., and Chow, W.H. (2007). GST, NAT1, CYP1A1 polymorphisms and risk of esophageal and gastric adenocarcinomas. Cancer Detect Prev *31*, 233-236.

Wikman, H., Thiel, S., Jager, B., Schmezer, P., Spiegelhalder, B., Edler, L., Dienemann, H., Kayser, K., Schulz, V., Drings, P., *et al.* (2001). Relevance of N-acetyltransferase 1 and 2 (NAT1, NAT2) genetic polymorphisms in non-small cell lung cancer susceptibility. Pharmacogenetics *11*, 157-168.

Wu, R.W., Tucker, J.D., Sorensen, K.J., Thompson, L.H., and Felton, J.S. (1997). Differential effect of acetyltransferase expression on the genotoxicity of heterocyclic amines in CHO cells. Mutat Res *390*, 93-103.

Zang, Y., Doll, M.A., Zhao, S., States, J.C., and Hein, D.W. (2007). Functional characterization of single-nucleotide polymorphisms and haplotypes of human N-acetyltransferase 2. Carcinogenesis *28*, 1665-1671.

Zhangwei, X., Jianming, X., Qiao, M., and Xinhua, X. (2006). N-Acetyltransferase-1 gene polymorphisms and correlation between genotype and its activity in a central Chinese Han population. Clin Chim Acta *371*, 85-91.

Zheng, W., Deitz, A.C., Campbell, D.R., Wen, W.Q., Cerhan, J.R., Sellers, T.A., Folsom, A.R., and Hein, D.W. (1999). N-acetyltransferase 1 genetic polymorphism, cigarette smoking, well-done meat intake, and breast cancer risk. Cancer Epidemiol Biomarkers Prev *8*, 233-239.

Zhu, Y., and Hein, D.W. (2008). Functional effects of single nucleotide polymorphisms in the coding region of human N-acetyltransferase 1. Pharmacogenomics J *8*, 339-348.

CURRICULUM VITAE

Name: Lori Michele Millner

Current Position Title: NIEHS Postdoctoral Fellow
University of Louisville, Department of Pathology, Louisville, KY 40292
Email: lmmill10@louisville.edu

Education/Training

Institution/Location	DEGREE	YEAR	FIELD OF STUDY
University of Kentucky, Lexington, KY	B.A.	2004	Chemistry and Biology
University of Louisville, Louisville, KY	M.A.	2008	Pharmacology and Toxicology
University of Louisville, Louisville, KY	Ph.D.	2011	Pharmacology and Toxicology

Positions and Employment

2002-2004	Undergraduate Researcher, University of Kentucky, Lexington, KY
2003	Undergraduate Researcher, NSF and University of South Florida, Tampa, FL
2003-2004	Pharmacy Technician, GeriCare Pharmacy, Lexington, KY
2004-2005	Humanitarian Aid, University of Saratov, Saratov, Russia
2005-2006	Chemist, New Products Development Lab, Valvoline World Headquarters, Lexington, KY
2006-present	Graduate Student, Department of Pharmacology, University of Louisville, Louisville, KY

Other Experience and Professional Memberships

2000-2004	Student Member of American Chemical Society
2008-present	Student Member American Association Cancer Research
2009-2010	Student Representative to the University of Louisville Medical School Faculty Forum
2010-present	Kentucky Academy of Science
2010	Instructor in Advanced Eukaryotic Genetics BIOC 641

Honors

2000-2004	Chancellor's Scholarship, University of Kentucky
2000-2004	Dean's List, University of Kentucky
2003	1st Place American Chemical Society Undergraduate Poster Competition
2003	2nd Place American Chemical Society Undergraduate Poster Competition
2008	Dean's Citation for Master's Thesis
2008	Recipient of AACR Scholar-In-Training Award funded by Susan G. Komen for the Cure
2008 – 2011	Recipient and PI of Department of Defense Breast Cancer Research Grant; N-acetyltransferase 1 Polymorphism and Breast Cancer; OGMB08961
2010	Platform Speaker 2010 5th International Workshop on Arylamine *N*-acetyltransferases, Paris, France
2010	Recipient of University of Louisville School of Medicine Travel Award
2010	Recipient of University of Louisville Center for Genetics and Molecular Medicine Travel Award
2010	Recipient of University of Louisville Graduate Student Council Travel Award
2011	Invited speaker to the 2011 St. Jude National Graduate Student Symposium

Selected peer-reviewed publications

Published Abstracts

1. Anna Rothert; Sapna K. Deo; Libby G. Puckett; Lori M. Millner, Marc J. Madou; Sylvia Daunert. Adaptation of a whole-cell based reporter gene assay for arsenite and antimonite to a compact disc centrifugal microfluidics platform. Abstracts, 55th Southeast Regional Meeting of the American Chemical Society, Atlanta, GA, United States, November 16-19, 2003, 979.

2. Jessica Feliciano; Anna Rothert; Sapna K. Deo; Libby G. Pucket; Lori M. Millner; Jan Roelof Van der Meer; Marc J. Madou, and Sylvia Daunert. Bacterial biosensing systems ror arsenic detection: from the laboratory to the field. Abstracts, Superfund Basic Research Program Annual Meeting Dartmouth College November 9-12, 2003.

3. Lori M. Millner and Mohammed Eddoudi. Design and synthesis of porous metal organic frameworks. Abstracts, 55th Southeast Regional Meeting of the American Chemical Society, Atlanta, GA, United States, November 16-19, 2003, 1002.

4. Lori M. Millner, Jean Bendaly, Mark A. Doll, David F. Barker, J. Christopher States and David W. Hein. Functional Effect of N-acetyltransferase Allele NAT1*10 in DNA Adduct Formation and Mutagenesis Following Exposure to Aromatic and Heterocyclic Amine Carcinogens. Abstracts, Ohio Valley Society of Toxicologists Meeting, Eli Lilly and Company, Indianapolis, Indiana, November 2, 2007.

5. Lori M. Millner, Jean Bendaly, Mark A. Doll, David F. Barker, J. Christopher States and David W. Hein. Functional effect of N-acetyltransferase 1 (NAT1*10) Polymorphism

in DNA adduct formation and mutagenesis following exposure to aromatic and heterocyclic amine carcinogens. Abstracts, Society of Toxicology National Meeting, Seatle, WA. March 18, 2008.

6. Lori M. Millner, David F. Barker, Ashley L. Howarth, Mark A. Doll, J. Christopher States, David W. Hein. Translational Effects of Alternative NAT1 mRNA Isoforms. Abstracts, AACR Frontiers in Cancer Prevention Research International Conference, Washington, DC. November 16-19, 2008.

7. Lori M. Millner, David F. Barker, Mark A. Doll, J. Christopher States, and David W. Hein. Functional effects of N-acetyltransferase 1 (NAT1*10) polymorphisms. *FASEB J.* 2009 23:LB394.

8. Lori M. Millner, David F. Barker, Mark A. Doll, J. Christopher States and David W. Hein. Functional Effects of Alternative *N*-acetyltransferase (*NAT1*10*) mRNA Isoforms. Environmental Health Sciences Showcase, NIEHS, University of Cincinnati, Cincinnati, Ohio. September 25, 2009.

9. Lori M. Millner, Mark A. Doll, J. Christopher States and David W. Hein. Differences in Arylamine-induced Mutagenesis Associated with N-acetyltransferase 1 Alternative mRNA Isoforms. Abstracts Midwest DNA Repair Symposium, University of Louisville, Louisville, KY, May 15, 2010.

10. Lori M. Millner, Mark A. Doll, Jian Cai, J. Christopher States and David W. Hein. Functional Effects of NAT1*14 Polymorphism in a NATb mRNA Construct. 5th International Workshop on Aryalmine N-acetyltrasferases, Université Paris Diderot, Paris France, September 2, 2010.

11. Lori M. Millner, Mark A. Doll, Jian Cai, J. Christopher States and David W. Hein. Differences in Arylamine-Induced Mutagenesis with N-acetyltransferase 1 Alternative mRNA Isoforms. 5th International Workshop on Aryalmine N-acetyltrasferases, Université Paris Diderot, Paris France, September 2, 2010.

12. Lori M. Millner, Mark A. Doll, Jian Cai, J. Christopher States and David W. Hein. Effects of *N*-acetyltransferase 1 (NAT1*10) polymorphisms in NATb and NATa derived mRNA constructs on DNA adducts and mutations from 4-aminobiphenyl. Society of Toxicology 50th Meeting. Washington, D.C. March 6 – 10, 2011.

13. Lori M. Millner, Mark A. Doll, Jian Cai, J. Christopher States and David W. Hein. Differences in Arylamine-induced Mutagenesis Associated with N-acetyltransferase 1 Alternative mRNA Isoforms. Era of Hope Department of Defense Conference, Orlando, Florida. August 2 – 6, 2011.

Published Manuscripts

1. Rothert, A; Deo, S. K.; Millner, L.; Puckett, L..; Madou, M..; Daunert, S. Whole-cell-reporter-gene-based biosensing systems on a compact disk microfluidics platform. *Analytical Biochemistry* 2005, 342(1), 11-19.

2. Dikici, E.; Qu X., Rowe, L.; Millner, L.; Logue, ;. Deo, S.; Ensor M.; and Daunert S. Aequorin variants with improved bioluminescence properties. *Protein Engineering Design and Selection.*
2009 22(4):243-248.

3. Bendaly, J., Doll, M.A., Millner, L.M., Metry, K.J., Smith, N.B., Pierce Jr., W. M., and Hein, D.W.: Differences between human slow N-acetyltransferase 2 alleles in levels of 4-aminobiphenyl-induced DNA adducts and mutations. *Mutation Research* 2009 Dec 1;671(1-2):13-9.

4. Hein, D.W., Millner, L.M., Leggett, C.S. and Doll, M.A.: Relationship between N-acetyltransferase 2 single nucleotide polymorphisms and phenotype. *Carcinogenesis* 2010 Feb;31(2):326-7

5. Millner, L.M., Doll, Mark A., Cai, J., States, J. Christopher, Hein, David W. NATb/*NAT1*4* promotes greater arylamine *N*-acetyltransferase 1 mediated DNA adducts and mutations than NATa/*NAT1*4* following exposure to 4-aminobiphenyl. In press to Molecular Carcinogenesis.

Manuscripts Pending Acceptance:

1. Millner, L.M., Doll, Mark A., Cai, J., States, J. Christopher, Hein, David W. Functional effects on kinetic properties of *N*-acetyltransferase 1 (NAT1*14) in a NATb or NATa construct. *Drug Metabolism and Disposition submitted and under review.

2. Millner, L.M., Doll, Mark A., Cai, J., States, J. Christopher, Hein, David W. Functional effect of *N*-acetyltransferase 1 (NAT1*10) polymorphism in DNA adduct formation and mutagenesis following exposure to 4-aminobiphenyl. *To be submitted to Cancer Research.

Research Support

R01 CA34627 Hein (PI) 09/30/83 - 06/30/09 NIH/NCI
Pharmacogenetics of drug and carcinogen metabolism
The major goal is to assess the effect of NAT1 and NAT2 acetylator genotypes on cancer risk.
Role: Graduate Student

5T32ES011564-07 Hein (PI) 05/01/2008 – 09/30/2008 NIEHS
Effect of N-Acetyltransferase 1 polymorphisms on mutagenesis and DNA adducts
The major goal is to determine effects alternative NAT1 transcripts and alleles on altered mutagenesis and cancer risk.
Role: Trainee

OGMB08961 Millner (PI) 10/30/08 – 10/30/2011 Department of Defense Breast Cancer Research Program. N-acetyltransferase 1 Polymorphism and Breast Cancer.The major goal is to discover effect of NAT1 polymorphism on cancer development.
Role: PI